Ph.D. Thesis

"Hydrogel Based Wound Dressing Material"

Submitted by:
PREETI GUPTA
(2k14/PhD/AC/05)

Under the Supervision of:
Prof. ROLI PURWAR

Discipline of Polymer Sciences & Chemical Technology,
Department of Applied Chemistry,
Delhi Technological University,
Shahabad, Daulatpur, Bawana Road,
Delhi-110042, India

March 2021

DELHI TECHNOLOGICAL UNIVERSITY

Shahabad, Daulatpur, Bawana Road, Delhi-110042, India

DECLARATION

I hereby declare that the thesis entitled "**Hydrogel Based Wound Dressing Material**" is an original work carried out by me under the supervision of **Prof. Roli Purwar**, Department of Applied Chemistry, Delhi Technological University, Delhi. This thesis has been prepared in conformity with the rules and regulations of the Delhi Technological University, Delhi. The research work reported and results presented in the thesis have neither partially nor fully submitted to any other university nor institute for the award of any other degree or diploma.

Place: Delhi
Date:

(Preeti Gupta)

(Roll No: 2K14/PhD/AC/05)
Research Scholar
Department of Applied Chemistry
Delhi Technological University,
Delhi-110042

DELHI TECHNOLOGICAL UNIVERSITY

Shahabad, Daulatpur, Bawana Road, Delhi-110042, India

CERTIFICATE

This is to certify that the work embodied in the thesis entitled "**Hydrogel Based Wound Dressing Material**" by **Ms. Preeti Gupta (Roll No 2K14/PhD/AC/05),** in the partial fulfilment of the requirements for the award of the degree of **Doctor of Philosophy**, is an authentic record of student's own work carried out by her under the supervision of **Prof. Roli Purwar**, Faculty of Polymer Science, Department of Applied Chemistry, Delhi Technological University, Delhi.

This is also certified that this work has neither partially nor fully submitted to any other Institute or University for the award of any other diploma or degree.

PROF. ROLI PURWAR
Department of Applied Chemistry
Delhi Technological University,
Delhi-110042.

PROF. SUDHIR WARKAR
HOD, Department of Applied Chemistry
Delhi Technological University,
Delhi-110042

ACKNOWLEDGEMENTS

It gives me immense pleasure to express my deep sense of gratitude to my supervisor ***PROF. ROLI PURWAR***, *Department of Applied Chemistry, Delhi Technological University, Delhi* for assisting me in identifying and formulating the research problem. Despite her busy schedule, *Prof. Roli Purwar* was always available for the advice and discussions. Her valuable comments and advice gave me the confidence to overcome the challenges in formulation of this Ph.D. thesis work.

I owe my heartfelt gratitude to ***Prof. Yogesh Singh***, *Hon'ble Vice-Chancellor, Delhi Technological University* for his kind permission and ***Prof. Sudhir Warkar***, *Head, Department of Applied Chemistry, DTU* for providing me the necessary facilities to carry out this research work. I wish to express my sincere thanks to the all faculty members of *Department of Applied Chemistry, DTU* for their help and support during this research work.

I would like to thank all technical and non-technical staff and my friends, seniors and fellow researchers: ***Dr. Chandra Mohan Srivastava, Dr. Meenakshi, Dr. Anuja Agarwal, Ms. Priya, Ms. Radhika, Ms. Ritu, Ms. Radha, Ms. Sharmilla, Ms. Mohini, Mr. Aman Verma, Mr. Ankesh Kumar, Mr. Jawed Alam*** who have supported me through their encouragement, support and friendship during this period of thesis research work. I would like to thank to all those who directly and indirectly supported me in carrying out this thesis work successfully. I wish to pay my sincere thanks to ***University Grant Commission (UGC)*** for providing me financial support to carry out this research work.

Furthermore, I am indebted to ***My Parents***, ***My Bua, Phuphaji***, My brothers ***Yashvardhan*** and ***Rishabh***, My sister ***Pooja,*** My sister in laws ***Khushi*** and ***Mansi*** for their endless inspiration, moral support and guidance throughout my whole life, Niece ***Nivika*** and Nephew ***Rudra, Vedansh and love*** for their selfless love and support, that has always been a driving force for the completion of my research work.

Above all, I owe to ***Almighty God*** for granting me wisdom, health and strength to accept the challenges of the life.

Place: Delhi

Date: (***Preeti Gupta***)

Abstract

Weak mechanical strength of hydrogels in wet condition limits their use for load bearing applications. Their mechanical strength can be raised by grafting them over some support or by converting them into nanofibrous form. Present thesis is focused on the preparation of poly (acrylamide-co-acrylic acid) hydrogel grafted over cotton fabric using two different cross-linkers i.e. PEG and MBAAm for making medicated dressing and nanofibers of hydrogel of poly (acrylamide-co-acrylic acid). FTIR was used to confirm the insertion of cross-links into the polymer chains. Grafting of uniform hydrogel layer on cotton surface and formation of hydrogel nanofibers were confirmed by using SEM. The average fibre diameter was found to be 275±94.5 nm.

Swelling of composite prepared using PEG followed first-order kinetic model at acidic and neutral pH whereas second-order kinetic model at pH 8.5 while that prepared using MBAAm followed second-order kinetic equation at all the pHs studied. The kinetics of swelling was also governed by Peppas model at all pHs. Release of drug from both the composites was studied in phosphate buffers having pH 5.5,7 and 8.5 at 37±0.1°C and observed that it was fastest in phosphate buffer having pH 7. On fitting drug release data into different models, it was observed that drug release was diffusion controlled and followed Fickian diffusion mechanism in case of composite prepared by using PEG as cross-linker whereas it was controlled by diffusion as well as chain relaxation in case of composite prepared by using MBAAm. Mechanical testing using Universal Testing Machine supported a higher mechanical strength of the hydrogel composite as compared to its film.

Swelling behaviour of Nanofibrous mats was found to be highest at neutral pH and it followed second order kinetics at all pHs. The drug release kinetics was further evaluated and found that it took place by Fickian diffusion ($n < 0.5$) and followed second order release kinetics. Antimicrobial tests were performed to show the effectiveness of drug loaded within the hydrogel samples.

Keywords: Hydrogel, poly (acrylamide-co-acrylic acid) composite, hydrogel nanofibers, cross-linker, swelling kinetics, drug release.

Table of Contents

List of Figures

List of Tables

List of Abbreviations

S.No.	Abbreviation	Full form
1.	AAc	Acrylic acid
2.	PAAc	Polyacrylic acid
3.	AAm	Acrylamide
4.	PAAm	Polyacrylamide
5.	APS	Ammonium persulphate
6.	MBAAM	N,N'-Methylene bisacrylamide
7.	PEG	Polyethylene glycol
8.	SEM	Scanning electron microscopy
9.	FTIR	Fourier transformed infrared spectroscopy
10.	TGA	Thermogravimetric analysis
11.	DSC	Differential scanning calorimetry
12.	PVA	Polyvinyl alcohol
13.	PMAAc	Polymethacrylic acid
14.	PDMAEMA	Polydimethylaminoethylacrylate
15.	PDEAEMA	Polydiethylaminoethylmethacrylate
16.	PET	Poly(ethylene terephthalate)
17.	MAAm	Methacrylamide
18.	CAN	Ceric ammonium nitrate
19.	NIPAAm	N-isopropyl acrylamide
20.	HEMA	Hydroxyethyl methacrylate
21.	PU	Polyurethane
22.	p(LLA-CL)	Poly (L-lactide-co-Ɛ-caprolactone)
23.	PEGMC	Poly (ethylene glycol) maleate citrate
24.	PEGDA	Poly (ethylene glycol) diacrylate

25.	VAc	Vinyl acetate
26.	PEO	Polyethylene oxide
27.	PP	Polypropylene
28.	MWCNT	Multiwalled carbon nanotubes
29.	PNIPAAM	Poly (N-isopropyl acrylamide)
30.	PLA	Polylactic acid
31.	PHEMA	Poly (2-hydroxy methyl methacrylate)

CHAPTER 1

INTRODUCTION & OBJECTIVES

1.1 Introduction

Wound care devices are the most lucrative and developing continuously with changes in their demand in prospect of recent research and development. A wound is any external or internal cut or break in the regularity of body tissue, especially skin, because of some injury or operation. It may be acute or chronic depending upon its nature and the time involved in its healing. An acute wound takes 8-12h for its curing based on its size, depth and extent of harm, while chronic wounds such as burn wound, ulcers take indefinite time for their curing and do not go through the normal stages of wound healing[1]. A firm belief until mid-1900 was fast healing of the wound in dry and uncovered conditions. Later it was observed that a covered wound remains in contact with proteinases, chemotactic and growth factors which enhance the healing process. Discoveries suggested that healing of wound is a complex and dynamic process and involves the following four overlapping phases: coagulation and haemostasis, inflammation, proliferation, maturation[2]. Any factor stimulating any of these phases enhance the healing process. Winter[3] for the first time proved that wet conditions help in faster healing of the wound. This is because scab formed in case of an open wound results in a decreased rate of epithelisation[4]. Modern dressings not only cover the wound but also enhance the healing process. These dressings were developed to match the properties of ideal dressings such as permeability to gases, providing a moist environment, non-permeability to micro-organisms, painless removal, exudate absorption, biocompatibility, and elasticity, stimulation of growth factors, non-toxicity and cost affectability. Till date near about more than 25 companies are supplying advanced dressings of more than 300 types. Some such

dressings include semi-permeable films, foams, alginate[5,6,7,8], hydrocolloids[9,10,11], amorphous hydrogels, hydrogel sheets, hydrogel gauzes, bioactive wound dressings, composite dressings, medicated dressings.

Hydrogels have gained remarkable attention, especially in the last 30 years[12], as they can imbibe a large quantity of water owing to their hydrophilic nature but can retain their existence due to three-dimensional network structure[13]. They can be used as absorbents in baby diapers[14], ion-exchange resins[15], biomedical substances like soft contact lenses[16] or carriers for the controlled release of drugs[17] and supports for catalysts[18,19]. They exhibit fast swelling, high normalised swelling, surface slipperiness which make them a good candidate for drug delivery. Polyacrylamide, a superabsorbent material, in the form of hydrogel widely found applications in various fields such as agriculture, drug release, food packaging products, water treatment, ophthalmic etc[20], but this hydrogel lacks hydrolytic stability.

Stimuli-responsive hydrogel, especially pH responsive, can be prepared using polyacrylic acid having trigger on/off point in an acidic environment. But its gel also exhibits inferior gel strength, dispersion and elastic properties in aqueous media[21]. Presence of pendant –COOH groups and structural similarity with acrylamide, makes acrylic acid a potent candidate for copolymerisation with acrylamide and making it pH-sensitive. Bajpai et al.[22] prepared a pH- respondent hydrogel system using acrylamide, methacrylamide and acrylic acid. Acrylamide and acrylic acid owing to their high water affinity and copolymerisation velocity were now chosen as the base materials for making hydrogels. Studies showed that hydrogel of the copolymer of poly (acrylamide-co-acrylic acid) have high water absorption tendency[23,24].

Hydrogel dressings can be supposed as the most promising candidate for covering wounds, especially where the moist environment is required. They possess

the tendency to provide moisture to the dry wound and at the same time absorption of extra exudate, if any, from the wound site. These dressings not only hydrate the wound but also re-hydrate scar and cause autolytic debridement. These produce a soothing and cooling effect which is more valuable in case of burn wounds. These dressings are available as amorphous hydrogels (e.g. Curafil, Hypergel, Intrasite gel) and sheet hydrogels. The former being soft and formless, become less viscous in contact of fluid and lead some allergic reactions while the latter being sheet-like swell in contact of fluid and maintain their integrity[25]. "Geliperm" (developed by Geistlich & Sons Co) was the first hydrogel based dressing made up of acrylamide cross-linked by using MBAAm (N, N-Methylene bisacrylamide) which fulfils almost every condition of an ideal wound dressing. Some other commercially available hydrogel dressings are Curasol, Tegagel, Carrasyn, DuoDerm, etc. These dressings require secondary dressings, have weak mechanical strength, cause maceration of skin around the wound and have limited absorption capacity which limit their use for wound dressing applications, especially in case of heavily exudating wounds.

Composite dressings, containing more than one physiologically distinct layers, are versatile and can be used conveniently for partial or full thickness wounds. Generally such dressings are less flexible and costlier. Hydrogels, on the other hand, flow away from the local target site or exhibit premature dissolution in wet conditions i.e. are extremely flexible. So their composite with some support may meet with the flexibility of ideal dressing or enhance their mechanical strength[26]. Such composites are prepared by grafting the hydrogel layer over some support such as cotton[27,28], chitosan[29] etc.

Medicated hydrogels containing drugs/antibiotic, reduce the bacterial infection at wound site have grown their importance in improving wound healing process[30,31].

Highly porous structure and aqueous swelling of hydrogels can easily be tuned by controlling the cross-links density in the gel network. Porous structure also allows loading of nutrients/drugs into the gel network and subsequently release it at a rate depending on the diffusion coefficient of the small molecules or large molecule through the gel network[32]. Preparation of any hydrogel involves three integral parts: Monomer, initiator and cross-linker. Cross-linker plays a key role in the conversion of polymer to its hydrogel form. An optimum concentration of the cross-linker is required to convert the copolymer into a form having optimum pore size. Below this concentration hydrogel is not formed due to less cross-linking. But above this concentration, excessive cross-linking hinders the swelling tendency of the hydrogel due to reduction in pore volume. Besides quantity, nature of the cross-linker also influences their swelling tendency. A cross-linker which is hydrophilic and has somewhat longer carbon chain may lead to the formation of pores of optimum size as compared to that having shorter (2-4 carbon) chains and the pores of optimum size are responsible for more swelling in a shorter period of time. Therefore, pore size and hence, swelling ability and drug holding capacity are related with the network elasticity which on the other hand, depends upon the nature of hydrophilic group present, extent of cross-linking and porosity in the network. Different cross-linkers like formaldehyde[33], N,N'-methylene bisacrylamide (MBAAm)[34,35] polyethylene glycol diglycidal ether[36], tetraethylene glycol[37], polyethylene glycol[26] had been used by different researchers. For developing poly (acrylamide-co-acrylic acid) hydrogel, MBAAm is widely and commercially used cross-linker but in literature use of PEG[27] has also been reported. Hydrogel films of copolymers of acrylic acid (AAc) with acrylamide (AAm) derivatives have been reported for the release of various

drugs[12,25,26,27,38] such as bovine serum albumin[39], gentamicin sulphate[40], theophylline[41], ascorbic acid[42], 5-fluorouracil[43] etc.

Electrospun nanofibrous mats have high surface to volume ratio, porous structure, good mechanical strength, more flexibility as compared to their film counterparts[44]. The swelling kinetics of hydrogels films are inversely related with the square of their dimension, so the rate of volume change can be increased by changing the morphology of the hydrogel material from films to nanofibrous form. Large surface area of hydrogel nanofibrous mats enables fast release of antibiotics or growth factors into the wound site[45,46]. The high porosity of nanofibrous mats able do fast absorption of body fluids and diffusion of waste. These alluring properties of hydrogel nanofibrous mats make them a good candidate for medicated wound dressing materials[47].

Recently, efforts have been made on the structure and composition design for achieving advance nanofiber-based hydrogel with high mechanical strength and multifunctional application performance. Electrospun hydrogel nanofibers from poly (styrene-co-maleic anhydride)[48], poly (styrene-co-maleic sodium anhydride) / cellulose[49], multiblock polyester urethane[32], PVA / Hyaluronic acid[50], polyvinyl alcohol / polyacrylic acid / MWCNT[51], Chitosan-g-PNIPAAM / Polyethylene oxide[52], polyaspartic acid[46], poly(vinyl caprolactam-co-hydroxymethyl acrylamide)[53] and Polyvinylpyrrolidone[54] have been explored for tissue engineering and drug delivery applications. An important shortcoming associated with the several hydrogel nanofibrous mats was their easy deformation in aqueous media i.e. an unstable fibre morphology in aqueous media makes them non-suitable for load bearing applications[48,55].

1.2 Motivation of Research

Hydrogel of poly (acrylamide-co-acrylic acid) finds several applications as super-porous material but their weak mechanical strength limits their use for wound dressing applications. Thus, there is a need to develop a structure which possesses high mechanical strength and release drug in a controlled manner. To raise mechanical strength, the hydrogel system was grafted over some support. The uniqueness here was that the hydrogel layers bind chemically while the available composite dressings have two layers - one adhered at the surface of other, from where the second layer can be detached.

The drug release property can be tuned by controlling pore size and increasing surface area. Cross-linker plays a important role in deciding the strength and pore size of a hydrogel system. This induced the idea of using two different cross-linkers PEG (polyethylene glycol) and MBAAm (N, N'-methylene bis acrylamide) for the preparation of poly (acrylamide-co-acrylic acid) grafted cotton fabric and study their effect on swelling and drug release properties of the composites. A higher cross-linker concentration may lead to less swelling or drug loading because of highly condensed structure. So, we also focused on predicting the adequate quantity of cross-linker for maximum swelling.

Nanofibers are the materials having high mechanical strength, more surface area and high porosity which introduced the idea of conversion of hydrogel into nanofibrous form to enhance its mechanical strength and porosity to achieve control release of drugs.

1.3 Objective

The broad objective of the thesis was design and development of poly (acrylamide-co-acrylic acid) hydrogel based wound dressing material for drug release.

The above objective was achieved under the following sub-objectives:

- Synthesis and characterization of hydrogel composite by graft copolymerization of poly (acrylamide-co-acrylic acid) over cotton fabric using PEG as cross-linker.
- Synthesis and characterization of hydrogel composite by graft copolymerization of poly (acrylamide-co-acrylic acid) over cotton fabric using MBAAm as cross-linker.
- Comparative study of swelling and drug release results of poly (acrylamide-co-acrylic acid) hydrogel composites prepared by using MBAAm and PEG as cross-linkers.
- Fabrication and characterization of poly (acrylamide-co-acrylic acid) hydrogel nanofibers.

CHAPTER 2

LITERATURE REVIEW

In the recent years, a considerable interest has been generated for the preparation of smart wound dressing material to induce fast healing in moist environment. But before going in their details, it is also essential to know about traditional dressings available and the problems associated with them. Thus, in this chapter, the properties and shortcomings of available wound dressings have been discussed and the recent research going on in this field has also been explored.

2.1 Wound and its Healing

Skin, the single largest body organ, protects the body from the external environment by keeping infection causing agents such as bacteria and viruses out and maintaining the internal environment such as temperature and water level of the body. Any injury like cut, shock etc., resulting in damaged dermis of the skin is termed as a wound. Injured skin also results in loss of tissue fluid. If the wound covered more than 10% of the total body surface area, it may result in potentially life-threatening loss of tissue fluid. Depending upon its cause and period of curing, a wound may beacute[56] or chronic[57]. The former is the result of some trauma and takes a limited period of time for its curing. Contrary to this, the latter is a result of some disease and hence, requires more care and time for curing[1,57].

Wound healing being a complex process, involves which several cellular and biochemical reactions[1,2]. It generally involves following four overlapping phases: coagulation and haemostasis, inflammation, proliferation, and maturation[2]. For the successful healing of a wound, these phases must occur in proper sequence and time

period. Any factor which interferes in any of these phases may result in delay in healing process. Smoking, age, stress, oxygenation, nutrition, medications etc., are some factors which individually or collectively impaired the healing process[2]. On the other hand, factors which stimulate any of these phases may fasten the healing process.

2.1.1 *Factors Affecting Wound Healing*

(i) Wound infection

An open wound is more prone towards the bacterial infection and in an infectious wound, the availability of growth factors reduces and fibrin essential for healing process degrades. Since the bacteria cause inflammation so the chances of their availability in chronic wounds are very high. Thus, the healing can be enhanced by reducing wound infection by covering it with some dressing. Secondly, release of some antibiotics also helps in controlling wound infection leading to its fast healing.

(ii) Role of wound pH in healing process

pH of normal skin is found to be acidic as first reported by Hesus et al.[58] and confirmed by Schade et al.[58] after more than 50yr. The pH value of normal skin varies from 4.0-6.0 depending upon the area of residence and age of the person and play a key role in protecting skin from external adverse factors such as bacteria, chemicals etc. In case of wound or injury the skin pH is disturbed because of the exposure of underlying layers having pH near about 7.4. Further bacterial growth is supported by weakly acidic or alkaline pH (more than 6.0) but reduces as pH approaches towards acidic media. Thus, the bacterial infection can be controlled at the wound site by shifting its pH towards acidic side. It is also evident by a clinical study where the bacterial load is reduced sufficiently by just applying some acidic ointment[144]. Thus,

the shifting of pH from alkaline to acidic media not only helps in controlling bacterial growth but also supports fast healing because of the more activity of the healing nutrients and antibiotics at lower pH. The innate defence of the body also works on the same fact.

The therapeutic inventions shifting the wound pH towards acidic site may reduce bacterial infection and supports fast healing[59].

(iii) Wound dressings

An open wound although cured readily as believed until mid-1900 but is more prone towards infection, so to heal a wound readily it is generally covered with some dressing[2]. For years, humans have used different materials such as linen, honey, animal fats, and vegetables fibres for wound dressing. All these dressings are resistant to infection causing bacteria, cheap and harmless. Honey besides aforesaid properties also make the smell of discharge less offensive, but quality control in honey production, its sensitiveness to pollen and lack of evidence base in therapeutic effects and chemical properties limits its use for this purpose[60].

Traditional dressings like gauze, lint, plasters, cotton wool etc[61]., are dry dressings and have been used to protect a wound from contamination since a longer period. In case of these dressings, wound becomes dry as they absorb the exudate. When the conditions of the wound are dry, its bed rapidly dries out resulting in scab formation made up of dead and dying cells. New epithelial cells migrate down underneath to find a moist area, so the healing phase was extended. Further at the time of dressing change, there occurs pain, dehydration, and adherence to the wound causing damage to newly formed tissue and bleeding, microbial invasion, and accumulation of exudate at the wound site due to its low absorption etc[62] and hence,

delay the healing time. These disadvantages make these dressings uncommon for wound dressing applications, mainly in case of chronic wounds. Therefore, it has been concluded that traditional dressings should be applied only in case of clean and dry wounds or as secondary dressing to absorb exudates for protecting the wound[63,64,65].

Winter et al.[4] in 1962 worked on covering wounds with some specific dressings in an experimental model (using the pig) and observed the rates of healing. Winter[3] observed that healing was faster in case of wounds covered with an occlusive dressing in comparison to an open wound. This work generated the principles of moist wound healing for the first time. Winter's results on a human subject were confirmed by Hinmen et al.[66] in 1963. In a moist environment, exudate bathes the wound bed with nutrients. Many modern dressing materials such as semi-permeable films, foams, alginate, hydrocolloids, amorphous hydrogels, hydrogel sheets, hydrogel gauzes, bioactive wound dressings, composite dressings, medicated dressings are now designed to fulfil many of the requirements of advanced dressings. These dressings have their own advantages and disadvantages.

Semipermeable dressings[8,67,68] are transparent (helps in continuous inspection), permeable to gases, impermeable to micro-organisms, cause autolytic debridement, highly elastic and flexible. Tegaderm™, Opsite™ etc., are some such commercially available semi-permeable dressings which differ in water vapour transmission rate, adhesive property, and comfortability. The disadvantages associated with these dressings are their low tendency to absorb exudate and maceration of the wound and nearby area[69].

Foam dressings fulfil most of the requirements but are not suitable in case of low exudating or dry wounds[9,10]. Moreover, these may adhere to the wound, if exudate

dries. Hydrocolloid dressings[11] are the combinations of inner layer of foming agents (which are colloidal in nature) and outer impermeable layer of elastomers and adhesives. These dressings fulfil the requirements like water vapour permeability, non-permeability to bacteria, exudate adsorption, debridement property etc., and can be used for low to moderately exudating wounds. Comfeel™, Granuflex™, Tegasorb™, DuoDerm™ etc., are some commercially available hydrocolloid dressings[69]. Use of these dressings initially leads to enlargement of wound and fouling smell. These dressings cannot be used for highly exudating wounds and wounds which involve anaerobic colonisation.

Alginate dressings[5,6,7] contain sodium or calcium salts of guluronic or mannuronic acid units. Their swelling ability is due to the formation of metal-alginate gel when these dressings come in contact of the wound fluid. Thus, these dressings maintain moisture at the wound site. These dressings also possess the properties like water vapour transmission, painless removal and non-permeability to bacteria. These can be applied on low to heavy exudate wounds. Sorbsan™, Curasorb™, Kaltostat™, Algisite™, etc are some commercially available alginate dressings. The major drawbacks associated with the alginate dressings are need of secondary dressings and gel formation only in the presence of fluid which limit their use for dry wounds, and third degree burn wounds[8].

Bioactive dressings are biomaterial (natural or synthetic) based dressings and possess properties like biocompatibility, non-toxicity, biodegradability. The synthetic materials used for their synthesis are chitosan, collagen, hyaluronic acid, elastin etc. Sometimes growth factors and antimicrobials have also been incorporated into these dressings to enhance the wound healing process.

Hydrogel dressings[70] can be suggested as a promising candidate for covering wounds especially where moist environment is required. Owing to their tendency of providing moisture, they can be used for dry wounds. At the same time, these dressings absorb the extra exudate, if any, from the wound site. These dressings not only hydrate the wound, but also re-hydrate scar and cause autolytic debridement. These generate soothing and cooling effect which is more valuable in case of burn wounds. Although weak mechanical strength in wet conditions and need of secondary dressings are the disadvantages associated with hydrogel dressings.

2.2 Hydrogels

Hydrogels, the three dimensional, crossed-linked network polymers made up of hydrophilic materials, have good water swelling ability (some of them can soak up as much as 500 times their weight in water), biodegradability, non-carcinogenicity and biocompatibility[71]. Their swelling ability is mainly due to the presence of hydrophilic groups such as –COOH, $-SO_3H$, $-NH_2$, -OH. They can be formulated into different forms such as slabs, films, coatings, nanoparticles, nanofibers etc. These are composed of homo-polymers or co-polymers, and are immiscible with water due to the presence of chemical cross-links (tie-points, junctions), or physical cross-links, such as entanglements or crystallites. The monomer used for the preparation of hydrogels may be natural or synthetic or a combination of both. These resemble in their physical properties with living tissue because of their relatively high water content and soft, rubbery consistency. Owing to their unique properties, hydrogels are widely used in the medical pharmaceutical and related fields such as tissue engineering[72], cell culture, wound dressings, contact lenses[75], artificial organs, barriers (to regulate biological adhesion), super absorbent and drug delivery systems[67].

The term hydrogel was first introduced by Bemmelen[73,74] whereas Wichterle et al.[75] were the first who prepared hydrogel of hydrophilic networks of PHEMA for making contact lenses. Afterwards several hydrogel systems have been developed. In recent years, particular interest has been devoted to the hydrogels showing phase transitions (i.e. volume change) in response to changes in external conditions such as pH, ionic strength, temperature, electric currents etc[76,77]. Such hydrogels have been termed as smart or intelligent gels. Some hydrogels are more common than the others towards a particular response.

2.2.1 *Important Features of Hydrogels*

Some of the features which make hydrogels unique materials for wound dressing applications are as follows:

(i) pH responsiveness

The hydrogels of PAAm, PAAc, PMAAc, PDMAEMA, PDEAEMA are generally pH responsive. Besides some phosphoric acid derivative containing hydrogels are also pH responsive. The pH responsiveness of these hydrogels is because of the presence of hanging ionisable acidic (like –COOH, $-SO_3H$) or basic (like NH_4^+) groups. These groups have the ability to gain or loss proton(s) from the environment. In basic environment, the acidic groups ionise and repel each other by similar charges. This strong electrostatic repulsion allows the penetration of polar solvent (or water) inside the polymer resulting in excessive swelling of the hydrogel. However, in acidic medium, these groups protonate resulting in reduced charge density and hence, collapsing polymeric chains. Due to which swelling reduces. The hydrogel containing basic groups ionise in acidic medium and hence, exhibit a reverse behaviour of the hydrogel containing acidic groups.

Figure2.1 Hydrogel Containing Acidic Hanging Groups

Figure 2.2 Hydrogel Containing Basic Hanging Groups

A hydrogel system containing acidic as well as basic hanging groups exhibits a two phase transition in acidic and basic medium rather than neural medium[78].

The efficiency of a hydrogel towards a response can be controlled by fine tuning the monomer concentration, monomer type, cross-link density, and pendent groups. A more expressive stimulus results in a highly substantial response.

(ii) Swelling behaviour of hydrogels

Hydrogels are porous materials and swelling is their one of the most studied properties[79,80]. It is related with the tendency of the hydrogels to hold water or any other biological fluids into their structures. When water (or solvent) enters into a dry hydrogel system, it first hydrates the most hydrophilic groups, and is known as the primary bound water. After that it gets attached with the hydrophobic group forming hydrophobically bound water, also known as the secondary bound water. The primary and secondary bound water collectively form the total bound water. After the

interaction of water with the hydrophilic and hydrophobic groups, the water imbibes into the gel matrix by the osmotic driving forces up to the infinite dilution. However existence of physical forces such as hydrogen bonding, opposed the additional swelling of the gel matrix. This additional water, after the saturation of hydrophilic and hydrophobic groups with water, is called free or bulk water. This water is assumed to be filled in the space present in between the polymeric chains and/or in the centre of voids and pores. Thus, the swelling ability of a hydrogel system is related with the presence of hydrophilic groups as well as the space present in between the polymeric chains i.e. pore size which in turn depends upon the nature and composition of monomers as well as cross-linker. Moreover, nature, composition, pH, temperature and ionic strength of the solvent or dissolution medium also affect the solubility of a hydrogel system.

Hydrogel swelling is governed by two factors: osmotic factor and counter elastic factor. The latter controls the stretching of polymeric matrix and hence, prevents its stretching. When these two forces counterbalance each other, the state of equilibrium is achieved i.e., equilibrium swelling is achieved. After achieving this stage there occurs no further swelling or deformation in the structure of hydrogel[81].

In case of degradable polymer chains or cross-links, the gel matrix disintegrates and dissolves at a rate dependent upon the composition of gel matrix[72].

The relative amount of total free and bound water present in a hydrogel matrix can be determined by DSC, NMR, and/or use of molecular probes. By using DSC technique, the relative amounts are calculated by assuming that only free water freezes, so the endothermic peak predicted while warming the sample is due to melting of free water and hence gives the amount of free water present in the water

sample. The amount of bound water can be predicted by subtracting the amount of free water from the total water content present in the hydrogel sample.

The water imbibing capacity of hydrogels also determines the permeation of nutrients in and movement of cellular matrix out of the cell. Hydrogels, owing to their porous structure, allow the loading of drugs or nutrients and their subsequent release. Porosity of hydrogels is an important physicochemical parameter, on the basis of which the hydrogels can be classified as non-porous, micro-porous, macro-porous, and super-porous [81]. In case of non-porous hydrogels, the pore size is below 100Å. It means that they contain mainly bound water and swelling is mainly governed by diffusion through free volume. For micro-porous hydrogels, the pore size varies from 100 -1000Å showing the presence of major amount of bound water and the swelling is governed by molecular diffusion as well as convention in the solvent containing pores. Macro-porous hydrogels have pore size greater than 1000Å and also contain a major fraction as bound water. Their swelling is governed by diffusion and is faster than micro-porous hydrogels. The pore size in case of super-porous hydrogels (SPHs) usually lies in the range of several micrometres. These hydrogels mainly contain free water and their swelling is due to capillary action. They exhibit very fast swelling which does not depend upon the size of the sample.

The porous network of the hydrogels can be tuned by controlling the cross-link density in between the polymeric network and affinity towards the aqueous media.

Swelling Kinetics

The discussion of hydrogels is not complete without describing the various mathematical models and equations of swelling kinetics. Various mathematical models have been proposed to describe the swelling kinetics of hydrogels. These

models quantitatively interpret the swelling data in terms of kinetic parameters[82]. According to the classification proposed by Bajpai[83], the movement of penetrant (solvent) into the hydrogel matrix follows one of the following mechanism:

(i) When the hydrogel matrix has high flexibility, the penetrant easily penetrates into the gel matrix or the rate of hydrogel matrix relaxation is much faster than the rate of diffusion of the penetrant. This is the case of Fickian diffusion or case-I transport.

(ii) When the hydrogel matrix is somewhat less mobile, the rate of hydrogel matrix relaxation becomes approximately equal to the rate of diffusion of the penetrant. This is the case of anomalous transport.

(iii) When the hydrogel matrix is very less mobile, it does not allow the urgent penetration of penetrant into the gel matrix or the rate of hydrogel matrix relaxation is much slower than the rate of diffusion of the penetrant. This is the case of non-Fickian diffusion or case - II transport. In this case, the swelling varies directly with time. Many researchers observed non-Fickian diffusion of the solvent into the gel matrix[41,84,85].

Korsermeyer–Peppas model[86] was the most widely used model showing the swelling kinetics of a hydrogel system. The empirical equation for this model is

$$\frac{M_t}{M_\infty} = kt^n$$

Where n is the swelling exponent exhibiting mode of movement of penetrate and k is the constant for the hydrogel, t is the time taken for swelling. While using this equation only one dimensional movement is considered. A hydrogel film having the value of $n \leq 0.5$ corresponds to Fickian diffusion, that having value $0.5 < n < 1$

corresponds to anomalous or non – Fickian transport and that having value ≥ 1 corresponds to case - II transport[86,87].

Zero-order kinetics model indicates a slower rate of penetration. A first-order kinetic model shows that the swelling varies directly with the water content present in the hydrogel before achieving the state of equilibrium, whereas the second-order kinetic model shows the variation of swelling with the square of water content present in the composite before achieving equilibrium.

(iii) Drug loading and releasing capacity

In the past few decades, the pharmaceutical research has mainly focused on the development of novel drug and the systems for administrating the drug, especially at a specific target. The unique physical properties of hydrogels have sparked particular interest in their use for drug delivery applications. The porous network of hydrogel allows loading of drug into its matrix and also its subsequent release at a rate dependent upon the diffusion coefficient of micro or macro molecules through the hydrogel matrix[68] or in other words, hydrogels have the property of sustained drug release. Hydrogels are known to reduce the problems of conventional dosage forms as well as of the novel drug delivery systems for which a biocompatible, convenient and stable drug delivery system is required to hold and release molecules as small as NSAIDs (Non-steroidal anti-inflammatory drugs) or as large as proteins and peptides[88]. Their porous network can easily be tuned by controlling the cross-link density in the gel matrix and the affinity of the hydrogels towards aqueous media in which they are swollen.

The hydrogel based drug delivery systems are usually pharmacokinetic but they may be sustained also. The drug or antimicrobial agents can be incorporated into a hydrogel system using one of the following methods:

(i) Blending of drug with the dope solution before subjecting to electrospinning,

(ii) Encapsulating the drug before mixing the solutions,

(iii) Attachment of the drug molecules with the fibre surface,

(iv) Post treatment of sample with the drug to load drug in to it.

Out of these the last one is supposed to be more effective because the chances of interaction between the drug and hydrogel system are less.

Dressings showing controlled and sustained drug release, exhibit continuous antimicrobial behaviour and reduces the chances of adverse effect. Drug release is governed by swelling, degradation, diffusion, affinity based mechanism. Drug release from a hydrogel system depends upon the pore size, pore volume fraction, interconnection of pores, and cross-link density. Type and strength of interaction of drug with the polymer chain also affects its release profile from the hydrogel system.

Recently a considerable progress has been observed to overcome the clinical and pharmacological challenges of hydrogel based drug delivery systems.

Drug Release Kinetics

Korsermeyer–Peppas model[86] also indicates the drug release profile of a hydrogel system. However, this model is applicable only for analysing initial data of drug release (near about 60% release). For analysing the data beyond this limit, other models like zero-order, first-order, second-order, Higuchi-model are used[89].

Zero-order kinetics model indicates a slow drug release profile due to no disaggregation of the hydrogels[90]. A first-order kinetics model indicates the direct variation of drug release (water soluble) from the matrix with the amount of drug

remaining in the hydrogel matrix[81,91]. When the drug molecules dispersed in a uniform matrix act as the dispersing medium, Higuchi model is used to describe it.

Therefore, the mathematical model, development of which needs the comprehension of all the phenomenon affecting drug release kinetics, is of great importance for the process optimization of controlled release formulation[82,92].

2.3 Different Forms of Hydrogels

Hydrogels can be prepared from any hydrophilic polymers, which differ in their chemical compositions and bulk physical properties. Furthermore, they can be formulated into various physical forms like slabs, coatings, films, micro particles, and nanoparticles. In general, the hydrophilic materials used for the development of a hydrogel are polyvinyl alcohol, polyacrylic acid, polyacrylamides, polyethylene oxide, or polyvinyl pyrrolidone etc[70,93].

2.3.1 *Hydrogel Films*

The hydrogels may be formed in the form of films by spreading their semi-solid form over a disc or plate before drying them. These films can hold more than 90% of water, thus they possess properties such as high biocompatibility, swelling ability, water holding capacity and rubbery consistency just like natural tissues.

Xie et al.[94] developed a non-cytotoxic biodegradable hydrogel system of PEGMC and PEGDA, which was able to take the wound shape and hence, covered the wound completely to protect it from bacterial invasion. This system offered excellent bacterial inhibition and enhanced wound healing.

Lian et al.[95] prepared carboxylated PVA through free radical solution polymerization of VAc and AAc followed by saponification and reported that with

increase in AAc content, storage modulus and mechanical strength decreases, due to which physical cross-link density decreases and the network structure becomes looser. The swelling rate constant and equilibrium swelling ratio are greatly improved by the addition of AAc onto PVA chains. However, this hydrogel system follows Higuchi model for drug release.

PAAm hydrogels can absorb relatively high amounts of water; however their swelling capacity is not very sensitive to pH or electrolytes[63]. On the other hand, hydrogel of acrylic acid possesses pH sensitivity but less water holding capacity. Moreover its gel also exhibits inferior gel strength, dispersion and elastic properties in aqueous media[21]. Presence of pendant –COOH groups and structural similarity with acrylamide makes acrylic acid a potent candidate for copolymerisation with acrylamide and making it pH-sensitive.

Bajpai et al.[22] prepared a pH respondent hydrogel system using acrylamide, methacrylamide and acrylic acid. Acrylamide and acrylic acid owing to their high water affinity and copolymerisation velocity were then chosen as the base materials for making hydrogels. Studies showed that hydrogel of the copolymer of poly (acrylamide-co-acrylic acid) have high water absorption tendency.

Solpan et al.[85] developed pH and temperature sensitive hydrogel of poly (acrylamide-co-acrylic acid) using irradiation technique and observed a high swelling (3000%) with increasing AAm concentration. They also predicted non-Fickian nature of swelling. This property suggested use of hydrogel for absorbing exudates from the wound.

Chavda et al.[24] prepared a composite of poly (acrylamide-co-acrylic acid) hydrogel and characterized its properties but they focused mainly on mechanical properties like density, tensile strength and swelling behaviour. They observed that the

tensile strength of the composite is much higher whereas its density and swelling ratio are low. Thus, they suggested the need of optimization of swelling ratio with tensile strength.

Li et al.[96] reported that the pK_a of the copolymer of acrylamide and acrylic acid is ~4.5 and the equilibrium swelling ratio was 120 at pH lower than 6.0 with an ionic strength, equivalent to 0.01M NaCl and 265 at low ionic strengths. They studied the material binding property of the hydrogel for the adsorption of metal ion.

Turan et al.[97] studied the effect of amount of acrylic acid in the composite material and reported that as the acrylic acid content increases, the porosity and hydrophilicity of the material increases resulting in increased response rate. Further, rate of de-swelling increases as pH goes down from 9.0 to 2.0. This is because of the disappearance of electrostatic repulsion generating hydrophobic interaction between the carboxylic and amide group.

Nesrinne et al.[34] also reported the pH sensitivity of poly (acrylamide- co-acrylic acid) hydrogels and different swelling ratio in different media. They suggested that the copolymer shows a slower saturation as compared to polyacrylamide sample, due to which their level of swelling is much higher. Further if some electrolyte is also present exo-osmosis takes place and hence, the hydrogels do not swell. Along with the characterization, they also studied the rheological behaviour and observed an increase in rigidity with increase in the amount of PAAc.

Katime et al.[41] loaded the hydrogel of acrylamide and acrylic acid with theophylline and reported that as the cross-linking increases, the rate of release of theophylline decreases. Further the release follows non-Fickian diffusion mechanism because the value of release index, *n* in each case is found to be greater than 0.5. A

similar study is done by Thakur et al.[40] when they loaded the hydrogel with gentamicin sulphate and reported release through Fickian diffusion mechanism i.e. the value of *n* here is less than 0.5. Ritger et al.[86] suggested that dimensionality index is necessary for giving an idea about drug release mechanism.

From the literature, it is clear that hydrogel system of poly (acrylamide-co-acrylic acid) is a pH and temperature responsive superabsorbent system. Some of this system studied so far along with its application is shown in the following table:

Table 2.1: Different Applications of Poly (acrylamide-co-acrylic acid) System

Sl. No.	Monomers	Redox Initiators	Cross-linker	Applications	Reference
1.	AAm & AAc	APS-TEMED	MBAAm	-------	[97]
2.	AAm & AAc	APS-TEMED	MBAAm	Gentamicin sulphate	[40]
3.	AAm & AAc	Controlled hydrolysis of AAm	MBAAm	Cu & Cd metal binding	[96]
4.	AAm & AAc	Potassium peroxo disulphate	MBAAm	Theophylline release	[41, 78]
5.	AAm & AAc	APS & sodium metabisulphite	MBAAm	Cu ion capture	[98]
6.	AAm & AAc	APS/TEMED	MBAAm	BSA release	[39]
7.	AAm & AAc	APS/TEMED	MBAAm	Ascorbic acid release	[90]
8.	AAm & AAc	APS/TEMED	MBAAm	5-FU drug release	[43]

Literature also suggested that the poly (acrylamide-co-acrylic acid) hydrogel were mainly prepared by using methylene bisacrylamide as the cross-linker. Moreover, all these have weak mechanical strength in wet conditions.

2.3.2 *Composite Hydrogels*

From the above literature, it is clear that hydrogels possess high swelling ability, biodegradability, non-carcinogenicity and biocompatibility but have low mechanical strength in wet conditions. A solution to this problem at that time was supposed to be the conversion of hydrogel film into composite membranes, where the hydrogel is coated (grafted) over a textile material. The fabric reinforcement enhances the strength of the hydrogel and the drug loaded hydrogel offer precise control of the release behaviour[99]. In these composite membranes, the layer which makes the physical contact with the wound surface is referred to as primary layer or base layer while that which covers the primary layer is called secondary or top layer. Different hydrogel systems have been grafted over various supports like cellulose[101,105], cotton[104], PET[103,114], PP[111,112] etc., using different cross-linking techniques. The grafting reaction was initiated by employing methods like chemical initiator[27], photo-irradiation[107], high energy radiation techniques[100, 106] etc.

Borbely et al.[101] grafted cellulose pulp with vinyl acetate monomer using ceric ion redox system as initiator to enhance the mechanical strength of hydrogel and optimized the conditions favourable for maximum grafting introduced a grafting technique. This technique can also be implied for grafting any hydrogel over a fabric. The above studies were also supported by J. Chen et al.[102]. They used plasma induced graft polymerization method for the grafting of PNIPAAm over non-woven fabrics, but the point of difference was that here the substrate was activated by using

radiations either in the presence or absence of monomer while in former case it was done using chemicals (chemical grafting), which being cheaper, is more advantageous. They also analysed the blood compatibility of the grafted material and predicted that it has been improved, related to platelet adhesion, plasma protein adsorption and thrombus.

Pour et al.[103] developed PAAm hydrogel on the surface of PET in well controlled manner and found that PAAm hydrogel-g-PET shows low adhesion to skin i.e. keratinocyte cells. They also predicted a good antimicrobial activity of the grafted material towards multidrug-resistant *Pseudomonas aeruginosa* when loaded with silver nanoparticles.

Mostafa[104] grafted MAAm onto the cotton yarn using potassium permanganate / nitric acid as initiator to enhance the tensile strength and observed increased tensile strength up to a certain grafting yield and then further reduction.

Khullar et al.[105] grafted acrylonitrile on cellulose derivative, obtained from Bamboo using chemical initiator CAN and observed that water retention value of the grafted material was less, showing its more hydrophobicity. Afterwards several attempts had been made for the grafting of different hydrogels over different supports.

A short description of some of the fabric supported hydrogel system is given in Table 2.2.

Table 2.2: Fabric Supported Hydrogel Systems

Fabric	Hydrogel	Technique used	Reference
Cotton	NIPAAm	Pre-irradiation	[106]
Cotton	NIPAAm	Photo-induced	[107]
Cotton	Methacrylamide	Chemical-induced	[104]
Cotton	NIPAAm/Chitosan	Plasma-induced	[108]
Cotton	AAm-co-itaconic acid	Chemical-induced	[27]
Chitosan	AAc/HEMA	Radiation-induced	[109]
Chitosan	NIPAAm	Plasma-induced	[102]
Chitosan	PU/NIPAAm	UV Radiation-induced	[110]
PP	NIPAAm/AAc	Radiation-induced	[111]
PP	Methylmethacrylamide	Radiation-induced	[112]
PP+PET	NIPAAm	Photo-induced	[113]
PET	NIPAAm/AAc	Radiation	[114]

Hydrogel of poly (acrylamide-co-acrylic acid) was studied for the release of various drugs and was suggested as a good drug delivery device, but no literature was observed showing an insight on the improvement of their mechanical strength in wet situation. An initial work of grafting of poly (acrylamide-co-acrylic acid) hydrogel system over the surface of cotton fabric using a chemical cross-linker was performed by Purwar et al.[26] Moreover, the use of a hydrophilic biodegradable cross-linker to this system was also first time reported by them.

2.4 Hydrogel Dressings

Hydrogels fulfils most of the desirable requirements of an ideal wound dressing such as they promote moist healing, they are non-adherent and provide cooling and soothing effect to the surface of the wound, which may have a marked reduction in pain and therefore, have high patient acceptability[71,115]. Hydrogels are biocompatible materials, so they have been recognized to function as drug protectors, especially in case of peptides and proteins, from *in vivo* environment i.e., they exhibit very low tendency to adsorb proteins from body fluids because of their low interfacial tension. Chauhan et al.[93] predicted that hydrogels meet with the two basic needs of drug delivery systems i.e., they release drug in predetermined rate and at the site of wound directly because of their three dimensional network structure. Further, they are biocompatible and biodegradable with minimum tendency of protein absorption and any kind of material can diffuse into and out of it. They are sensitive towards external stimuli like pH, temperature etc., and hence, are called intelligent gels. All of the above properties make hydrogel a good material for wound dressings.

Several hydrogel dressings are also available in the market. Some of the common dressings along with their advantages and disadvantages are shown below:

Table 2.3: Available Hydrogel Dressings with their Applications

Hydrogel Dressings	Manufactured by	Components	Applications	Ref.
Aquaderm™	DermaRite industries	2-Acrylamido-2 methyl-1-propanesulfonic acid sodium, Propylene Glycol, Poly (ethylene glycol) dimethacrylate, 2-Hydroxy-2-methylpropiophenone	Pressure ulcers Minor Burns	116
DermaSyn®	DermaRite industries	Acrylate polymer	Acute or chronic partial and full thickness wounds Ulcers,	117
Suprasorb®	Lohmann &Rauscher	Acrylic polymers, polyethylene, phenoxyethanol	Dry Wound, first and second degree burn wounds, Pressure ulcers.	74
Neoheal®	Kikgel	PEG, polyvinylopyrrolidone, and agar	Some chronic wounds Ulcers, abrasions, burns, bed sores	118
Simpurity™	Safe n'Simple	polyethylene oxide, polyvinyl alcohol, acrylate, polyurethane,	Dry wounds, skin burns and dry scab	74
Intrasite Gel	Smith and Nephew	Carboxymethyl cellulose and propylene glycol.	Pressure ulcers, Diabetic foot ulcers Surgical incisions	74
Restore Hydrogel	Hollister Incorporated	Hydrogel impregnated gauze pad contains hyaluraonic acid	Partial and full thickness wound	74
Solosite gel	Smith and Nephew	sodium salt of carboxymethyl cellulose and glycerol	skin tears, Venous ulcers, Surgical incisions, Diabetic foot ulcers, Pressure ulcers,cuts	74
Woun'Dres®	Coloplast	Carbomer and collagen with other	Dry wounds	74
Geliperm	Geistlich Sons Ltd	Polyacrylamide, polysaccharide, agar	skin and tissue loss, chronic, acute wounds, superficial pressure sores. Low acoustic impedance.	119

The main disadvantages associated with these dressings are their weak mechanical strength in wet conditions and need of secondary dressings to keep them in their place, which limit their use in this field.

2.5 Nanofibers

Nanofibers are the fibres having diameter in the nanometre or micrometre range. Unique properties like high surface area to volume ratio, easy surface functionalization and tuneable porosity opens the doors for applications of nanofibers in numerous fields, especially for biomedical applications such as wound dressings, tissue engineering, antibacterial mats, drug delivery system. Several techniques are available for the spinning of a polymer dope solution into nanofibrous form such as solution blowing[129], electrospinning[48] etc. Out of the various techniques electrospinning being simple, cost effective and versatile, appealed the material scientists globally.

A typical electrospinning machine is a combination of high voltage power supply unit, spinneret, and collector. The fibre morphology can be controlled by modifying the units of the apparatus as well as the concentration and viscosity of the dope solution. Nanofibrous mats resemble with the extracellular matrix and hence, help in promoting proliferation and cell migration phases leading to rapid wound healing. Thus, they may be supposed to be a material for the use as wound dressing applications. The main problem associated with most of the nanofibers was their easy deformation in wet conditions. To overcome this problem the concept of development of nanofibers-hydrogel composite was introduced.

2.5.1 *Nanofibers-Hydrogel Composite*

If nanofibers are incorporated into hydrogel, they may result in hydrogels composite having improved mechanical properties[120,121,122]. Further incorporation of nanofibers may also potentially enhance the cell activity in the resultant composite. Hydrogels are usually prepared from a solution state, so the constructed nanofibers can be easily unravelled (by manual tearing or cutting of the membrane) and mixed with their solution[123]. The nanofibers can also be incorporated in to a hydrogel system by layer by layer assembly. The hybrid nanofibers and the three dimensional hydrogel can be prepared by simultaneous electrospinning and electrospraying of hydrogel[120,124]. Researchers have reported the incorporation of nanofibrous membrane or yarn into hydrogel blocks in their chopped state[120,122].

Anderson et al.[125] used electrospun polycaprolactone as scaffold for supporting the vertical stability of standing swollen hydrogel that surrounds micro fabricated sensor hairs. Focusing ring was used to concentrate electrospun polycaprolactone fibres such that it rest vertically on the sensor hairs before the hydrogel was added over it.

Mo et al.[126] electrospun p(LLA-CL) into nanofibrous form and then mixed it (in chopped state) with the collagen solution in 1:1 ratio. The storage modulus of this hydrogel-nanofibers composite was found to be very high as compared to that of hydrogel of pure collagen.

The nanofibers can also be encapsulated within hydrogel network without further modifications to prepare the nanofibers-hydrogel composite. Because of the hydrophilic nature of the hydrogels, the nanofibers used should also be hydrophilic so that the hydrogel solution integrates completely within the pores of the nanofibers.

A major drawback associated with the hydrogels was that they generally do not affect direction of cell growth. Electrospun scaffolds in contrast are able to orient cells through contact guidance when the fibres are aligned. An advantage of the nanofibers-hydrogel composite was that cells can be easily encapsulated within the hydrogel before attaching with the nanofibers.

2.5.2 *Hydrogel Nanofibers*

Hydrogel nanofibers possess the properties of both hydrogels and nanofibers. Like hydrogels they exhibit sustained swelling in aqueous media and like nanofibers they possess very high surface area and diameter in the submicron range. Owing to biocompatibility and a faster response rate as compared to other hydrogel structures such as slab, disc, rod, film, hydrogel nanofibers have enhanced applications in the field of drug delivery, wound dressing, tissue engineering etc. Three dimensional cross-linked structure of hydrogels make them insoluble in water or any other medium and non-fusible. So their direct electrospinning is not possible. They are converted into nanofibrous form using specific methods such as photo-induced cross-linking polymerisation, hydrolysis reaction, heat induced esterification etc. Among these techniques the last one i.e. heat induced esterification being simple was widely used. Liu et al.[127] prepared the hydrogel nanofibers of poly [acrylamide-co-(maleic acid)] using this technique.

The idea of conversion of hydrogel into nanofibrous form was first incorporated in 2002 by Ding et al.[55]. They prepared the nanofibers of PVA hydrogel using electrospinning technique and glyoxal as a cross-linker. However, the nanofibers formed have beaded structure. The cross-linked nanofibers were insoluble

in water and possessed a good mechanical strength than the non-cross-linked nanofibers in wet condition.

Xie et al.[128], in 2003, prepared the nanofibers of PEO and PVA using chemical cross-linker 4,4'-methylenebis(phenyl diisocyanate) to enhance catalytic activity of lipase enzyme.

Xu et al.[129] developed the hydrogel nanofibers of Chitosan / PLA / PEG cross-linked with glutaraldehyde, using solution blowing method for wound dressing application. They studied the properties like swelling, air permeability and antimicrobial activity.

Afterwards hydrogel nanofibers of poly (styrene-co-maleic anhydride)[48], poly (styrene-co-maleic sodium anhydride) / cellulose[49], multiblock poly ester urethane[32], PVA / Hyaluronic acid[50], PVA / PAAc / MWCNT[51], chitosan-g-PNIPAAM / PEO[52], polyaspartic acid[46], poly (vinyl caprolactam-co-hydroxymethyl acrylamide)[53] and polyvinylpyrrolidone[54], have been prepared and explored for tissue engineering and biomedical applications. Out of these, hydrogel nanofibers of polyester urethane were thermo-responsive[32].

Some of them along with the cross-linking techniques used and applications are tabulated below:

Table 2.4: Some Hydrogel Nanofibers and Their Applications

Hydrogel Nanofibers	**Cross-linker**	**Application**	**Reference**
Poly(2-hydroxyethyl methacrylate)	Photoinduced	Enzyme and cell immobilization	[130]
Poly(styrene-co-maleic anhydride)	Diethylene glycol	--	[48]
Poly(acrylamide-co-maleic acid)	Diethylene glycol	--	[127]
Poly (vinyl alcohol)	Glutaraldehyde	Hyaluronic acid	[50]
Poly (styrene-co-maleic sodium anhydride)/cellulose	Diethylene glycol	---	[49]
PVA/PAA/MWCNT	Glutaraldehyde	Ketoprofen release	[51]
Chitosan-g-PNIPAAM/PEO	3-mercaptopropanoic acid	BSA release	[52]
Poly aspartic acid	Ethylene diamine	----	[46]
Chitosan/PLA/PEG	Glutaraldehyde	------	[129]
PNIPAAM/PAA	PVA or Na_2HPO_4	-----	[45]

Literature suggested that hydrogel system of poly (acrylamide-co-acrylic acid) has not been electrospun till date although this hydrogel system was found to be a superabsorbent system and studied widely for the release of various nutrients/drugs.

CHAPTER 3

EXPERIMENTAL WORK

In this chapter, an insight have been provided on the materials and methods used in the research work. An idea about the various techniques used to characterise the samples prepared has also been given. Here, the various methods and formulae used to predict the swelling and drug release behaviour of the samples developed have also been discussed.

3.1 Materials

Acrylic acid (AAc), N, N'-Methylene bisacrylamide (MBAAm) and Ammonium per sulphate (APS) were purchased from Central drug house (Delhi, India), Acrylamide (AAm) of reagent grade was bought from Sisco Research Laboratories (Mumbai, India), Polyethylene glycol (PEG-6000) from LOBA CHEMI (Mumbai, India), Potassium dihydrogen phosphate, Ortho- phthalaldehyde, Methanol, Mercaptoethanol, 2-propanol, Borax, Sodium hydroxide were procured from Sigma Aldrich, Gentamicin sulphate and Amoxicillin were purchased from HIMEDIA Laboratories Pvt (India) Ltd, Cotton fabric ($139gm^{-2}$), Distilled water was used to carry out all the experiments.

3.2 Methods of Preparation

3.2.1 *Preparation of Hydrogel Composite using PEG as Cross-linker*

The hydrogel composite using PEG as cross-linker was prepared in the following steps:

(i) Active sites generation

Washed, dried and weighed cotton fabric of 3×3 cm^2 was immersed in APS initiator solutions of the concentrations 1% to 7% (w/V) to generate active sites over the surface of cotton fabric. The fabric treatment temperature was varied from 30°C to 60°C and its time was varied from 15minutes to 45minutes.

(ii) Grafting of copolymer over the activated fabric

The activated fabric was graft copolymerized by varying the concentration of the monomers i.e., AAc and AAm from 5% to 15% (w/V). The reaction time was varied from 15minutes to 55minutes and the reaction temperature was varied from 30°C to 60°C.

(iii) Insertion of cross-links

After graft copolymerization, PEG [0.05 to 1% (w/w) w.r.t weight of the monomer] was added to convert the graft copolymer into hydrogel form by inserting cross-links. The reaction was carried out for 10minutes to 30minutes.

In terms of grafting yield the following reaction parameters were optimized: -

1. Monomer concentration,
2. Reaction time,
3. Reaction temperature,
4. Initiator concentration,
5. Initiator treatment time and temperature,
6. Cross-linker concentration.

The cross-linker concentration was also optimised in terms of percentage swelling.

Schematic diagram for the development of hydrogel composite using PEG as cross-linker is shown in Figure 3.1.

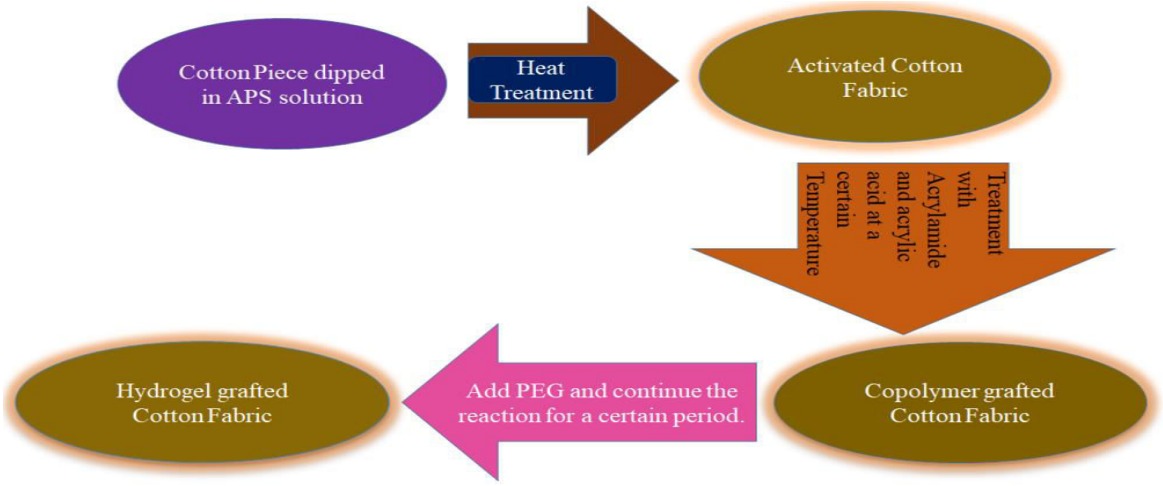

Figure 3.1 Schematic Diagram Showing Development of Hydrogel Composite using PEG

3.2.2 *Preparation of Hydrogel Composite using MBAAm as Cross-linker*

The hydrogel composite using MBAAm as cross-linker was also developed by a three-step process. In the first step, a 3×3cm^2 sample of the support, i.e., cotton fabric, was activated by treating it with an initiator, APS. The concentration of the initiator was varied from 1% to 7% (w/V) and the treatment temperature and treatment time were varied from 30°C to 60°C and 15minutes to 45minutes respectively. The activated substrate was then treated with monomers [AAc and AAm] by varying the net concentration from 5%-17% (w/V), temperature from 30°C to 60°C and time from 15minutes to 55minutes to graft a layer of their copolymer over the surface of the substrate. Further cross-linker MBAAm [0.05% to 1% (w/w)] was added, and the reaction was continued to induce cross-links in the grafted copolymer. The cross-linking reaction time was varied from 10minutes to 30minutes. The reaction parameters were optimised in terms of grafting yield.

Schematic diagram for development of hydrogel composite using MBAAm as cross-linker is shown in Figure 3.2.

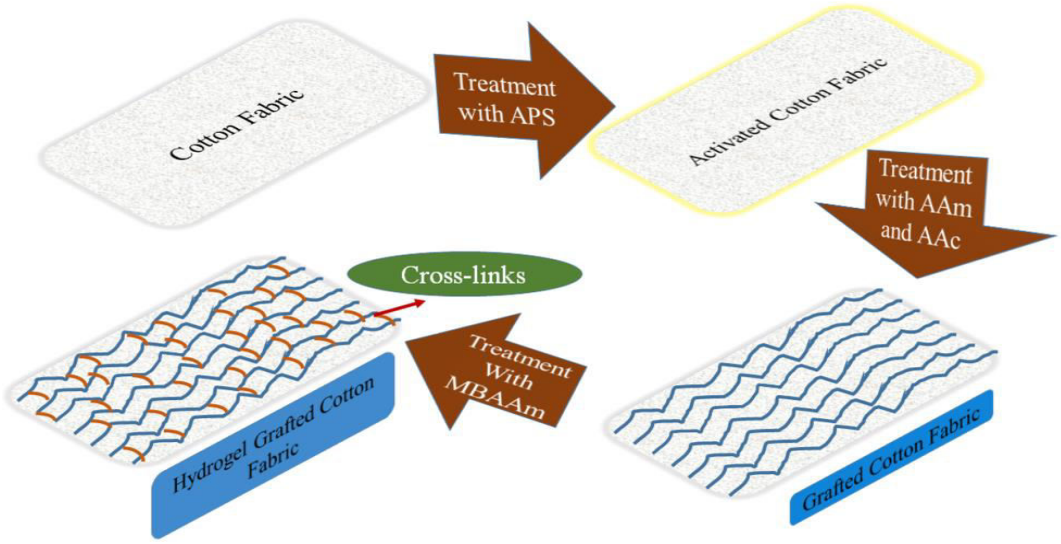

Figure 3.2 Schematic Diagram Showing Development of Hydrogel Composite using MBAAm

3.2.3 *Preparation of poly (acrylamide-co-acrylic acid) Hydrogel Nanofibers*

The poly (acrylamide-co-acrylic acid) hydrogel nanofibers were prepared via the following two steps:

(i) Development of copolymer of poly (acrylamide-co-acrylic acid)

Copolymer of poly (acrylamide-co-acrylic acid) was developed using solution polymerisation method. In a 1M aqueous solution of AAm, a 10ml mixture of 0.1mole AAc and 0.076g APS was added drop wise with constant stirring. The reaction was carried out for about 3h at a temperature of 70°C. The copolymer precipitated out and was washed with a methanol water mixture of ratio 1:1. The copolymer was filtered and kept in a vacuum oven at 60°C for about 10h to make it moisture free.

(ii) Development of hydrogel nanofibrous mat

The dope solution for electrospinning was prepared by dissolving poly (acrylamide-co-acrylic acid) copolymer [8% (w/V)] in distilled water with continuous stirring at room temperature. PEG (2% w/w) was added in the dope solution. The copolymer dope solution was electrospun using a voltage of 23kV, tip to collector distance of 15cm and feed rate of 3.5–4μLmin^{-1} on a drum collector. Cotton fabric is used for collecting the nanofibrous mats. The nanofibrous mats were converted into hydrogel form by placing it in an oven at 150°C for 10minutes and the obtained hydrogel nanofibrous mats were dried in a vacuum oven at 80°C for 10h to 12h.

Schematic diagram for development of hydrogel nanofibrous mats is shown in Figure 3.3.

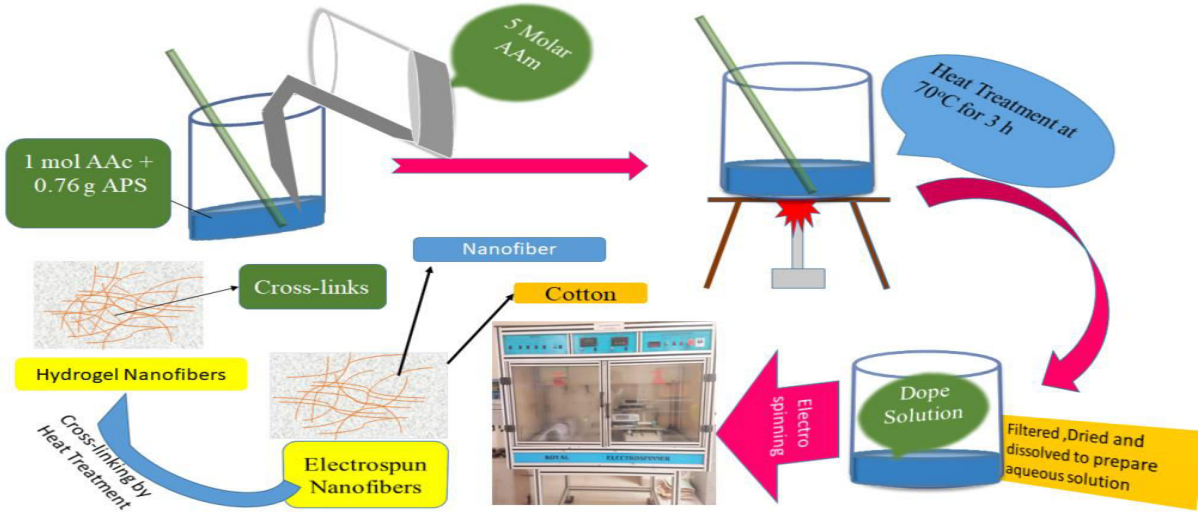

Figure 3.3 Schematic Diagram Showing Development of Hydrogel Nanofibrous Mats

3.3 Grafting Yield

The conditions for composite preparation were optimized by plotting grafting yield obtained by varying a single parameter fixing the others as constant. Grafting yield of dried and weighed poly (acrylamide-co-acrylic acid) hydrogel grafted cotton fabric was calculated using the formula

$$Grafting\ yield = \frac{w_g - w_d}{w_d} \times 100 \quad \text{---------- (1)}$$

Where w_g = Weight of grafted material, w_d = Weight of fabric before grafting

3.4 Characterisation

The following techniques were utilized to characterize the hydrogel grafted cotton fabric (composite) and hydrogel nanofibers –

3.4.1 *Fourier Transformed Infrared Spectroscopy (FTIR)*

Thermo-scientific Nicolet 380 spectrophotometer, USA, in ATIR mode was used for the structural analysis of the hydrogel composites prepared by using PEG or MBAAm and poly (acrylamide-co-acrylic acid) hydrogel nanofibers. The scanning was performed setting frequency range 500- 4000cm^{-1} and a resolution of 4cm^{-1}.

3.4.2 *Scanning Electron Microscopy (SEM)*

Morphologies of hydrogel composite samples and poly (acrylamide-co-acrylic acid) hydrogel nanofibers were studied using SEM (model no. S-3700N, Hitachi, Germany). Before mounting in SEM, the samples were made conductor of electricity by gold-sputter coating and then fastened using adhesive tape in the sample stage.

Diameter distribution of the hydrogel nanofibers was obtained by analysing the SEM images for 50 fibres using J-image software.

3.4.3 *Thermo Gravimetric Analysis (TGA)*

The thermal properties of the poly (acrylamide-co-acrylic acid) hydrogel nanofibers were tested using Perkin Elmer TGA 4000 instrument under nitrogen atmosphere with scanning rate of 10°C/min and temperature range of 30°C to 700°C.

3.4.4 *Differential Scanning Calorimetry (DSC)*

The differential scanning calorimetry of the poly (acrylamide-co-acrylic acid) hydrogel nanofibrous mats was carried out using Perkin Elmer DSC8000 instrument in the temperature range of 30°C to 160°C and scanning rate 10°C /min under nitrogen atmosphere.

3.4.5 *Porosity*

Porosity of the poly (acrylamide-co-acrylic acid) hydrogel nanofibrous mat was evaluated using liquid displacement method. For this, solvent used was *n*-hexane as it shows unhindered motion through interlinked pores and has no effect on the morphology of nanofibrous mat. For measurement known amount of solvent, here 7ml, was taken in a measuring cylinder and then the sample of specific size was kept inside it for 10min. The volume of the solvent was measured after immersion of sample and after removal of hexane-soaked sample. Following formula is used to calculate the porosity of nanofibrous mats from the volumes obtained

$$\% \, Porosity = \frac{(V_0 - V_2) \times 100}{V_1 - V_2} \quad \text{---------- (2)}$$

Where V_0 = Volume of n-hexane taken, V_1 = Volume of solvent after dipping the mat, V_2 = Volume of solvent after removing hexane soaked mat.

3.4.6 *Swelling Studies*

For swelling studies hydrogel composites of size 1×1cm^2 and hydrogel nanofibers of size 3×4 mm^2 were immersed in phosphate buffer solutions of different pH(4.5, 7.0,and 8.5). At regular time intervals, the sample were taken out and weighed. The pHs selected for swelling test simulates with wound pH in fresh and curing conditions. Chronic wound has pH in the range of 7.15–8.9 and it becomes neutral and then acidic with the curing of the wound [58],[59]. Before weighing, the surface water was wiped out using tissue paper. The swelling ratio (α) was calculated using the formulae

$$Percent\ swelling\ (Sw_t) = \frac{(W_w - W_i)}{W_i} \times 100\% \quad \text{---------- (3)}$$

Here, w_w = Weight of wet composite and w_i = Initial weight of dry composite.

$$Swelling\ ratio\ (\alpha) = Sw_t/SD_{eq} \text{---------- (4)}$$

Where SD_{eq}= Equilibrium swelling degree at a certain temperature and pH.

The experiments were performed in triplicate.

Network parameters

Swelling behaviour of the hydrogel composites can also be explained by their number average molecular mass between cross-links ($\bar{M}_c$), cross-link density (q) and mesh size (ξ).

1. *Number average molecular mass between cross-links ($\bar{M}_c$)*

Following equation was used to predict the number average molecular mass between cross-links ($\bar{M}_c$)[35],[131].

$$\frac{1}{M_c} = -\frac{\frac{\bar{v}}{V_1}[\ln(1-v_{2,s}) + v_{2,s} + \chi v_{2,s}^2]}{(v_{2,s}^{\frac{1}{3}} - \frac{1}{2}v_{2,s})} \quad \text{---------- (5)}$$

Where, V_1 = molar volume of water≃ molar mass of water = 18.1gmol^{-1} [132]

χ = Flory Huggins polymer –water interaction parameter ≃ 0.5[132,133]

$\bar{v}$ = Specific volume of the polymer = Volume of the polymer/mass

$v_{2,s}$ = Polymer volume fraction in the swollen condition, it was predicted from equilibrium swelling results using the relation

$$v_{2,s} = \frac{v_d}{v_s} \quad \text{---------- (6)}$$

v_d = Volume of dry polymer, v_s = Volume of the swelled hydrogel at equilibrium condition

2. *Cross-link density, q*

The cross-linking ratio, q was obtained in terms of mole fraction of cross-linked units[134], i.e.

$$q = \frac{M_o}{M_c} \quad \text{---------- (7)}$$

Where M_o = Molar mass of the repeating unit, its value was obtained using the following relation[135]

$$M_o = \frac{n_{AAm} \times M_{AAm} + n_{AAc} \times M_{AAc} + n_{CL} \times M_{CL}}{n_{AAm} + n_{AAc} + n_{CL}} \quad \text{---------- (8)}$$

Where n_{AAm} , n_{AAc}, n_{CL}= number of moles of acrylamide, acrylic acid, and cross-linker respectively and M_{AAm}, M_{AAc}, M_{CL} = molar masses of acrylamide, acrylic acid, and cross-linker respectively.

3. *Mesh size (ξ)*

The mesh size (ξ) was calculated using $\bar{M}_c$ and Flory characteristic ratio of the polymer C_n by the following relation

$$\xi = v_{2,s}^{-1/3} \sqrt{\frac{2C_n M_c}{M_o}}\, l \quad \text{---------- (9)}$$

Where l = length of C-C bond along the backbone of the polymer = 1.54 Å[132]

In the above equation value of C_n was used as the weight average of C_n values of poly (acrylamide) and poly (acrylic acid) chains in accordance to their mole ratio used in the hydrogel matrix. The C_n values for poly (acrylamide) chain and poly (acrylic acid) chain are 2.74 and 6.7 respectively[35].

Swelling kinetics

The swelling data of hydrogel composite was fitted in different models like Peppas-model, Higuchi-model, zero-order, first-order and second-order kinetic equations. Models / Equation having the highest value for correlation coefficient (R^2) was supposed to be the best model showing swelling kinetics.

The mathematical expression for the Peppas-model is

$$\frac{M_t}{M_\infty} = kt^n \quad \text{----------} \quad (10)$$

Where M_t/M_∞ = Normalized swelling ratio, n = Swelling exponent exhibiting mode of movement of penetrate,

k = Constant for the hydrogel, t = Time taken in Swelling.

The mathematical expression for the Higuchi-model is

$$\frac{M_t}{M_\infty} = kt^{1/2} \quad \text{----------} \quad (11)$$

Where M_t/M_∞ = Normalized swelling ratio, k = Constant for hydrogel, t = Swelling time.

The integrated equation for zero-order kinetic model is

$$M_t = M_\infty + kt \quad \text{----------} \quad (12)$$

The integrated equation for first-order kinetic model is

$$\alpha = (1 - Ae^{-kt}) \quad \text{----------} \quad (13)$$

Where, A = pre-exponential factor.

The integrated equation for second-order kinetic model is

$$\frac{t}{M_t} = \left(\frac{1}{kM_\infty^2}\right) + \left(\frac{1}{M_\infty}\right)t \quad \text{---------- (14)}$$

Where M_∞= Weight of composite at equilibrium, M_t = Weight of composite at time *t*. After performing swelling experiment, the dry weight of the sample was measured to calculate total weight loss in wet conditions in 24h.

3.4.7 *Antimicrobial Activity*

The antimicrobial activity of the hydrogel composites and hydrogel nanofibers were analysed using the zone inhibition method[136]. Here discs of drug loaded hydrogel samples were sterilized in a laminar airflow under UV light for 24h. The sterilized samples were mounted on agar plates cultured with *E.coli* (Gram-negative bacteria) and *S.aureus* (Gram-positive bacteria) as model bacteria. The plates were kept in an incubator at 37°C for 24h. Development of a clear zone below and around the discs on the plate medium recognized the release of drug and antimicrobial behaviour of the composite. The experiments were performed in triplicate.

3.4.8 *Drug Release Studies*

Drug release kinetics of the hydrogel composites and the hydrogel nanofibrous mat were studied using Carry 300 UV-Visible spectrophotometer (Agilent Technologies). Drug loaded samples were prepared by immersing dried composite or nanofibers sample into 20mL of drug (gentamicin sulphate or amoxicillin) solution (1mgmL^{-1}) for 48h. The samples were then separated and dried. The concentration of the drug in the remaining solution was measured using the calibration curve of the drug loaded. The amount of drug loaded was calculated by subtracting the remaining concentration of the drug from its initial concentration in the solution.

To check release profile, the dried drug loaded samples were placed separately in 10mL phosphate buffers having pH 4.5 (acidic), 7.0(neutral) and 8.5(basic). At a regular time interval, 1.0mL aliquot was taken out with subsequent mixing of the same amount (1.0mL) of the fresh buffer. Here the homogeneous distribution of drug molecules in the composite was assumed. The concentration of the drug in the aliquots was also measured using the calibration curve of the drug loaded. The percentage cumulative release was calculated by using the formula

$$\%\ Cumulative\ Release = \frac{V_e C_1 + V_0 C_n}{m} \times 100 \quad \text{---------- (15)}$$

Where V_e = sampling volume, V_0 = initial volume, C_1 and C_n are the initial concentration and concentration at sampling time *n*, *m* = mass of drug containing sample.

The experiments were carried out in triplicate and their mean value was used for analysis.

Drug release kinetics

The drug release data were fitted in different models like Peppas-model, Higuchi-model, zero-order, first-order and second-order equations. Equations of Peppas-model, first-order, second-order models have been given in swelling studies. The mathematical formulation for the Higuchi-model is

$$M_t = M_\infty + k_H t^{1/2} \quad \text{---------- (16)}$$

Where k_H = Higuchi constant, an indicator of characteristics of a hydrogel system.

The model having the maximum value of correlation coefficient (R^2) was considered the best model for showing the drug release mechanism.

3.4.9 *Mechanical Testing*

Universal Testing Machine (Instron-2700) in tension mode was used to study the mechanical properties of the hydrogel films and hydrogel composite in wet conditions. Dog bone shape (70×10×0.4mm) wet sample was clamped between the two arms[137]. The gauze length of the sample was 50mm. The ends were fixed using tape to avoid the slipperiness. The clamped sample was stretched at a rate of 5mm min^{-1}. The test results were reported as stress-strain curves. Three samples of each were tested and their mean value was used for comparing mechanical properties.

CHAPTER 4

SYNTHESIS AND CHARACTERIZATION OF HYDROGEL COMPOSITE BY GRAFT COPOLYMERIZATION OF POLY (ACRYLAMIDE-CO-ACRYLIC ACID) OVER COTTON FABRIC USING PEG AS CROSS-LINKER

In this chapter, the mechanism of the grafting and cross-linking reaction were predicted. The effect of various parameters on the grafting of the copolymer of poly (acrylamide-co-acrylic acid) over the cotton fabric and insertion of cross-links in between the chains of the grafted copolymer have also been studied in terms of grafting yield. The characterisation of the composite by using FTIR spectroscopy and SEM techniques; and comparison of its mechanical properties with hydrogel film has also been done.

4.1 Mechanism of Reaction

The mechanism of the grafting reaction is shown in Figure 4.1. The cotton fabric got activated when treated with APS solution. In this reaction, the APS solution abstracted the cellulosic hydrogen to generate cellulose macro radicals. These radicals initiated graft polymerization reaction in the presence of AAm leading to the generation of a new free radical which combined with AAc to generate another free radical. In this way, a chain reaction started. Subsequent monomer addition to the activated chain propagates the grafting reaction onto the cotton fabric. The grafting reaction may be terminated by coupling or combination with the initiator, or by disproportionation with cross-linker. After grafting reaction, the addition of PEG inserted cross-links among the poly (acrylamide-co-acrylic acid) chains by forming an ester linkage with some of the –COOH groups in between the chains.

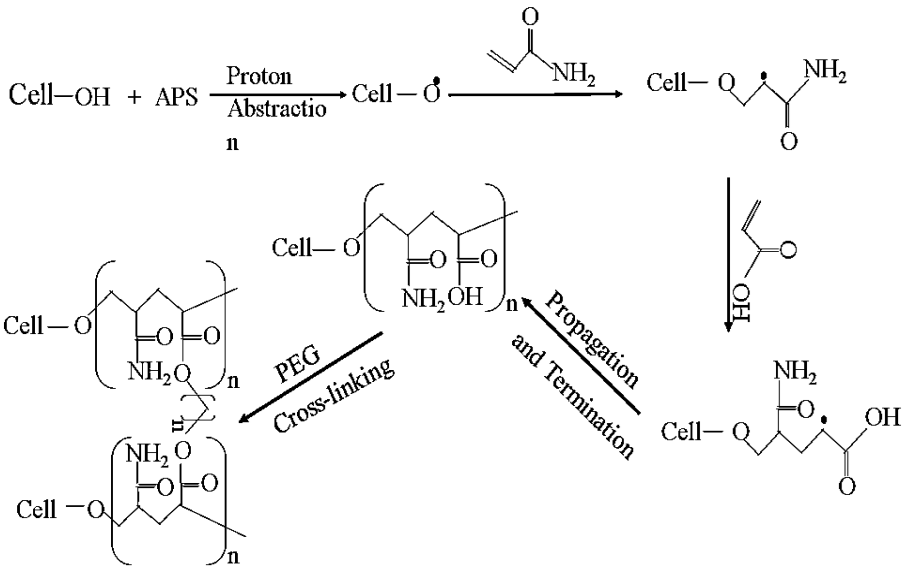

Figure 4.1 Mechanism of Grafting Reaction

4.2 Optimisation of Reaction Parameters

4.2.1 *Effect of Initiator Concentration*

The initiator concentration was plotted with the % grafting and the plot obtained is shown in Figure 4.2.

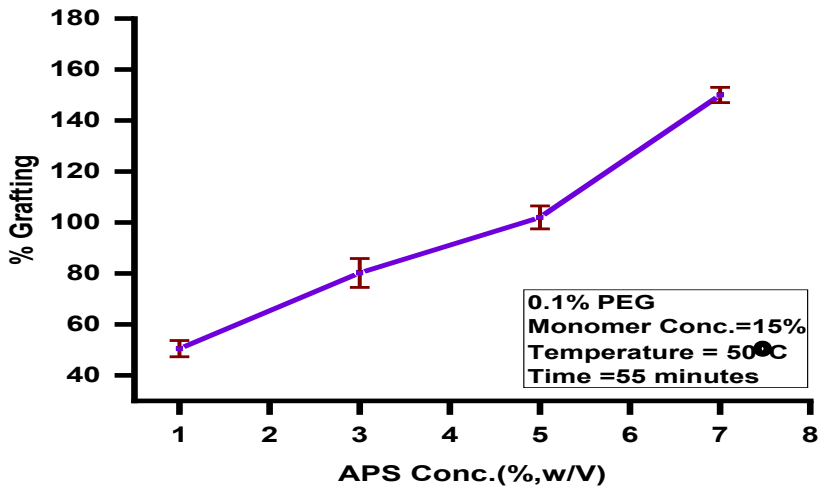

Figure 4.2 Effect of Initiator Concentration

The plot revealed a hike in grafting yield with rise in APS concentration indicating that APS was responsible for generating active sites over the surface of the substrate. A 0.23±0.05mm thick (approximately equal to the thickness of the cotton fabric) hydrogel layer was grafted using 5% (w/V) APS concentration. At 5% (w/V) APS concentration, the grafting yield was 102±5%. Further rise in APS concentration might weaken the bonds present among cotton fibers leading to the rupturing of fabric. It was reported that an initial increase and then decrease in the percentage grafting with increasing APS concentration shows more homo-polymerization due to the presence of initiator in the complete reaction mixture[105]. In our case, homo-polymerization was almost negligible as the initiator was available only over the substrate surface.

For further studies, the optimized APS concentration was 5% (w/V) as it led to the grafting of a sufficiently thick hydrogel layer over cotton fabric.

4.2.2 *Effect of APS Treatment Time and Temperature*

At lower temperature, the fabric was not activated but it got activated when the temperature was increased. This was because the initial increase in temperature increased the rate of dissociation of the initiator and at the temperature of 55±5°C maximum active sites were generated. Further increase in temperature might lead to weakening of the bonds present among cotton fibers leading to the rupture of the fabric. The fabric was treated with APS for a period of 30minutes. Treatment for longer period also caused weakening of the bonds present among cotton fibers leading to the rupture of fabric.

4.2.3 *Effect of Monomer Concentration*

The copolymer of poly (acrylamide-co-acrylic acid) was grafted over the cotton fabric and the percentage grafting was plotted with the monomer concentration. The plot obtained is revealed in Figure 4.3.

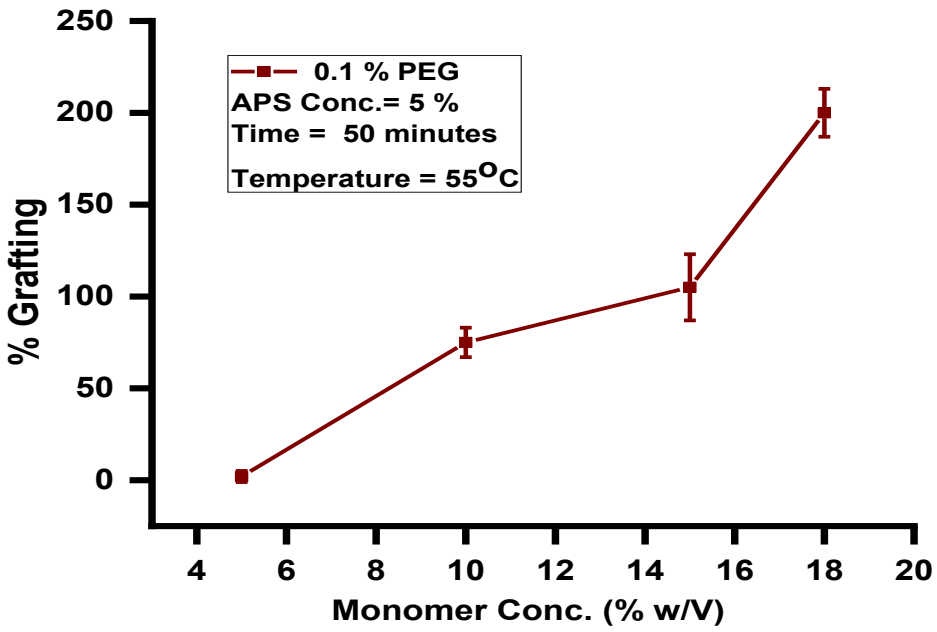

Figure 4.3 Effect of Monomer Concentration

A gradual increase in the percentage grafting was observed with increase in monomer concentration (Figure 4.3). It may be justified with the availability of more reaction sites at higher monomer concentration. Sufficiently thick (0.23±0.05mm thick, resembling with the thickness of the cotton fabric) hydrogel layer was grafted with 15% (w/V) monomer concentration. Grafting gradually increases with further rise in monomer concentration. Chun et al.[28] also observed the same findings for acrylic acid-acrylamide grafted polypropylene.

A thicker hydrogel layer left the fabric surface when equilibrated with water, due to rupture of forces between hydrogel and cotton owing to the bulkiness of hydrogel film in wet conditions. At 15% monomer concentration, the grafting yield was found to be 105±5%.

Thus, for further studies the optimized monomer concentration was 15% (w/V).

4.2.4 *Effect of Monomer Type*

The nature of monomer also affects the grafting yield. Polyacrylamide, polyacrylic acid and poly (acrylamide-co-acrylic acid) were grafted over the cotton fabric and the data was plotted in terms of grafting yield. The plot is shown in Figure 4.4.

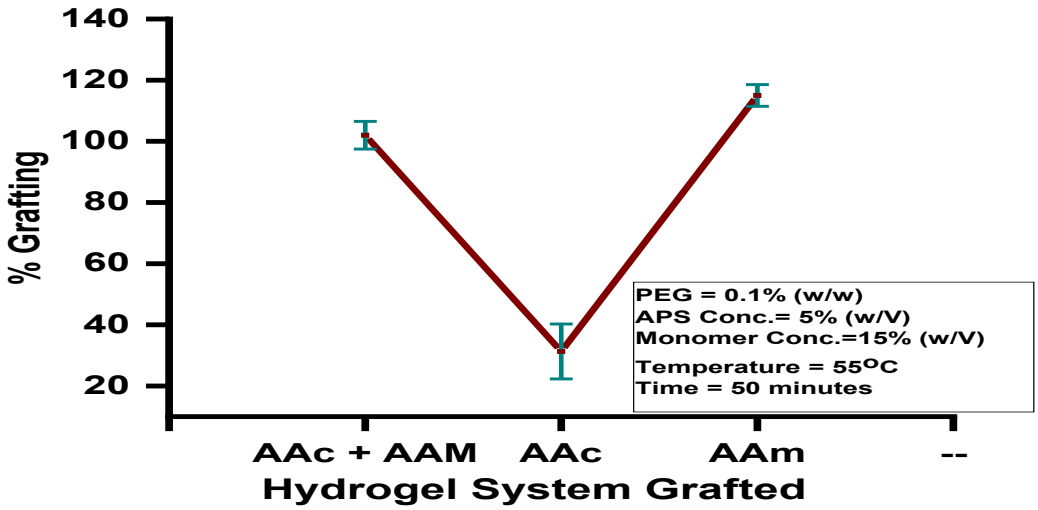

Figure 4.4 Effect of Hydrogel System Grafted

The plot shown in Figure 4.4 suggested the highest grafting for the polyacrylamide system, followed by grafting of its copolymer with acrylic acid. Least grafting was observed in case of polyacrylic acid. This may be due to repulsive

interactions between the chains owing to ionisation of carboxylic groups of the acrylic acid in the reaction medium (having pH above than the pK_a of acrylic acid) in case of acrylic acid systems.

4.2.5 *Effect of Temperature*

The percentage grafting was also obtained by varying the temperature of the reaction and it was plotted with temperature. The plot is shown in Figure 4.5. The plot revealed a rise in % grafting up to 50±5°C and then a decrease. This was because the initial increase in temperature increases the monomer's diffusion and mobility from the aqueous phase to the fabric phase resulting in increased grafting yield. A further rise in temperature (above 50±5°C) might accelerate radicals' termination, leading to a decrease in % grafting.

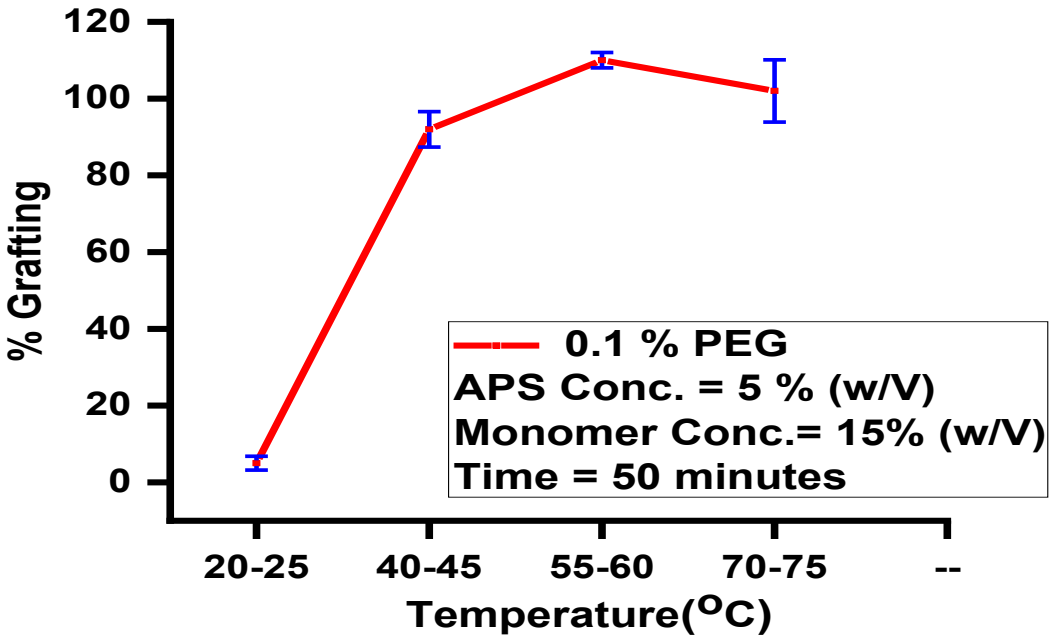

Figure 4.5 Effect of Temperature

4.2.6 *Effect of Reaction Time*

The percentage grafting was also obtained by carrying out the propagation reaction for different times and the results were plotted with time. The effect of reaction time on % grafting is shown in Figure 4.6.

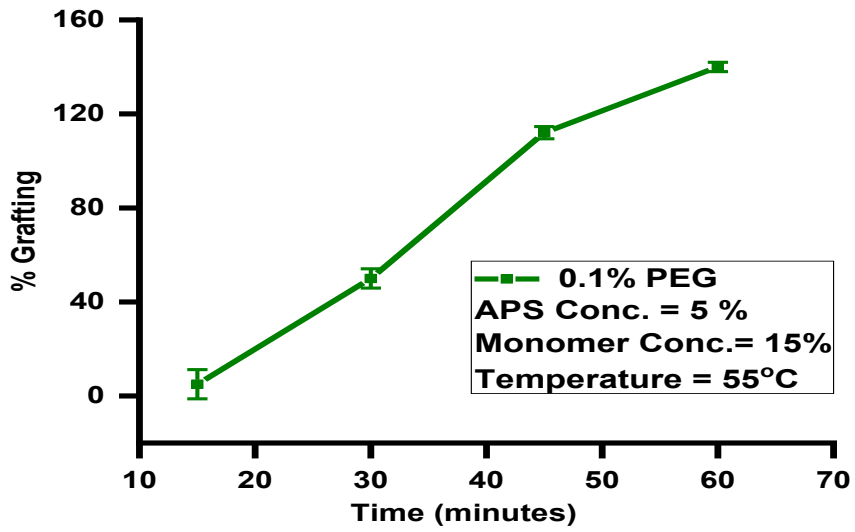

Figure 4.6 Effect of Propagation Reaction Time

The results suggested that grafting yield increased with increase in time, and 55minutes was the sufficient time to graft a hydrogel layer of requisite thickness (0.23±0.05) over the cotton fabric. A prolonged reaction may lead to the deposition of a thick hydrogel layer which in wet condition would detached easily from the fabric due to its bulkiness.

4.2.7 *Effect of Cross-linker Concentration*

The effect of variation of cross-linker concentration was predicted in terms of percentage grafting as well as percentage swelling. The grafting and swelling results were plotted w.r.t. cross-linker concentration. The plots are shown in Figure 4.7(a) and 4.7(b).

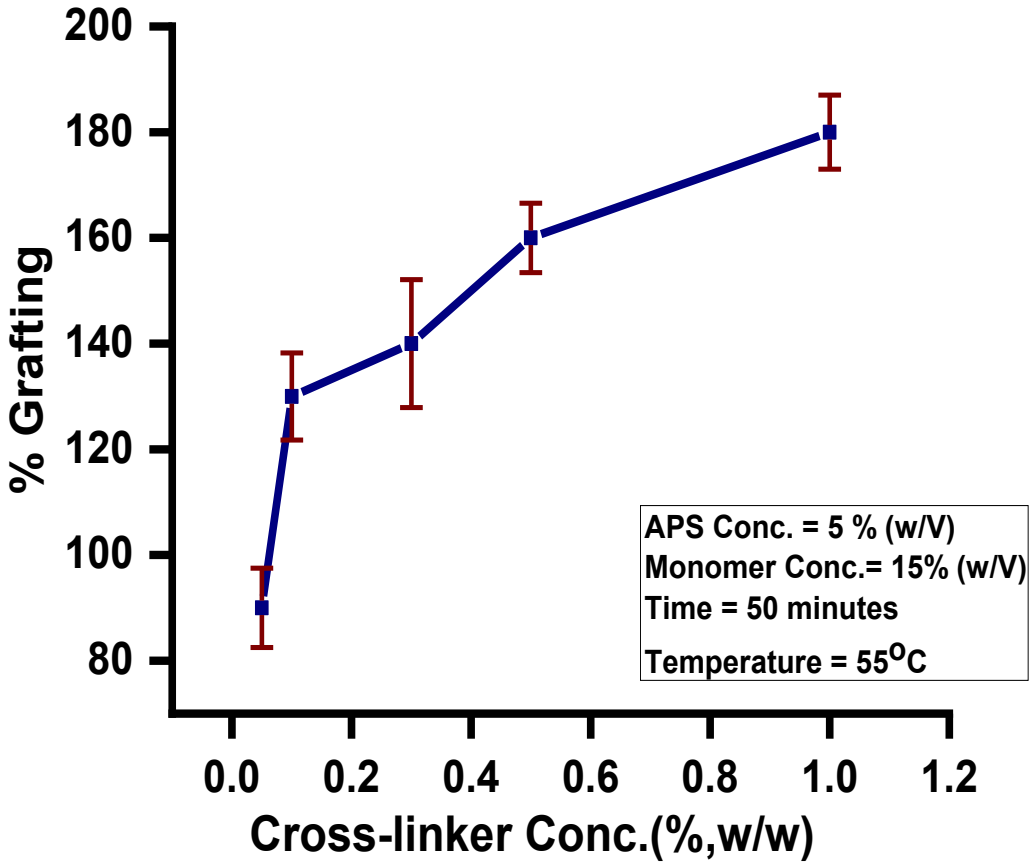

Figure 4.7(a) Effect of Cross-linker Concentration on % Grafting

Figure [4.7(a)] indicated a regular increase in grafting yield with increasing cross-linker concentration but there appeared a decrease in percentage swelling after a certain cross-linker concentration [Figure 4.7(b)].

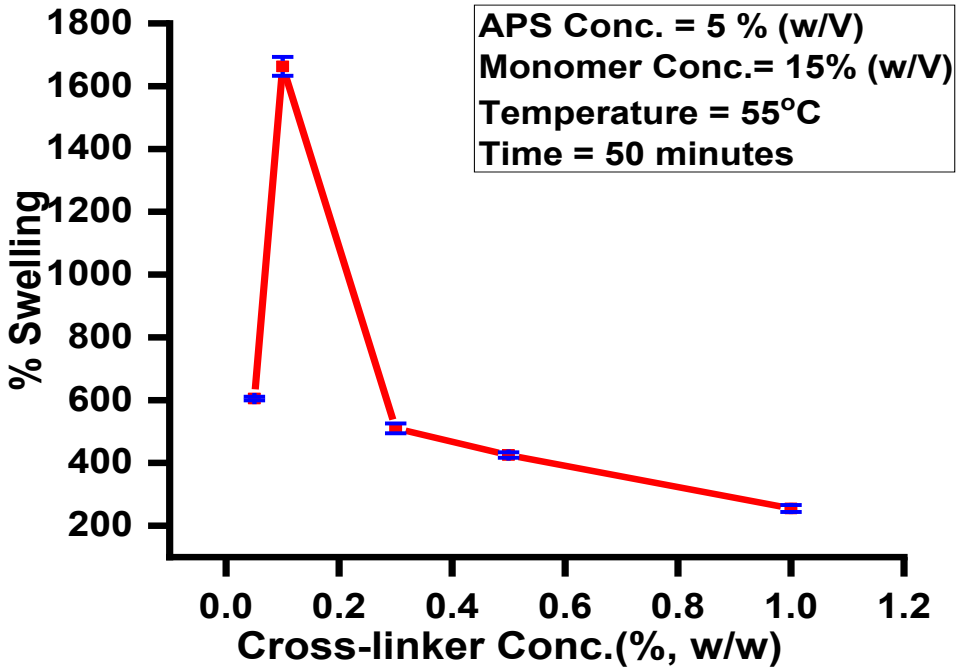

Figure 4.7(b) Effect of Cross-linker Concentration on % Swelling

This may be attributed to reduced space present between the polymer chains with raising cross-linker concentration[97] resulting in decreased pore size and hence, reduced swelling.

4.3 Structural Analysis

FTIR spectra of the cotton and the poly (acrylamide-co-acrylic acid) hydrogel composite are shown in Figure 4.8(a) and 4.8(b) respectively. The characteristic bands of cotton at 3300cm^{-1}(for –OH group) and 1027cm^{-1}(C—O str.) were appeared in Figure 4.8(a).

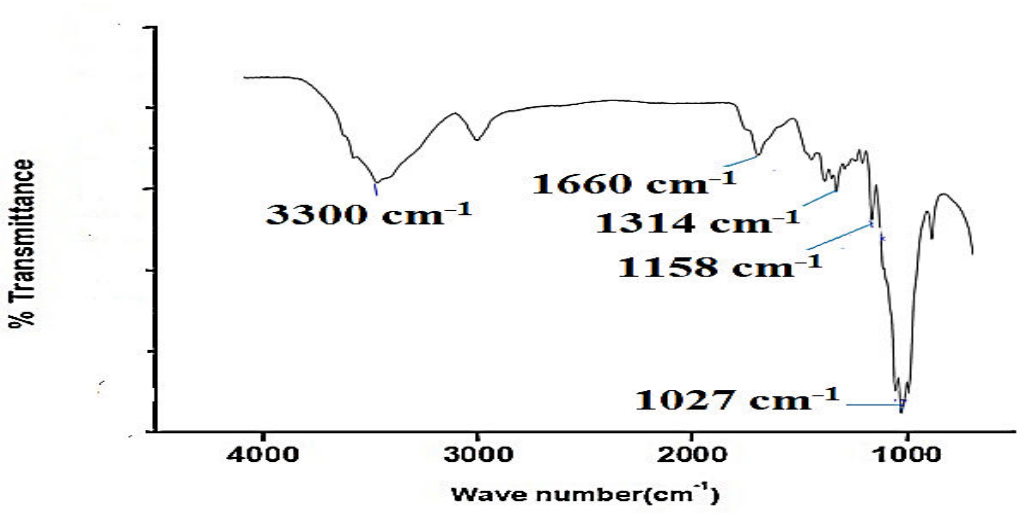

Figure 4.8(a) FTIR Spectra of Cotton

The characteristic bands of polyacrylic acid, acrylamide and PEG were appeared in FTIR spectra of hydrogel composite as shown in Figure 4.8(b).

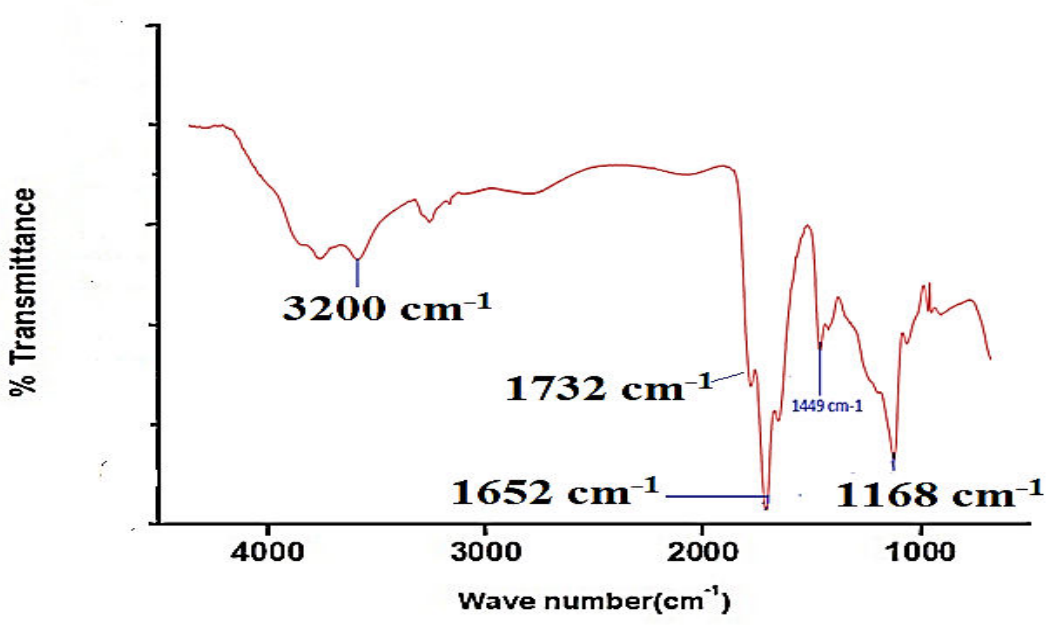

Figure 4.8(b) FTIR Spectra of Cell-o-$(AAm)_n$-co-$(AAc)_n$-PEG

Bands in the range of 3100-3500cm^{-1} (due to O-H and N-H stretching) confirmed the formation of the copolymer of AAm and AAc and that in the range of 2990-2700cm^{-1} were due to asymmetric and symmetric stretching of C–H of acrylate unit. Band for carbonyl, C=O (C=O of ester group) stretching appeared at 1732cm^{-1} and for C=O (C=O of acrylamide group) stretching appeared at 1652cm^{-1}. A band at 1449cm^{-1} was due to symmetrical stretching of COO[34]. Cross-linking by PEG in the hydrogel was revealed by a characteristic band of C-O-C stretching at 1168cm^{-1} showing the presence of ester linkage in it.

4.4 Morphological Analysis

The morphology of the cotton fabric and the composite prepared was observed by their SEM micrographs. Figure 4.9 (a) and 4.9(b) show the SEM images of pure cotton and composite respectively.

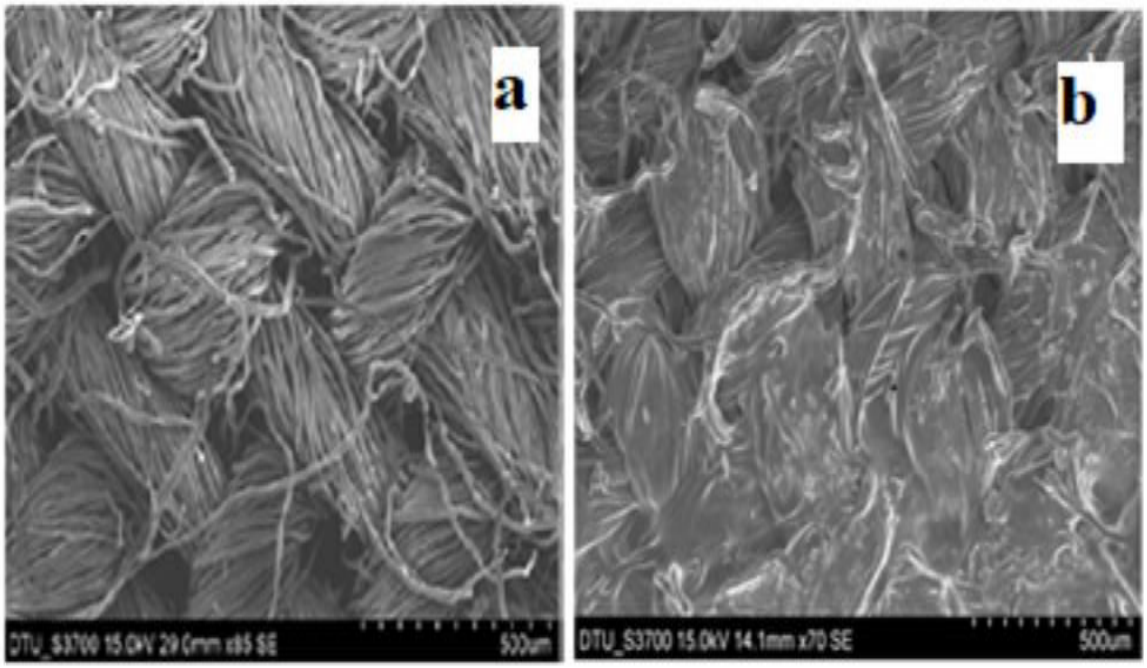

Figure 4.9 SEM Micrographs of (a) Pure Cotton (b) Cell-o-$(AAm)_n$-co-$(AAc)_n$-PEG

There appeared no layer over the surface of cotton fabric in Figure 4.9(a) but uniform layers of hydrogel appeared over the surface of cotton fabric in Figure 4.9(b), which was a clear indication of grafting of the hydrogel layer over cotton fabric.

4.5 Mechanical Properties

The mechanical properties of hydrogel film and composites were evaluated under wet conditions. The data is shown in Table 4.1.

Table 4.1: Mechanical Properties of Hydrogel Film and Hydrogel Composite Prepared by using PEG in Wet Conditions

Materials	Tensile Stress at Max Load (MPa)	Tensile Modulus (MPa)	Extension at Break (mm)
Hydrogel Film	3.07±.5 (0.03)	31.3±1.4(0.03)	26.8±5(0.02)
Cell-o-$(AAm)_n$-co-$(AAc)_n$-PEG	4.21 ± 0.5(.01)	91.6±5 (.02)	7.51±0.6 (.01)

Values in the bracket show coefficient of variation (CV).

The tensile strength was lower (3.0MPa) but extension at break was much higher (26.8mm) in case of hydrogel film as compared to hydrogel composite, in case of which tensile strength was 4.2MPa and extension at break was 7.5mm. Hydrogel composite showed very high modulus as compared to hydrogel film. These results supported the reinforcement of the strength of the hydrogel after grafting over the fabric.

CHAPTER 5

SYNTHESIS AND CHARACTERIZATION OF HYDROGEL COMPOSITE BY GRAFT COPOLYMERIZATION OF POLY (ACRYLAMIDE-CO-ACRYLIC ACID) OVER COTTON FABRIC USING MBAAM AS CROSS-LINKER

In this chapter, the mechanism of the grafting and cross-linking reaction, effect of various parameters on the grafting of copolymer of poly (acrylamide-co-acrylic acid) over cotton fabric and insertion of cross-links in between the chains of grafted copolymer using MBAAm in terms of grafting yield were explored. The study was also focused on the characterisation of the composite using FTIR (Fourier transformed infrared spectroscopy) and SEM (scanning electron microscopy) techniques. The mechanical strength of the composite has also been compared with that of the hydrogel film by using UTM data.

5.1 Reaction Mechanism

The active sites were generated when the cotton fabric was treated with APS solution. The APS abstracted cellulosic hydrogen and generate cellulose macro radicals which initiated graft polymerization reaction in the presence of acrylamide. It gave a new free radical which combined with acrylic acid to generate another free radical. In this way, a chain reaction initiated. Subsequent addition of the monomers to the activated chain propagated the grafting reaction over the cotton fabric. The grafting reaction might ceased by coupling or combination with the initiator, or by disproportionation with the cross-linker.

After grafting of copolymer over cotton fabric, the addition of MBAAm inserted cross-links among poly (acrylamide-co-acrylic acid) chains by introducing an amide

group in between the polymeric chain. In this reaction, MBAAm attacked at the unsaturated chain and generated new free radicals. The mechanism of the reaction is shown in Figure 5.1.

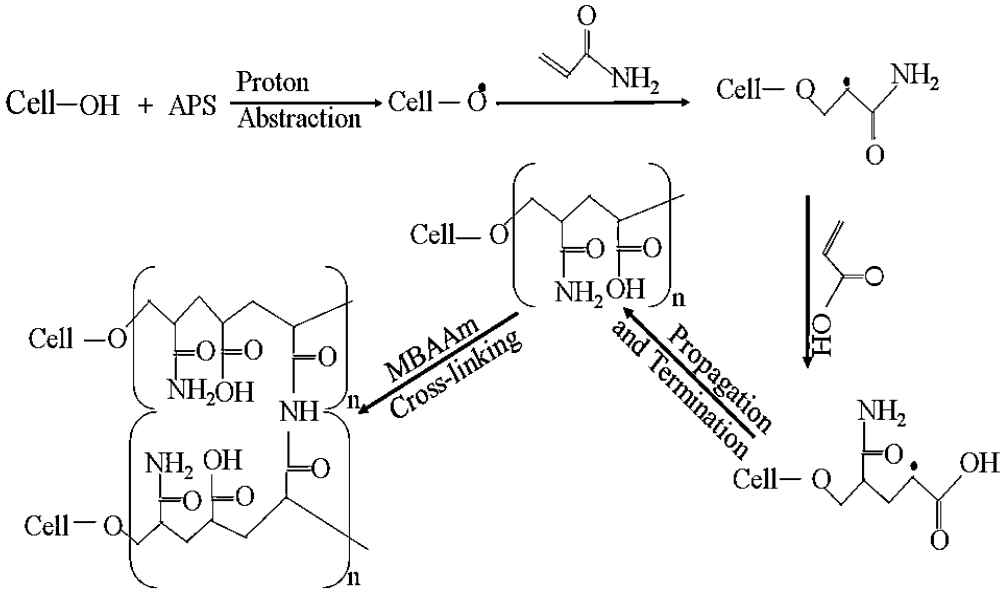

Figure 5.1 Mechanism of Grafting Reaction using MBAAm

5.2 Optimisation of Reaction Parameters

5.2.1 *Effect of Initiator Concentration*

The grafting yield was calculated by preparing the composite using different APS concentration and the obtained yields were plotted with the respective concentrations of APS. The plot is shown in Figure 5.2.

The plot indicated an increase in percentage grafting with increase in APS concentration. This is due to the generation of active sites over the surface of the cotton fabric by the use of APS. A 0.30±0.04 mm thick hydrogel layer was grafted with 5% (w/V) APS concentration. A further rise in APS concentration may weaken

the bonds present among fibers leading to the rupturing of the fabric. At 5% (w/V) APS concentration, the grafting yield was 184±5%.

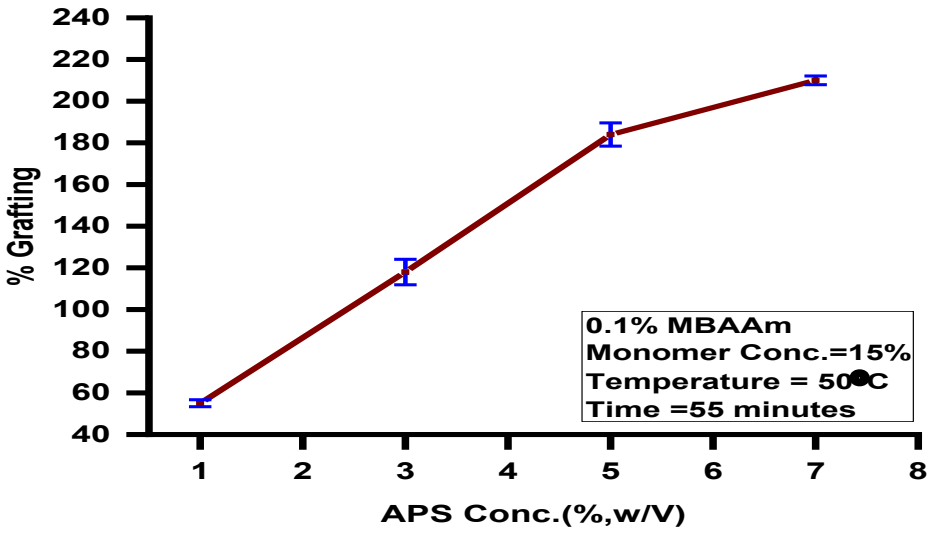

Figure 5.2 Effect of Initiator Concentration

Literature review showed an initial increase and then decrease in percentage grafting with rise in APS concentration because of the homo-polymerization as the initiator was present in the complete reaction solution[30]. However, in our case, presence of initiator only over the surface of the fabric reduced the chances of homo-polymerization. For further studies, the optimized APS concentration was 5% (w/V) as it leads to the grafting of a sufficiently thick hydrogel layer over cotton fabric[26].

5.2.2 *Effect of Monomer Concentration*

The percentage grafting was also obtained by varying monomer concentration and the obtained results were plotted with the respective monomer concentration. The plot is shown in Figure 5.3. This plot revealed the effect of monomer concentration on percentage grafting.

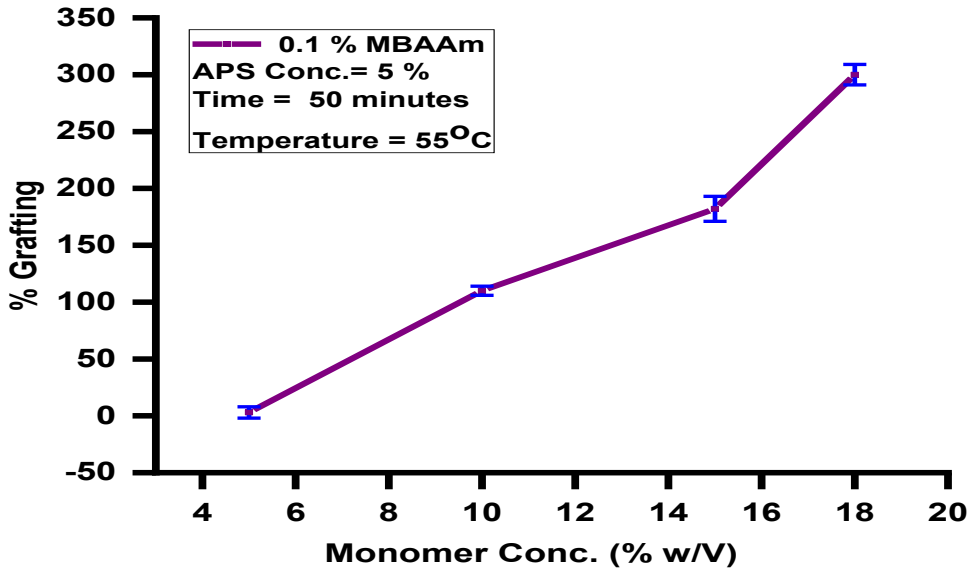

Figure 5.3 Effect of Monomer Concentration

The percentage grafting gradually increased with increase in monomer concentration. It might be because of the availability of more reaction sites at higher monomer concentration. Similar findings were observed in case of AAc-AAm grafted polypropylene composite prepared by Chun et al[28]. Sufficiently thick (0.23±0.05mm thick, resembling with the thickness of the cotton fabric) hydrogel layer was grafted with 15% (w/V) monomer concentration. A thicker hydrogel layer left the fabric surface when equilibrated with water due to rupturing of the forces existing between the hydrogel layer and cotton fabric owing to the bulkiness of hydrogel film in wet conditions. At 15% monomer concentration, the grafting yield was 182±5%. For further studies, the optimized monomer concentration was 15% (w/V).

5.2.3 *Effect of Monomer Type*

Different hydrogel systems were grafted over the cotton fabric and the percentage grafting for these systems were plotted. The plot is shown in Figure 5.4.

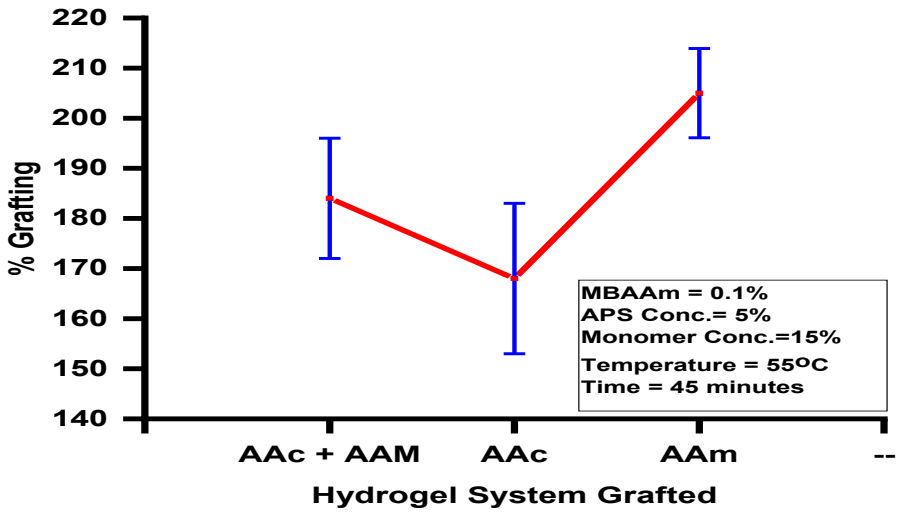

Figure 5.4 Effect of Hydrogel System Grafted

The percentage grafting was found to be highest in case of polyacrylamide system, followed by grafting of its copolymer and least grafting was observed in case of polyacrylic acid system. This might be due to repulsive interactions between the chains owing to ionisation of carboxylic groups of the acrylic acid in the reaction medium (having pH above than the pK_a of acrylic acid) in case of acrylic acid systems.

5.2.4 *Effect of Temperature*

The plot shown in Figure 5.5 indicated the effect of the temperature of propagation reaction on the grafting yield of the hydrogel system over the cotton fabric.

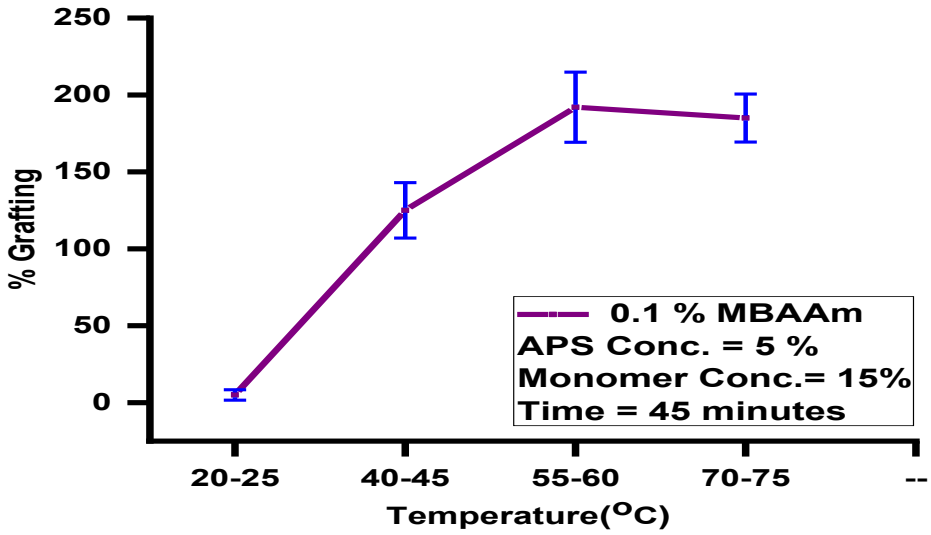

Figure 5.5 Effect of Temperature

.An initial rise in % grafting was observed with increase in temperature up to 50±5°C and then a decrease. This is because the initial rise in temperature raised the rate of monomer diffusion and their mobility from the aqueous phase to the fabric phase. Hence, the percentage grafting increases. A further rise in temperature (above 50±5°C) may accelerate radicals' termination, leading to a decrease in % grafting.

Thus, 50±5°C was the optimised temperature for the grafting reaction.

5.2.5 *Effect of Reaction Time*

Figure 5.6 shows the effect of reaction time on the percent grafting of hydrogel over cotton fabric using MBAAm as cross-linker.

The results indicated a regular increase in percentage grafting with passage of time and a sufficiently thick layer (0.23±0.05mm) was grafted in 55minutes. If the reaction was continued for a longer period, the thickness of hydrogel layer increased and the bulky layer readily detached from the fabric surface in wet condition.

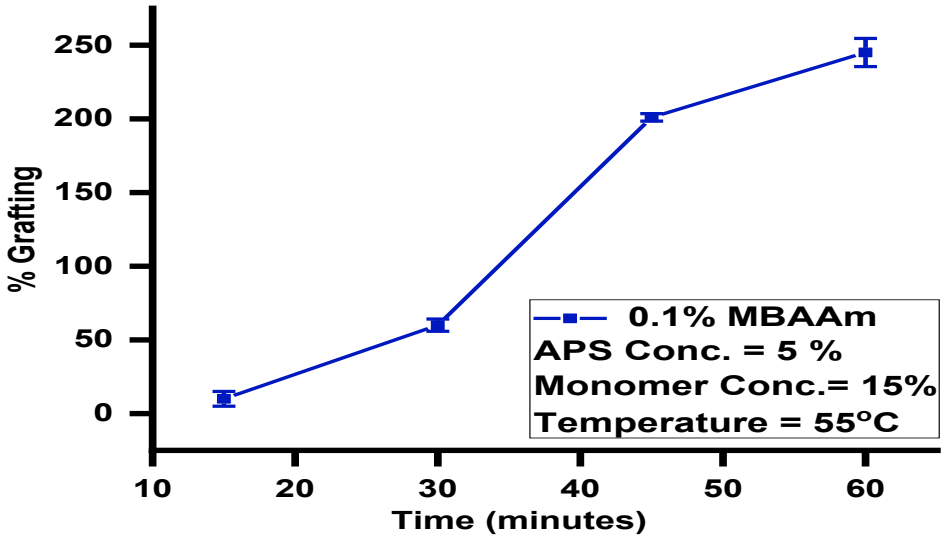

Figure 5.6 Effect of Propagation Reaction Time

Thus, 55minutes was optimised as the sufficient time to graft the hydrogel layer of requisite thickness over the fabric.

5.2.6 *Effect of Cross-linker Concentration*

The effect of cross-linker concentration was studied in terms of percentage grafting and percentage swelling. For this the percentage grafting and percentage swelling calculated for a specific cross-linker concentration were plotted with the respective cross-linker concentration. The plots are shown in Figure 5.7(a) and 5.7(b).

The plot shown in Figure 5.7(a) indicated an increase in percentage grafting with increase in cross-linker concentration up to a certain concentration and then it became constant because no sites are available for further cross-linking.

The percentage swelling first increased and then reduced after a certain cross-linker concentration as indicated in Figure 5.7(b) because initial addition of cross-linker generates pores for holding water. However, a higher cross-linker concentration increased the compactness of the gel matrix resulting in reduced pore size and decreased swelling.

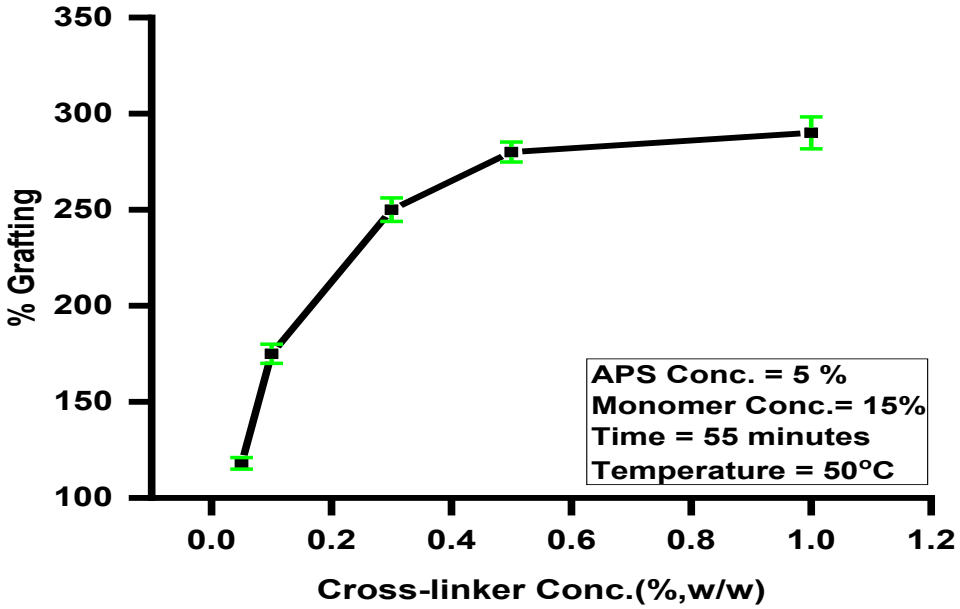

Figure 5.7(a) Effect of Cross-linker Concentration on % Grafting

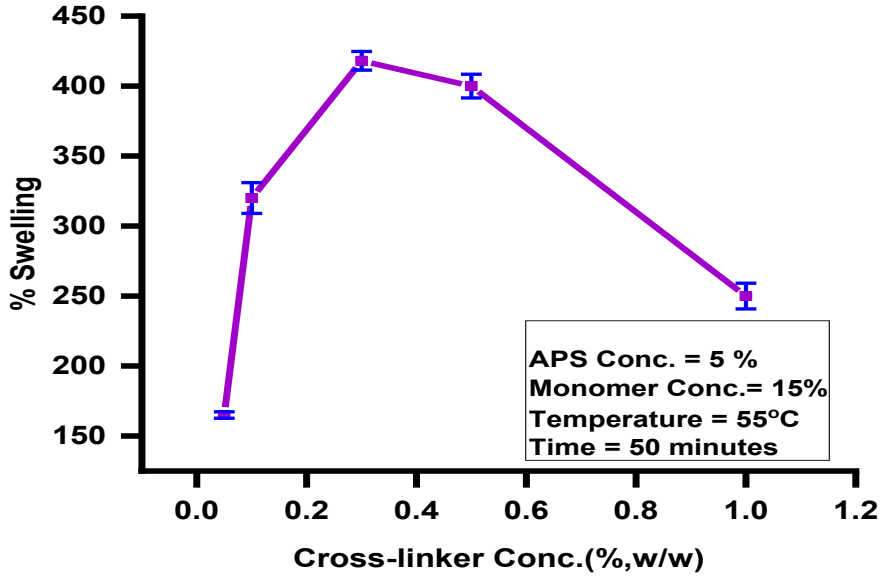

Figure 5.7(b) Effect of Cross-linker Concentration on % Swelling

5.3 Structural Analysis

FTIR spectra of pure cotton and hydrogel composite are shown in Figure 5.8(a)

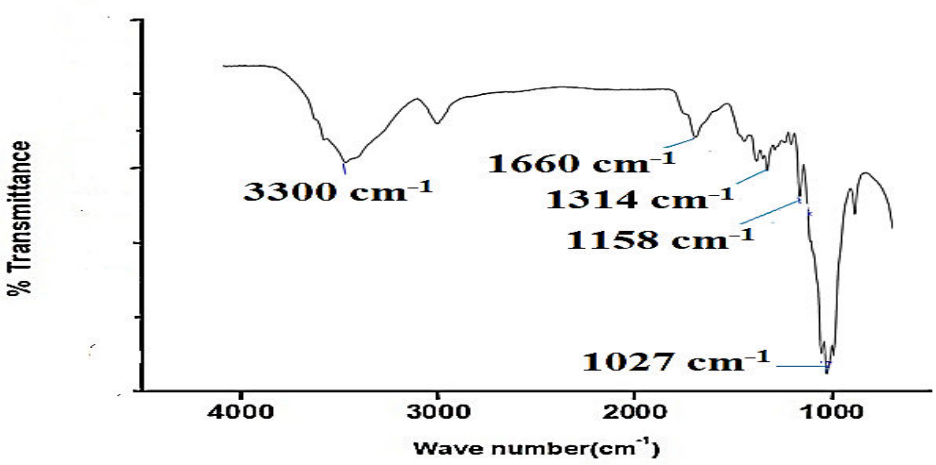

Figure 5.8(a) FTIR Spectra of Pure Cotton Fabric

and 5.8(b).

The characteristic bands of cotton at 3300cm^{-1} (for –OH group), 1027cm^{-1}(C—O str.) were appeared in Figure 5.8(a).

Figure 5.8(b) also revealed characteristics band in the range of 3100-3500cm^{-1} (due to O-H and N-H stretching) showing the formation of the copolymer of

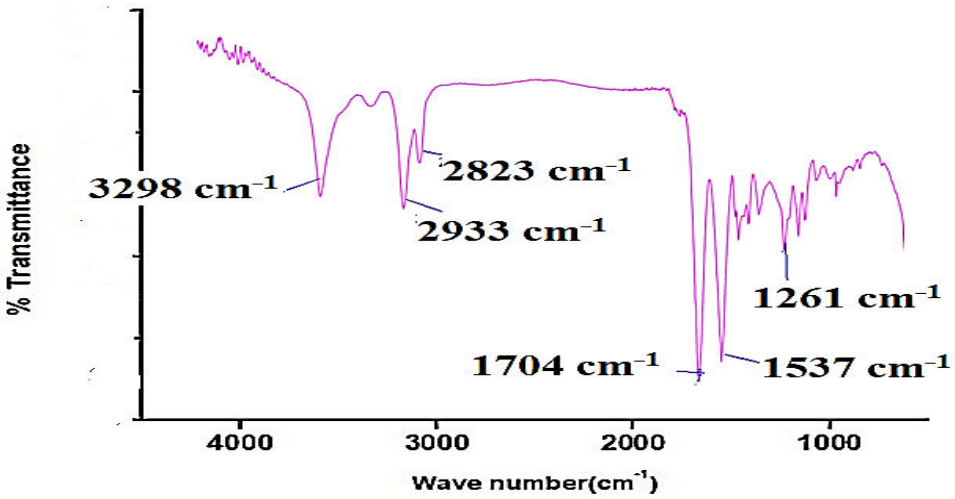

Figure 5.8(b) FTIR spectra of Cell-o-$(AAm)_n$-co-$(AAc)_n$-MBAAm

acrylamide and acrylic acid and those in the range of 2990-2700cm^{-1} showing asymmetric and symmetric stretching of C–H of acrylate unit [138]. Carbonyl band at 1537cm^{-1} showed the presence of secondary (2°) amide group. It, indeed, indicated N-H bending *trans* to the carbonyl oxygen[34]. A weak band 1420cm^{-1} was an indication of C–N stretching showing the presence of cross-linking agent MBAAm.

5.4 Morphological Analysis

Figure 5.9(a) and 5.9(b) show the SEM images of pure cotton and Cell-o-$(AAm)_n$-co-$(AAc)_n$-MBAAm respectively.

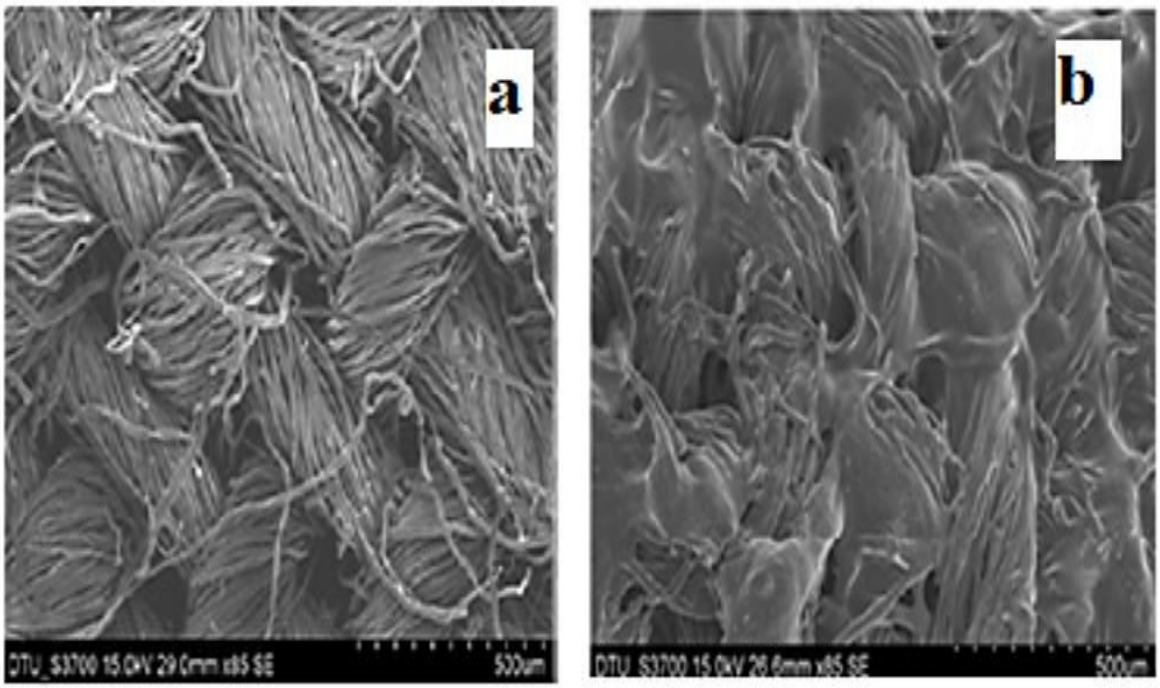

Figure 5.9 SEM Micrographs (a) Pure Cotton and (b) Cell-o-$(AAm)_n$-co-$(AAc)_n$-MBAAm

There was no layer over the surface of cotton fabric as indicated by Figure 5.9(a) but uniform layers of hydrogel appeared over the surface of cotton fabric in Figure 5.9(b), which was a clear indication of grafting of the hydrogel layer over the cotton fabric.

5.5 Mechanical Properties

The mechanical properties of hydrogel film and composites were evaluated under wet conditions. The data are shown in Table 5.1.

Table 5.1: Mechanical Properties of Hydrogel Film and Hydrogel Composite Prepared by using MBAAM in Wet Conditions

Materials	Tensile Stress at Max Load (MPa)	Tensile Modulus (MPa)	Extension at Break (mm)
Hydrogel film	3.07±.5 (0.03)	31.3±1.4(0.03)	26.8±5(0.02)
Cell-o-$(AAm)_n$-co-$(AAc)_n$-MBAAm	6.23± 0.6(.03)	275.37±4.9 (.04)	9.73±1.7 (0.05)

Values in the bracket show coefficient of variation (CV).

The tensile strength was found to be lower (3.0MPa) but extension at break was much higher (26.8mm) in case of hydrogel film as compared to hydrogel composites, having tensile strength of 6.23MPa and extension at break 9.7mm. Hydrogel composites revealed a very high modulus as compared to hydrogel film. These results supported the reinforcement of the strength of the hydrogel after grafting over the fabric.

CHAPTER 6

COMPARATIVE STUDY OF SWELLING AND DRUG RELEASE RESULTS OF POLY (ACRYLAMIDE-CO-ACRYLIC ACID) HYDROGEL COMPOSITES PREPARED BY USING MBAAM AND PEG AS CROSS-LINKERS

In this chapter, the swelling and drug release profile of the poly (acrylamide-co-acrylic acid) hydrogel grafted over cotton fabric composites prepared by using two different cross-linkers (PEG and MBAAm) have been discussed because cross-linker tuned the pore-density (volume) and thus, affects the swelling and drug release behaviour of the hydrogels. In this chapter, the composite prepared by using PEG as cross-linker is represented as cell-$(AAm)_n$-$(AAc)_n$-PEG and that prepared by using MBAAm as cross-linker as cell-$(AAm)_n$-$(AAc)_n$-MBAAm. The kinetics of swelling and drug release has also been explored by using various models.

6.1 Swelling Behaviour

The hydrogel composites were pH responsive as revealed in Figure 6.1(a)-(c).

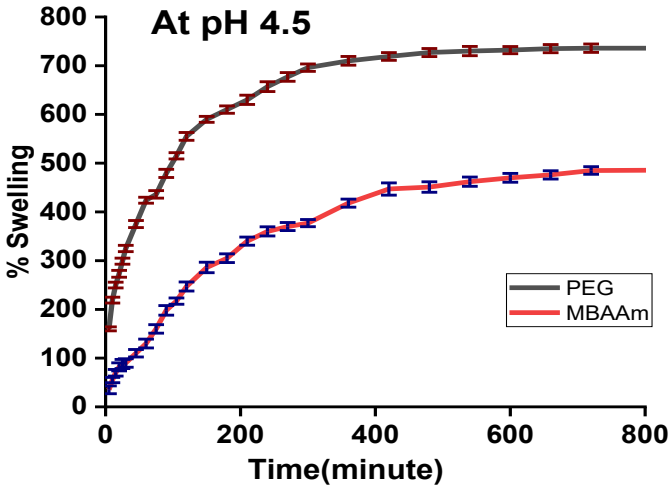

Figure 6.1(a) Swelling Behaviour of Hydrogel Composites at pH 4.5

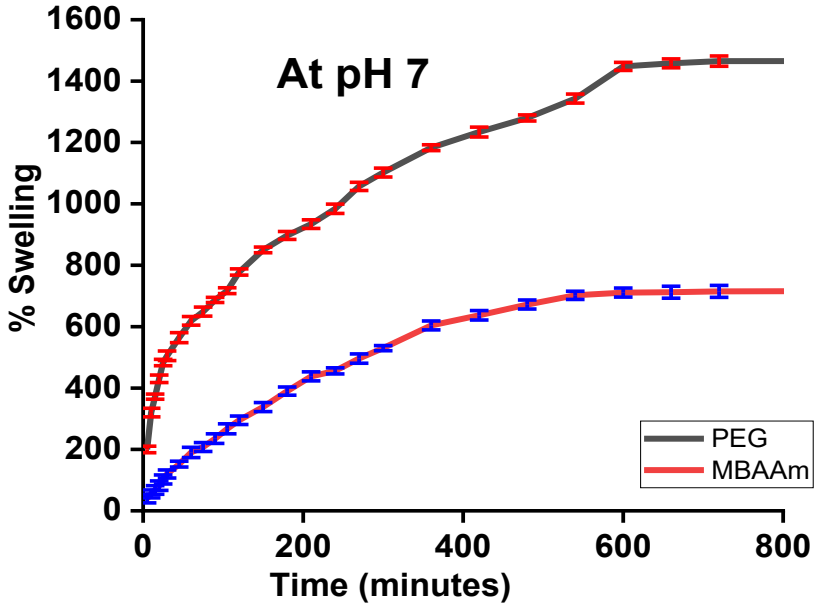

Figure 6.1(b) Swelling Behaviour of Hydrogel Composites at pH 7

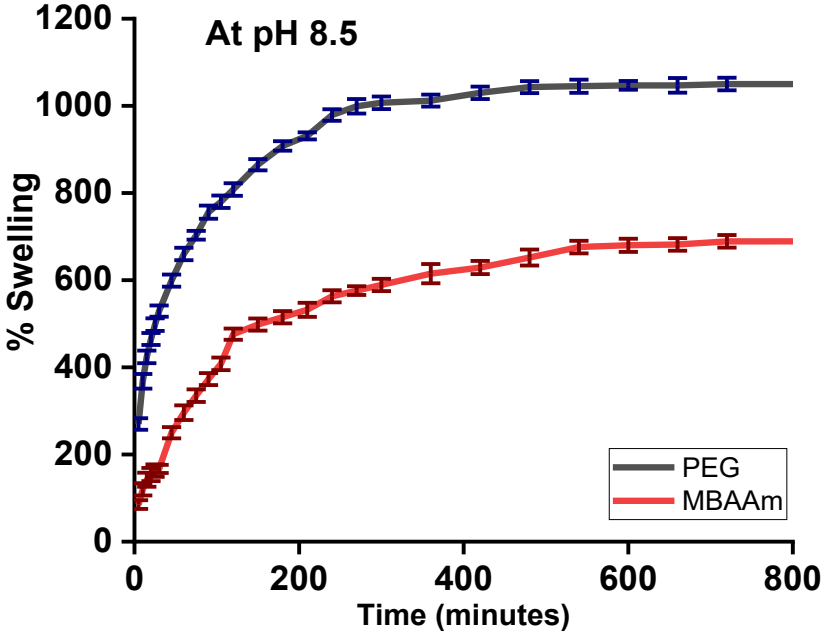

Figure 6.1(c) Swelling Behaviour of Hydrogel Composites at pH 8.5

There appeared a gradual sweep in swelling up to a certain point and then it became constant. This constant value was taken as the equilibrium swelling of the composites. Equilibrium swelling was maximum [i.e., 1466 % and 720 % respectively for cell-$(AAm)_n$-$(AAc)_n$-PEG and cell-$(AAm)_n$-$(AAc)_n$-MBAAm] at neutral (7.0) pH and minimum [i.e., 736 % and 490 % respectively for cell-$(AAm)_n$-$(AAc)_n$-PEG and cell-$(AAm)_n$-$(AAc)_n$-MBAAm] in acidic medium below the pK_a of acrylic acid (below pH 4.7). In alkaline medium, however, the equilibrium swelling was intermediate of these two [i.e., 1050 % and 690 % respectively for cell-$(AAm)_n$-$(AAc)_n$-PEG and cell-$(AAm)_n$-$(AAc)_n$-MBAAm]. This is because at lower pH (below the pK_a of AAc), the carboxylic groups, which were not involved in cross-linking with the hydroxyl group of PEG, remain unionised and form hydrogen bonds with the amine group of acrylamide. Thus, polymer-polymer interaction becomes more dominant over the polymer-solvent (water) interactions[97]. So the hydrogel shrank and aggregate together in absence of any repulsive forces causing less swelling. With rise in pH, the repulsion generated due to ionisation of carboxylic groups leads a large pore size and hence, results in more swelling. In alkaline media, the structure and physical forces get weaken due to the dissociation of the carboxylic group leading to smaller pore size and hence, somewhat less swelling.

At all the pHs swelling was higher in the case of cell-$(AAm)_n$-$(AAc)_n$-PEG as compared to cell-$(AAm)_n$-$(AAc)_n$-MBAAm. This might be attributed to the difference in the hydrophilicity and chain structure of the cross-linker used. In cell-$(AAm)_n$-$(AAc)_n$-PEG, hydrophilicity and comparatively longer chains of PEG might lead to larger pores for holding more water. It can also be justified through the network parameter such as polymer volume fraction, average molar mass between cross-links

M_c, cross-link density, q and mesh size (ξ) for cell-$(AAm)_n$-$(AAc)_n$-PEG and cell-$(AAm)_n$-$(AAc)_n$-MBAAm[81]. These parameters are shown in Table 6.1.

Table 6.1: Network Parameters of Hydrogel Composites, Cell-$(AAm)_n$-$(AAc)_n$-PEG and Cell-$(AAm)_n$-$(AAc)_n$-MBAAm

Network Parameter	Hydrogel Composite	
	Cell-$(AAm)_n$-$(AAc)_n$-PEG	**Cell-$(AAm)_n$-$(AAc)_n$-MBAAm**
Polymer volume fraction,$v_{2,s}$	0.28	0.67
Average molecular weight between cross-links, M_c	1.293×10^{6}	6.827×10^{4}
Cross-link density, q	4.53×10^{-5}	1.05×10^{-3}
Mesh size,(ξ) (in Å)	1120	193

This table revealed a higher M_c value in the case of cell-$(AAm)_n$-$(AAc)_n$-PEG showing its more water absorbing tendency as compared to cell-$(AAm)_n$-$(AAc)_n$-MBAAm. As the average molar mass between cross-links M_c increased, cross-link density decreased, which was also evident from the values obtained by calculations. This table also revealed an increase in mesh size (ξ) with decrease in polymer volume fraction showing a high water content which was observed in case of cell-$(AAm)_n$-$(AAc)_n$-PEG.

6.1.1 *Swelling Kinetics*

To study swelling kinetics the swelling data was fitted in different models like Peppas-model, first-order and second-order kinetic equations. The results have been reported in Figure 6.2 for cell-$(AAm)_n$-$(AAc)_n$-PEG and cell-$(AAm)_n$-$(AAc)_n$-MBAAm.

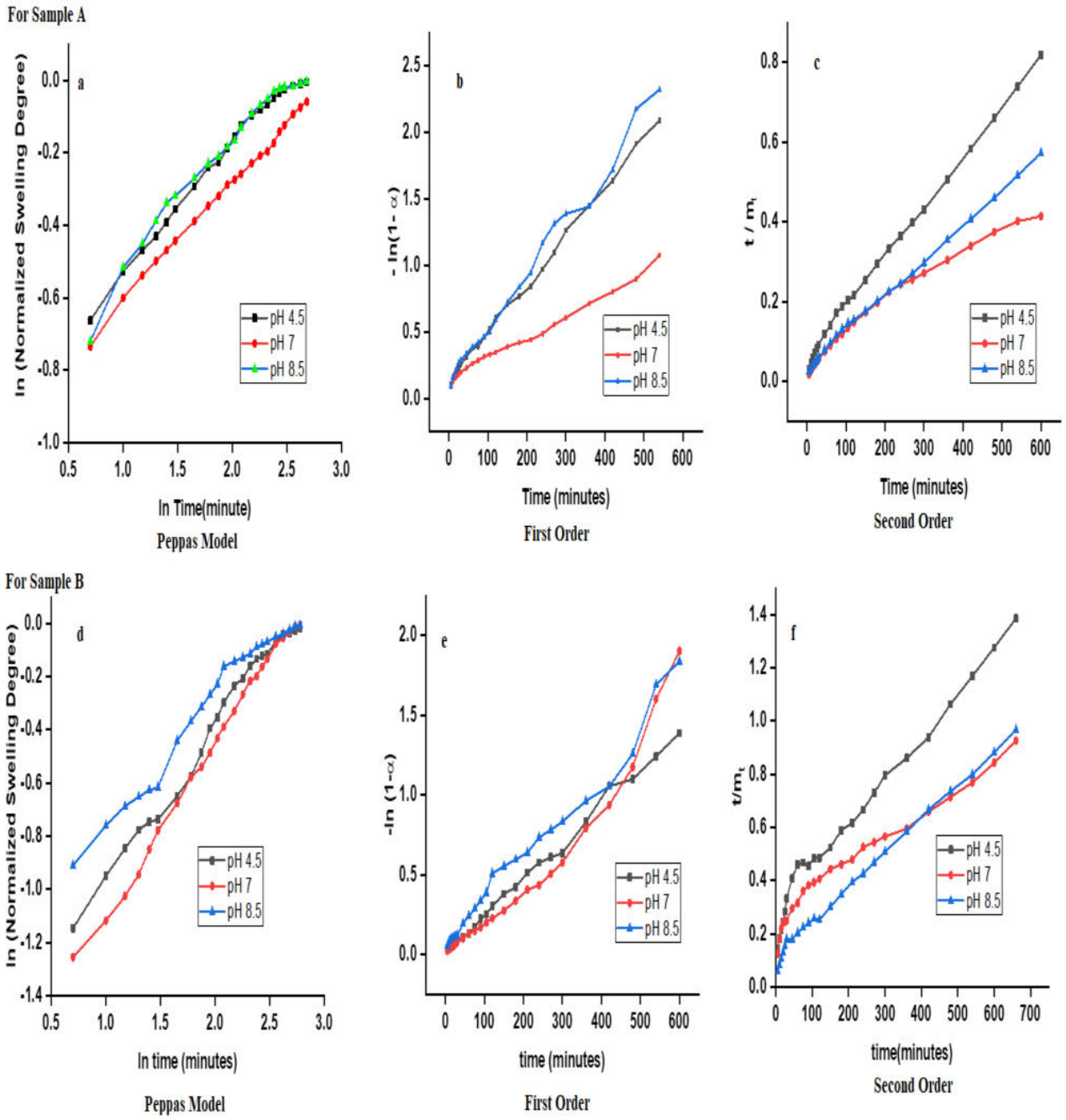

Figure6.2 Swelling Kinetics for Sample A (a) Peppas Model (b) First-order (c) Second-order, and Sample B (d) Peppas Model (e) First-order (f) Second-order

Where Sample A= cell-$(AAm)_n$-$(AAc)_n$-PEG, and Sample B = cell-$(AAm)_n$-$(AAc)_n$-MBAAm

Related kinetic constants have been summarised in Table 6.2.

Table 6.2: Kinetic Constants for Swelling at Different pH for Sample A and Sample B

pH value		Model Name						
		Peppas Model			First-order		Second-order	
		R^2	n	k	R^2	$k(s^{-1})$	R^2	$k(Lmol^{-1}s^{-1})$
4.5	Sample A	0.978	0.324	0.432	0.998	0.0036	0.997	3×10^{-5}
	Sample B	0.987	0.57	0.21	0.94	0.0022	0.97	1×10^{-5}
7	Sample A	0.997	0.327	0.392	0.989	0.0016	0.971	1×10^{-5}
	Sample B	0.997	0.65	0.173	0.62	0.56	0.96	4.2×10^{-6}
8.5	Sample A	0.976	0.35	0.416	0.994	0.004	0.998	2.3×10^{-5}
	Sample B	0.97	0.56	0.294	0.84	0.58	0.99	1.6×10^{-5}

Where Sample A =cell-$(AAm)_n$-$(AAc)_n$-PEG, and Sample B = cell-$(AAm)_n$-$(AAc)_n$-MBAAm

From Table 6.2, in case of cell-$(AAm)_n$-$(AAc)_n$-PEG, highest R^2 values for first-order kinetics at pHs 4.5 and 7.0 suggested a first-order swelling kinetics in acidic and neutral medium which showed that the swelling varied directly with the water content present in the hydrogel before achieving the state of equilibrium. However, at pH 8.5, the R^2 value was highest for second-order kinetics showing a second-order swelling kinetics in alkaline medium, which indicated a direct relation of swelling with the square of water content present in the composite before achieving equilibrium. Table 6.2 also revealed that the value of *n* for cell-$(AAm)_n$-$(AAc)_n$-PEG in all the cases was below 0.5 which was a case of Fickian diffusion i.e., swelling took place mainly by diffusion rather than chain relaxation[86]. A similar trend was reported by Purwar et al. for a similar type of hydrogel composite[139].

Contrary to this, swelling in case of cell-$(AAm)_n$-$(AAc)_n$-MBAAm followed second-order kinetics at all the tested pHs (as revealed by R^2 values). For cell-$(AAm)_n$-$(AAc)_n$-MBAAm, *n* value was greater than 0.5 at 4.5 and 7.0 pH, showing anomalous (Non-Fickian) diffusion at these pHs. It showed the nearly equal

contribution of diffusion and chain relaxation towards the swelling of hydrogel composites. Although the behaviour turned from anomalous to slight Fickian at higher i.e., 8.5 pH as suggested by *n* value (0.46). Thakur et al[35] also observed a second-order swelling kinetics and non-Fickian mechanism for poly(acrylamide-co-acrylic acid) hydrogel system prepared by using MBAAm as cross-linker.

The weight loss after swelling experiment in the case of cell-$(AAm)_n$-$(AAc)_n$-PEG was 40% whereas in the case of cell-$(AAm)_n$-$(AAc)_n$-MBAAm it was only 8%. It suggested that cell-$(AAm)_n$-$(AAc)_n$-PEG disintegrated faster as compared to cell-$(AAm)_n$-$(AAc)_n$-MBAAm because it hold more water due to its more hydrophilicity and large pores but the inter particles entanglement were weaker as compared to that generated by MBAAm as cross-linker.

6.2 Antimicrobial Behaviour

Results of antimicrobial tests are revealed in Figure 6.3(a) and 6.3(b). A clear zone of inhibition of growth of bacterial colonies below and around the drug loaded composite was observed whereas a dense population of bacterial colonies appeared in the control set that contained hydrogel composite having no drug. The zone diameter for *E.coli*. and *S. aureus.* were 17.5mm and 14.0mm in case of cell-$(AAm)_n$-$(AAc)_n$-PEG whereas these were found to be 15.0mm and 11.0mm for cell-$(AAm)_n$-$(AAc)_n$-MBAAm because drug (gentamicin sulphate) destroyed the bacterial cell when comes in its contact. Inhibiting action of drug-loaded composite material was a piece of evidence for drug release from both the composite samples.

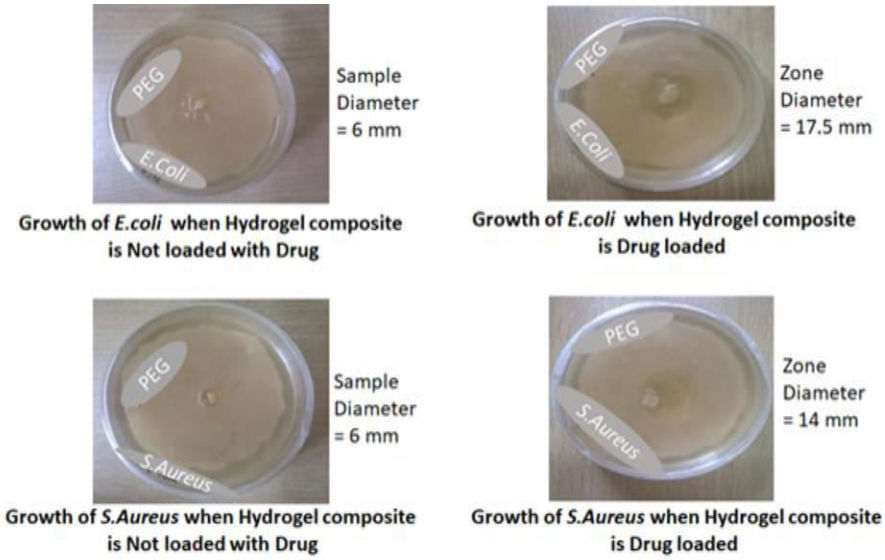

Figure 6.3(a) Antimicrobial Behaviour of Cell-$(AAm)_n$-$(AAc)_n$-PEG

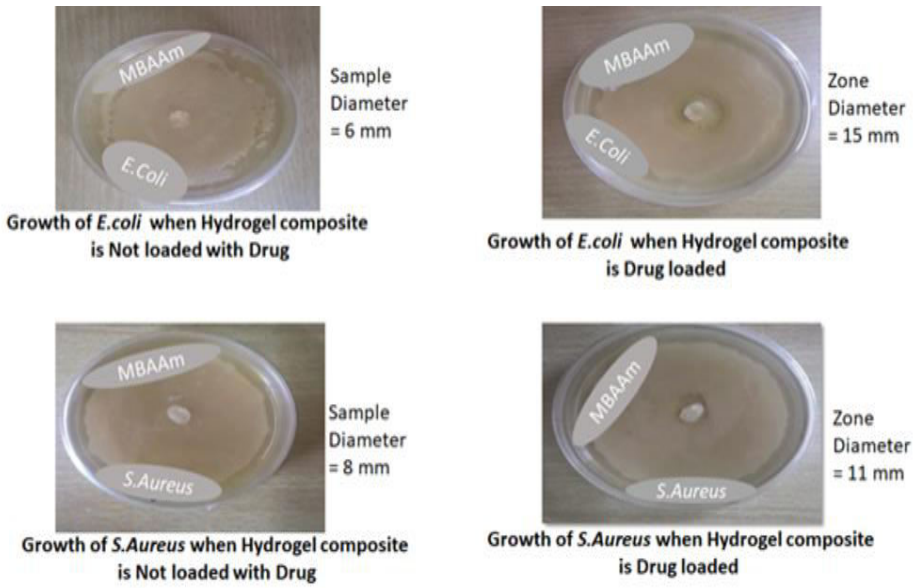

Figure 6.3(b) Antimicrobial Behaviour of Cell-$(AAm)_n$-$(AAc)_n$-MBAAm

More diameter of zone of inhibition in cell-$(AAm)_n$-$(AAc)_n$-PEG as compared to cell-$(AAm)_n$-$(AAc)_n$-MBAAm supported the dependency of bactericidal action of composite material upon the amount of drug released, i.e., upon the swelling and drug loading property of the composite.

6.3 Drug Release Studies

When gentamicin sulphate drug was used, the aliquot was derivatized using the method proposed by Pishbin et al[140]. In this method, a reactive solution was prepared by dissolving 130.0mg ortho-phthalaldehyde in 0.5mL methanol and then mixing it with 3.8mL borate buffer (pH 10.4) and 290.0µL 2-mercaptoethanol. Final volume of the reactive mixture was made 5.0mL using borate buffer. For derivatization, mixture of 1.0mL aliquot, 0.4mL reactive mixture and 1.2mL 2-propanol was kept in a heating bath at 40°C for 5minutes. The calibration curve was made using gentamicin sulphate derivative solutions having concentrations in the range 0.0 to 0.1mgml^{-1} at 333nm. The aliquot derivatives were analysed spectrophotometrically at 333nm using Cary 300 UV-VIS spectrophotometer.

UV-VIS spectrophotometer was used to check the amount of drug loaded in the composites. This amount was calculated from the difference of amount taken initially and the amount of drug remaining in the mother liquor after loading in the composites. The amount of drug loaded was found to be 76.45 % and 55.89 % respectively for cell-$(AAm)_n$-$(AAc)_n$-PEG and cell-$(AAm)_n$-$(AAc)_n$-MBAAm. Although a good amount of drug was loaded in both the cases but more drug was loaded in case of cell-$(AAm)_n$-$(AAc)_n$-PEG due to more hydrophilicity and optimum pore size in this case.

Figure 6.4 reveals plots of drug release as a function of time.

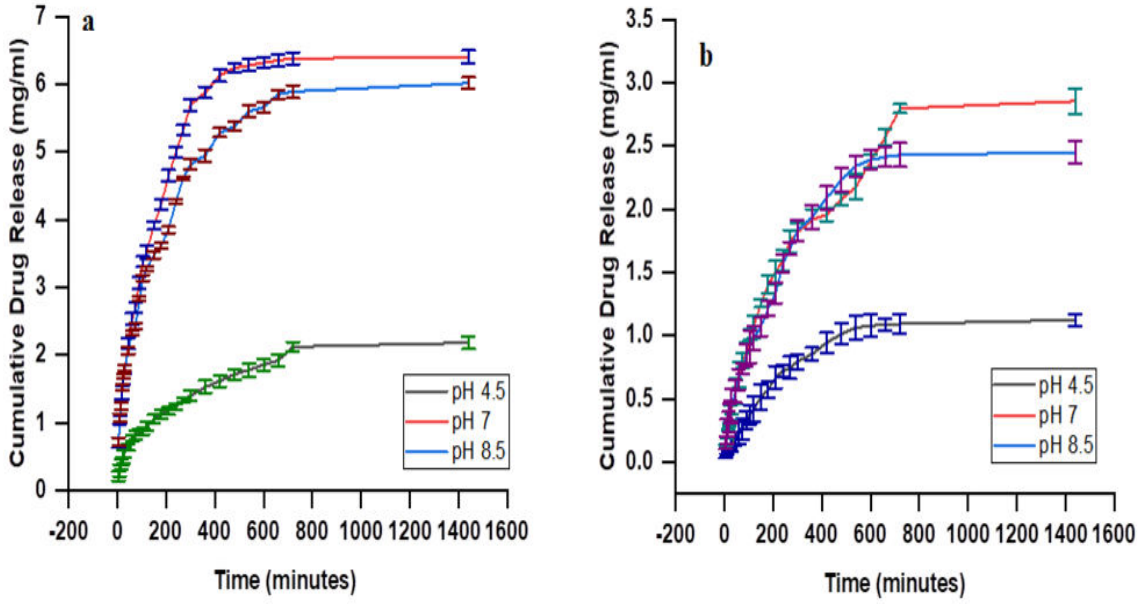

Figure 6.4 Cumulative Drug Release from (a) Cell-$(AAm)_n$-$(AAc)_n$-PEG (b) Cell-$(AAm)_n$-$(AAc)_n$-MBAAm

From these plots, it was evident that maximum drug release was observed at pH 7.0. Below and above this pH, hydrogen bonding and weakening of physical forces between polyacrylic acid and polyacrylamide respectively resulted in lesser release. Up to 68% drug was released in the first 12 h in the case of cell-$(AAm)_n$-$(AAc)_n$-PEG while it was only 62% in the case of cell-$(AAm)_n$-$(AAc)_n$-MBAAm.

6.3.1 *Drug Release Kinetics*

Drug release data were fitted in different kinetic models like Peppas-model, Higuchi-model, zero-order, first-order and second-order equations. These plots for cell-$(AAm)_n$-$(AAc)_n$-PEG and cell-$(AAm)_n$-$(AAc)_n$-MBAAm are shown in Figure 6.5.

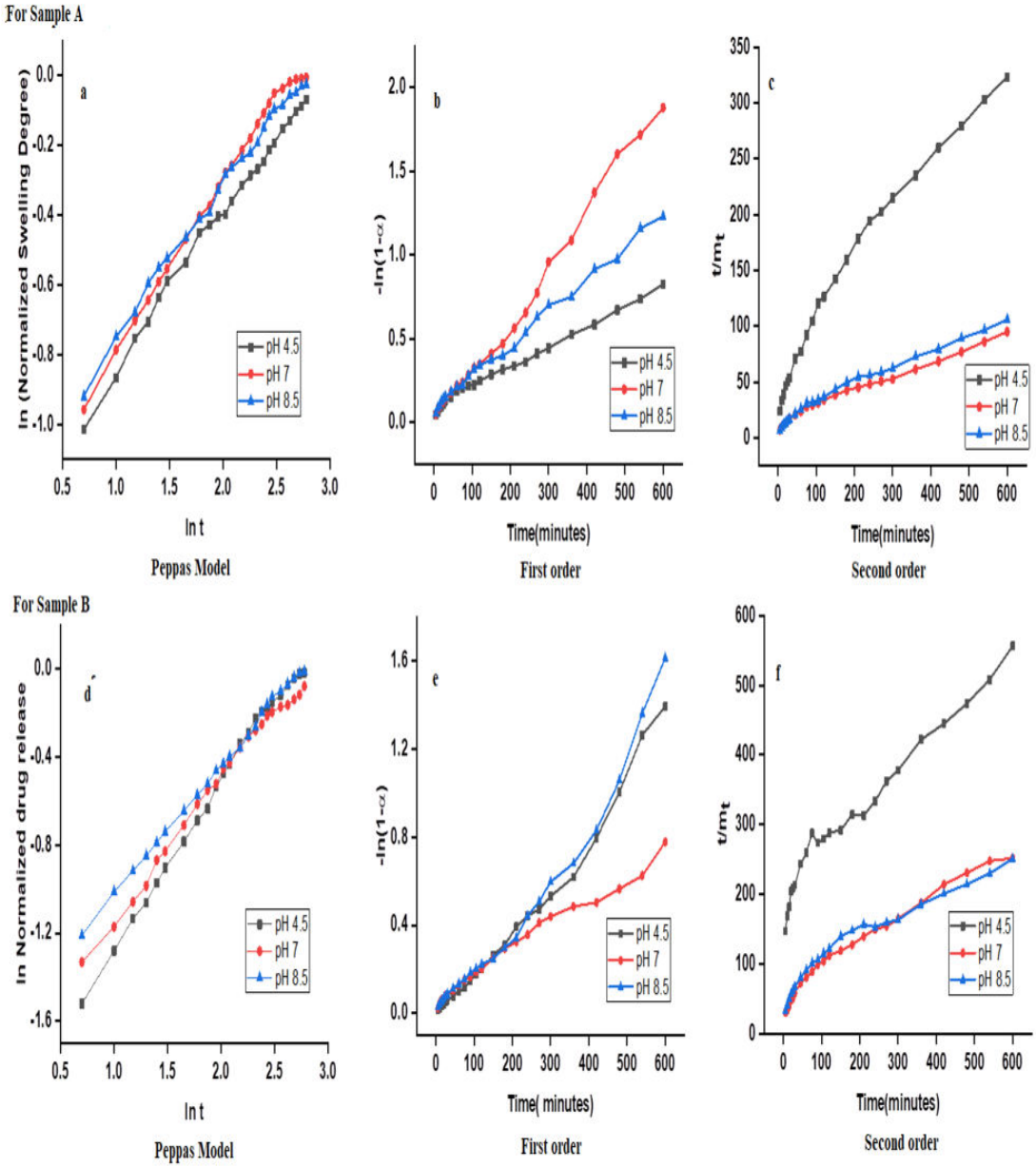

Figure 6.5 Drug Release Kinetics for Cell-$(AAm)_n$-$(AAc)_n$-PEG (a-c) and for Cell-$(AAm)_n$-$(AAc)_n$-MBAAm (d-f)

[Where, Sample A= cell-$(AAm)_n$-$(AAc)_n$-PEG and Sample B= cell-$(AAm)_n$-$(AAc)_n$-MBAAm]

The plots showing maximum linearity, was supposed to be the best fit model in each case. The kinetic constants of different models for these two composites at different pHs are summarized in Table 6.3.

Table 6.3: Kinetic Constants for Drug Release at Different pH for Composite Cell-$(AAm)_n$-$(AAc)_n$-PEG and Cell-$(AAm)_n$-$(AAc)_n$-MBAAm

pH Value		Model Name						
		Peppas-Model			First-order		Second-order	
		R^2	n	k	R^2	$k(s^{-1})$	R^2	$k(Lmol^{-1}s^{-1})$
4.5	**Sample A**	0.994	0.438	0.28	0.993	0.0012	0.97	5×10^{-3}
	Sample B	0.995	0.74	0.134	0.977	0.0036	0.96	1.8×10^{-3}
7	**Sample A**	0.99	0.43	0.29	0.99	0.0017	0.98	2.6×10^{-3}
	Sample B	0.991	0.62	0.174	0.984	0.0012	0.98	2×10^{-3}
8.5	**Sample A**	0.99	0.416	0.32	0.995	0.0019	0.98	1.8×10^{-3}
	Sample B	0.998	0.586	0.199	0.96	0.0023	0.93	1.7×10^{-3}

[Where, Sample A= cell-$(AAm)_n$-$(AAc)_n$-PEG and Sample B= cell-$(AAm)_n$-$(AAc)_n$-MBAAm]

From the table, it was evident that the value of correlation coefficient was highest for Peppas-model at all the studied pHs. It means drug release followed Peppas-model in both cases. According to this model, for a slab like drug delivery system, value of release exponent provides information about the type of diffusion. A system having the value of $n \leq 0.5$ corresponds to Fickian diffusion, that having value $0.5 < n < 1$ corresponds to anomalous or non –Fickian transport and that having value ≥ 1 corresponds to case II transport[86,87].

Table 6.3 also revealed the value of *n* below 0.5 showing Fickian type drug release i.e. drug release was mainly controlled by diffusion rather than chain relaxation in case of cell-$(AAm)_n$-$(AAc)_n$-PEG. Value of constant k also increased with a rise in pH of medium showing its dependency upon the structural constitution of the hydrogel composite. At lower pH hydrogen bonds formed by unionised

carboxylic group resulted in smaller pores. At a pH greater than pK_a of AAc (pK_a = 4.7) repulsion among negatively charged carboxylate ions led to the formation of larger pores. In alkaline medium diminishing of physical forces between PAAc and PAAm further resulted in somewhat smaller pore size. These results were in agreement with that reported by Purwar et al[139]. Table 6.3 shows value of *n* greater than 0.5 supporting a non-Fickian diffusion. It means drug release was governed by diffusion as well as chain relaxation in the case of cell-$(AAm)_n$-$(AAc)_n$-MBAAm.

Mesh size calculation revealed a higher mesh size in case of cell-$(AAm)_n$-$(AAc)_n$-PEG i.e. it had more surface area so drug release was governed by diffusion rather than chain relaxation, a case of Fickian diffusion. On the other hand, drug release from cell-$(AAm)_n$-$(AAc)_n$-MBAAm was governed by diffusion as well as chain relaxation (a case of non-Fickian diffusion) because of its lesser mesh size (as represented in Figure 6.6).

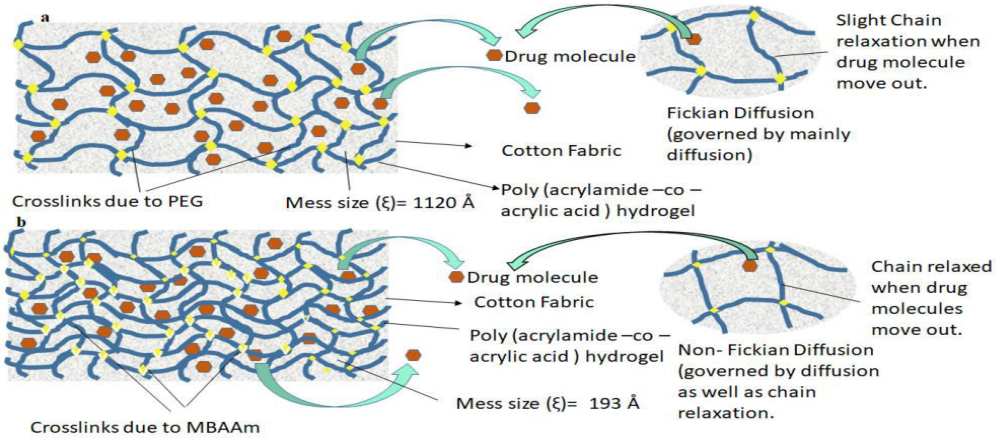

Figure 6.6 Schematic Diagram Showing Mechanism of Drug Release from (a) Cell-$(AAm)_n$-$(AAc)_n$-PEG (b) Cell-$(AAm)_n$-$(AAc)_n$-MBAAm

CHAPTER 7:

FABRICATION AND CHARACTERIZATION OF POLY (ACRYLAMIDE-CO-ACRYLIC ACID) HYDROGEL NANOFIBERS

In this chapter, the reaction mechanism involved in the preparation of hydrogel nanofibers has been discussed. The morphological and structural analysis of the poly (acrylamide-co-acrylic acid) hydrogel nanofibers have also been revealed by using FTIR, SEM, DSC and TGA techniques. The swelling and drug release behaviour of the hydrogel nanofibers have also been explored

7.1 Reaction Mechanism

When AAc was treated with APS, it attacked at the unsaturated carbon generating free radicals. When this solution was added to the solution of acrylamide, the free radicals attacked at the unsaturated carbon of acrylamide forming another free radicals. Thus, a chain reaction was initiated. Subsequent addition of monomer units

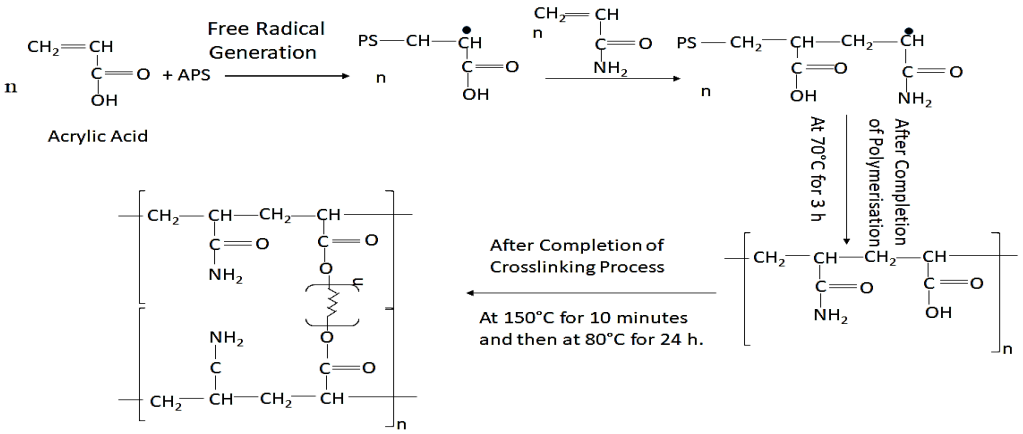

Figure 7.1 Reaction Mechanism Showing Formation of Poly (acrylamide-co-acrylic acid) Copolymer Dope Solution

resulted in the propagation of the chain leading to the formation of copolymer of poly (acrylamide-co-acrylic acid). The dope solution was electrospun and subjected to heat treatment at a temperature of 150°C for 10 minutes to introduce ester linkage in between the polymer chains. The reaction mechanism for the formulation of hydrogel nanofibrous mat was shown in Figure 7.1.

7.2 Morphological Analysis

Morphology of hydrogel nanofibrous mats was shown by its SEM images as given in Figure 7.2(a).

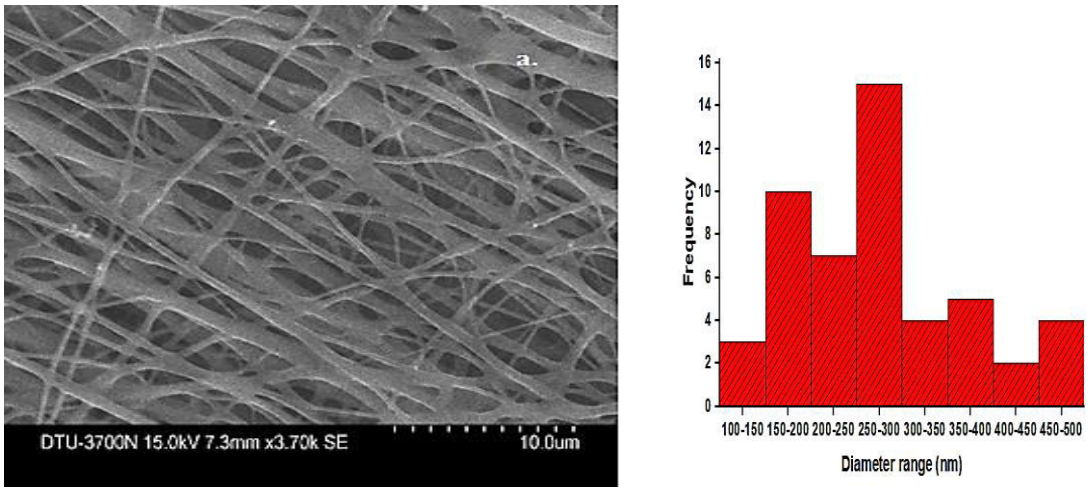

Figure 7.2 (a) SEM Image of Hydrogel Nanofibrous Mat (b) J Image Analysis for Fibre Diameter

Bead less nanofibrous morphology was obtained at 23kV voltage. However, there appeared a large variation in the fibre diameter. Figure 7.2(b) showed the diameter distribution of different nanofibers. The average diameter of the nanofibers was found to be 275nm±94.5. This was due to the change in viscosity of the solution with passage of time. The average diameter and bead less structure of nanofibers depended on the concentration of polymer in the dope solution, molecular weight of the polymer, and process parameters of the electrospinning machines. Similar

diameter range were reported for hydrogel nanofibers made from CTS-g PNIPAAm / poly (ethylene oxide)[52] and PVA[141]. The diameter of poly (acrylamide-co-maleic acid) hydrogel nanofibers was found to be lower i.e., 120nm[127]. The average diameter of chitosan / PLA / PEG[129] and chitosan / PVA[142] hydrogel nanofibers were reported to be 341nm and 430nm respectively.

7.3 Structural Properties

In Figure 7.3 FTIR spectra of non-cross linked and cross-linked nanofibrous mats are shown.

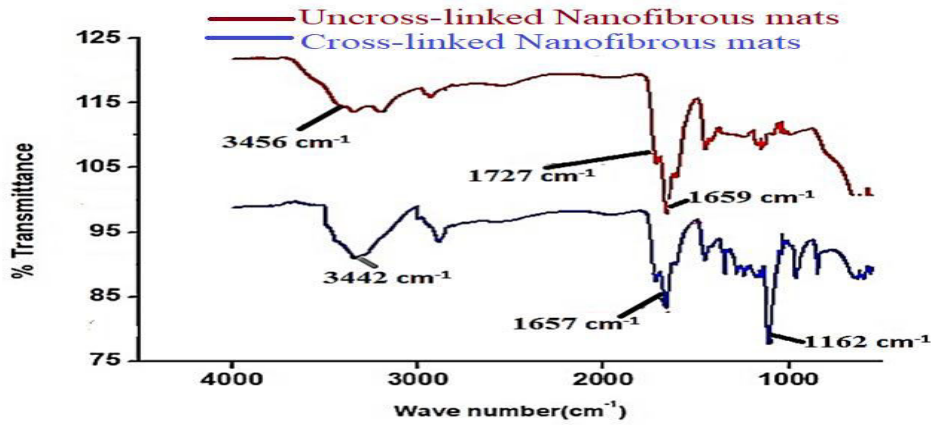

Figure 7.3 FTIR Spectra for Uncross-linked and PEG Cross-linked Nanofibrous Mats

Figure 7.3 clearly revealed the characteristic bands of copolymer of poly (acrylamide-co-acrylic acid). In this spectra, band at 3456cm^{-1} was due to N-H stretching, at 1727cm^{-1} it was for C=O (C=O of acidic group) stretching, and at 1659cm^{-1}, it was for C=O (C=O of acrylamide group) stretching. In the spectra of cross-linked nanofibrous mats, an extra band at 1167cm^{-1} was for C-O-C stretching showing the presence of PEG cross-linking in hydrogel. Other characteristic bands of poly (acrylamide-co-acrylic acid) cross-linked with PEG such as N-H stretching at

3442cm^{-1}, C=O (C=O of acrylamide group) stretching at 1658cm^{-1} and C=O (C=O of acidic group) stretching at 1727cm^{-1} also appeared in it.

These results were in close agreement with the FTIR results reported by Purwar et al[26]., where they examined the cotton grafted poly (acrylamide-co-acrylic acid) hydrogel.

7.4 Thermal Properties

These properties of cross-linked and non-cross-linked nanofibrous mats were analysed through DSC and TGA.

Figure 7.4 shows the DSC thermogram of cross-linked and non-cross-linked nanofibrous mats.

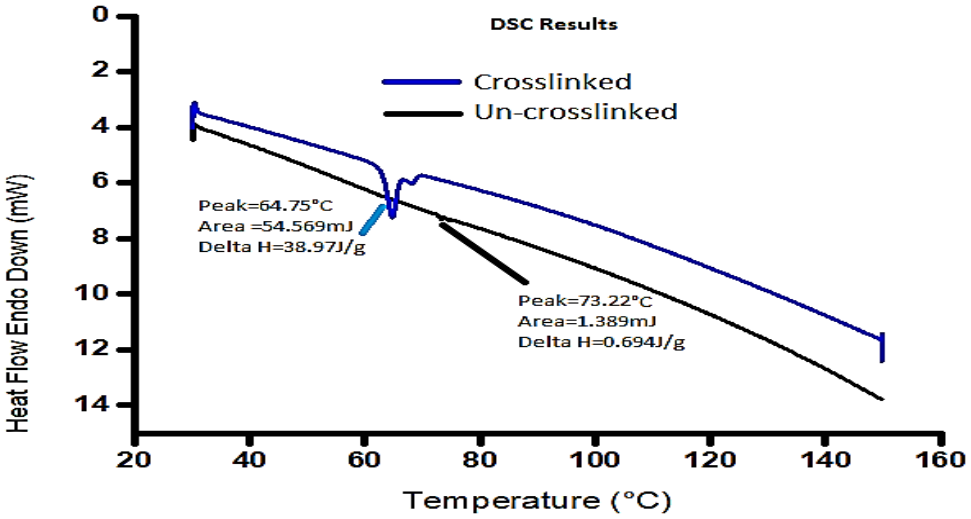

Figure 7.4 DSC Thermogram of Uncross-linked and PEG Cross-linked Nanofibrous Mats

The non-cross-linked sample and cross-linked nanofibrous mats showed endothermic peaks at 73.22°C and 64.75°C due to loss of water[34]. The values of enthalpy are 0.694Jg^{-1} and 38.97Jg^{-1} at endothermic peak of 73.22°C and 64.75°C

respectively. The higher enthalpy value for cross-linked nanofibrous mats as compared to that of uncross-linked sample suggested that the nanofibrous hydrogel had more capacity to hold water as compared to its non-cross-linked counterpart.

The thermal degradation behaviour of non-cross-linked and cross-linked nanofibrous mats is shown in Figure 7.5.

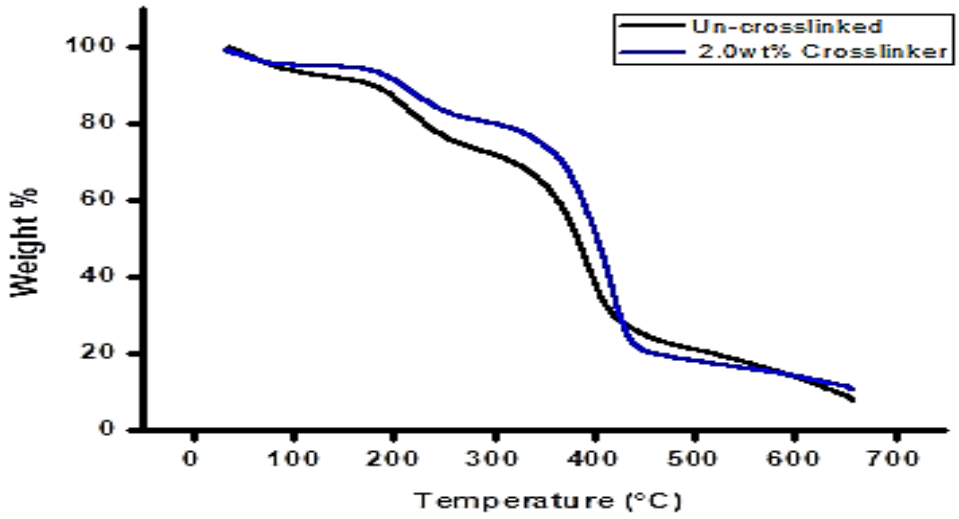

Figure 7.5 TGA Thermogram of Non-cross-linked and PEG Cross-linked Nanofibrous Mats

Both the samples showed three steps degradation behaviour. Initially up to 100°C, the mass loss was due to water content. The cross-linked sample showed higher thermal stability as compared to non-cross-linked sample above 400°C.

7.5 Swelling Behaviour

The swelling behaviour of hydrogel nanofibrous mat as a function of time was studied at different pHs (in the range of 2.0 to 8.5) and the results are shown in Figure 7.6.

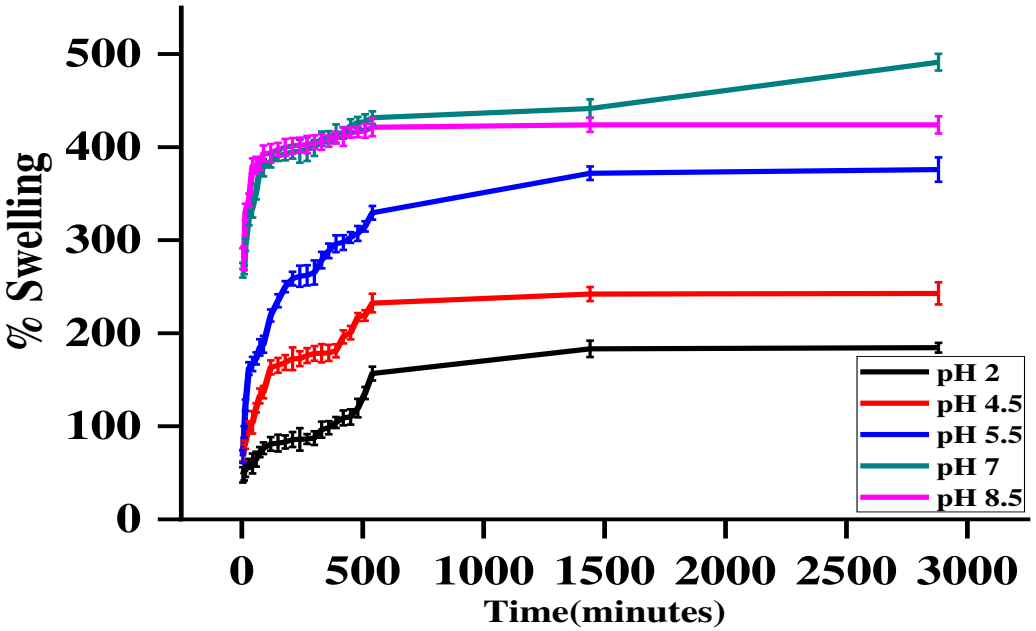

Figure 7.6(a) Swelling Behaviour of Hydrogel Nanofibrous Mat at Different pHs

It was observed that the hydrogel nanofibrous mats i.e., cross-linked nanofibrous mats, attained the maximum percentage swelling within 8h at all the pHs. However, a continuous swelling was observed up to 30h. The percent swelling increased with increase in pH upto pH 7.0 and then decreased. The maximum percent swelling (430%) was achieved at pH 7.0 (neutral medium). This swelling behaviour of poly (acrylamide-co-acrylic acid) hydrogel nanofibrous mat can be explained by the fact that at lower pH i.e., below the pK_a of AAc, all the pendant groups exist in unionized form and some hydrogen bonds may exist between carboxylic acid and

amino groups. Formation of hydrogen bonds reduces the available space for holding water molecules resulting in low percentage swelling.

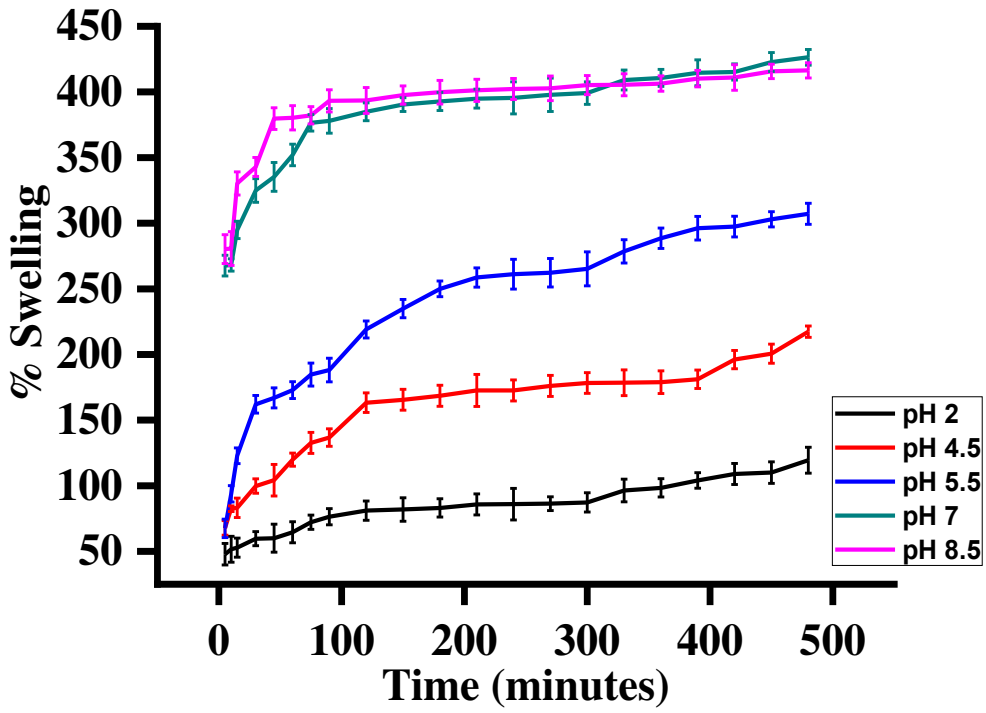

Figure 7.6(b) Swelling Behaviour of Hydrogel Nanofibrous Mats in First 500 Minutes

In alkaline pH (8.5), a decline in percent swelling was because of the dissociation of carboxylic group in alkaline medium. Due to which the physical forces existing between poly acrylic acid and poly acrylamide became weak, hence pores got diminished. Similar results were observed in our previous study where poly (acrylamide-co-acrylic acid) hydrogel cross-linked with polyethylene glycol was grafted over cotton fabric.

A major observation was found that the hydrogel nanofibrous mat achieved equilibrium swelling in 10h. In case of grafted hydrogel films the equilibrium swelling was achieved after 20h, however the amount of maximum swelling percentage

achieved 800%[139]. The swelling percentage of polyacrylic acid nanofibers cross-linked with β-cyclodextrin was reported 1800% at pH 7.0. Jin et al.[143] have compared swelling behaviour of hydrogel films and nanofibrous mat prepared with polyvinyl alcohol / polyacrylic acid blend and reported that percent swelling increased with rise in pH. The mass swelling of films were found higher than that of nanofibrous mat. The nanofibrous hydrogel attained equilibrium swelling within 10minutes as compared to 30minutes in the film form.

7.5.1 *Swelling Kinetics*

Swelling kinetics of the hydrogel nanofibrous mats was studied by fitting the swelling data into different kinetic models namely Peppas-model, Higuchi-model, zero-order, first-order and second-order kinetics equations. The plots of the models / equations, having higher value of R^2, are shown in Figure 7.7(a) to (c).

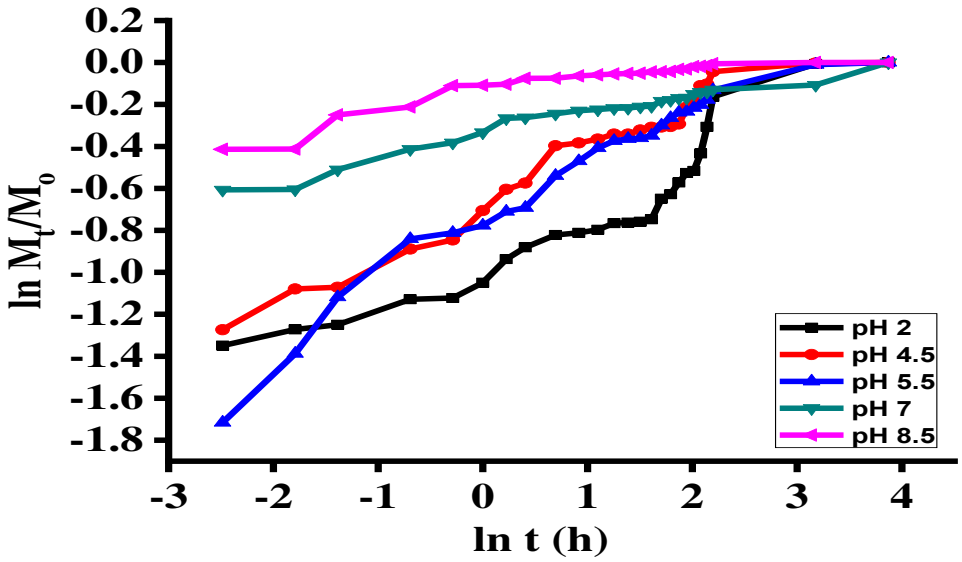

Figure 7.7(a) Peppas-Model

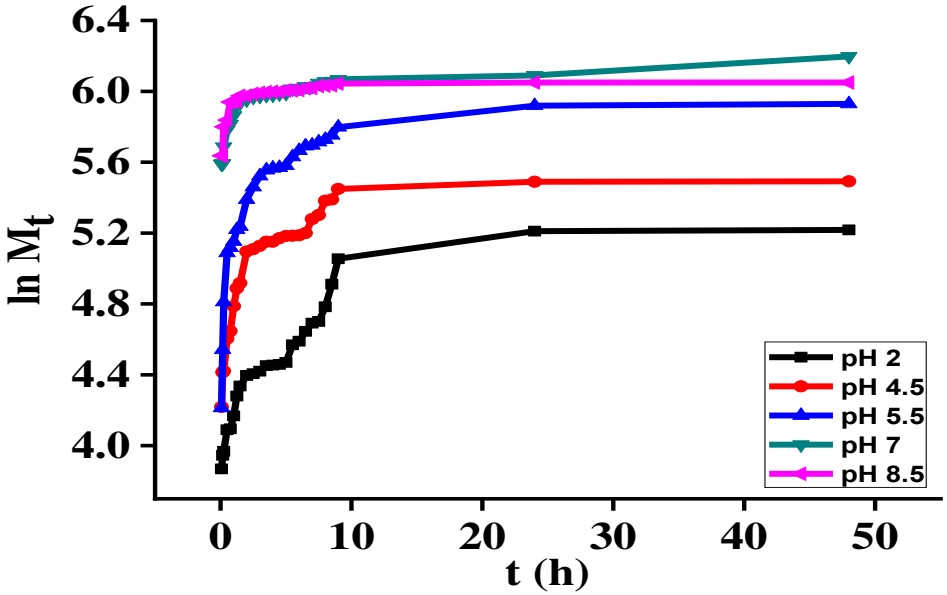

Figure 7.7(b) First-order

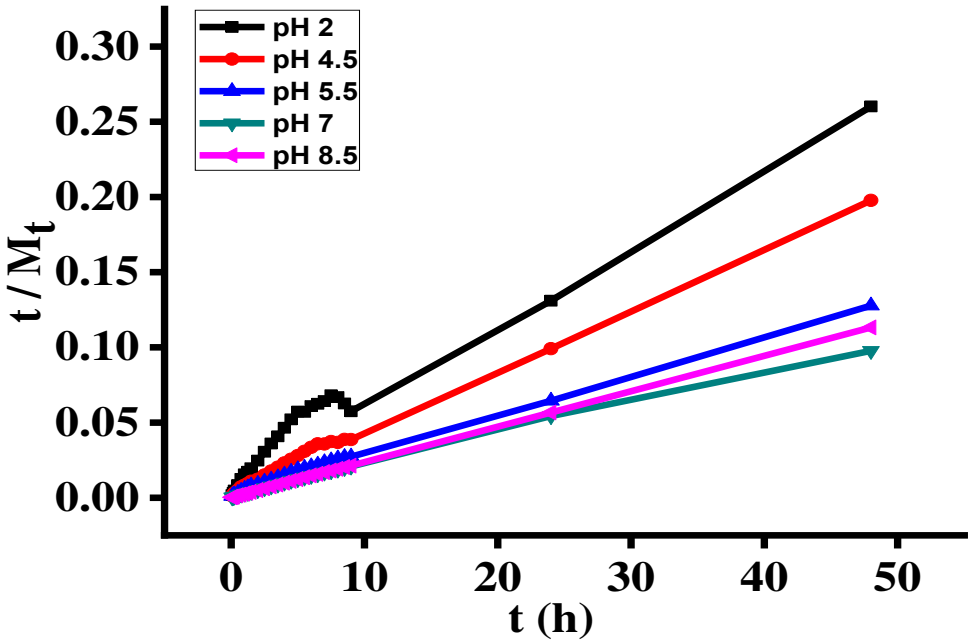

Figure 7.7(c) Second-order

Out of these, the plot having maximum linearity was considered as best fit kinetic model. Kinetic constants for swelling at different pHs using various kinetic models have been summed up in Table 7.1.

Table 7.1: Kinetic Constants for Swelling at Different pH

	Peppas Model			First-order Model		Second-order Model	
pH	**$(R^2)^a$**	**n^b**	**k^c**	**$(R^2)^a$**	**k^c**	**$(R^2)^a$**	**k^c**
2	0.89	0.23	0.11	0.57	0.027	0.96	0.0017
4.5	0.955	0.23	0.21	0.32	0.02	0.99	0.0032
5.5	0.95	0.27	0.164	0.30	0.029	0.99	0.0018
7	0.98	0.094	0.451	0.399	0.009	0.99	0.0027
8.5	0.86	0.066	0.7	0.19	0.0046	1	0.013

[a]Correlation coefficient,[b] Release exponent,[c] Constant of hydrogels

Value of correlation coefficient (R^2) clearly indicated that swelling followed second order kinetics at all the pHs taken for study (2.0, 5.5, 7.0, 8.5). Literature review revealed that swelling kinetics of polymer hydrogel may be either diffusion controlled (Fickian) or relaxation controlled (non- Fickian). The mechanism of water insertion into the hydrogel nanofibrous mats was governed by diffusion of water molecules into the gel matrix and subsequent relaxation of polymeric chain of hydrogel nanofibers. Literature also revealed first-order swelling kinetics for poly (acrylic acid) hydrogel at all the pHs studied while second-order swelling kinetics for poly (acrylamide-co-itaconic acid) / chitosan and chitosan-g-PAAm hydrogel[91]. In this study, swelling kinetics was of second order at all the pHs studied. It suggested swelling rate varied directly with the square of water content retained in the hydrogel nanofibrous mat before attaining equilibrium. With passage of time, swelling rate decreased rapidly because of its dependence upon the osmotic pressure difference.

Swelling kinetic of poly (acrylamide-co-acrylic acid) hydrogel films emulate first order kinetics at pH 5.5 and 7.0 while at pH 8.5 it emulates second order kinetics[54].

7.6 Antibacterial Activity

A clear inhibition zone was generated within and around the drug loaded samples in the 24h incubated agar plates. This shows the bactericidal behaviour of the hydrogel nanofibrous mats. The growth of inhibition zone, for both Gram-positive and Gram-negative bacteria, were measured. From Figure 7.8, the mean diameter of inhibition zone for Gram-positive bacteria *S. aureus.* was found around 13.5mm and for Gram-negative bacteria *E. coli.* it was found 12mm.

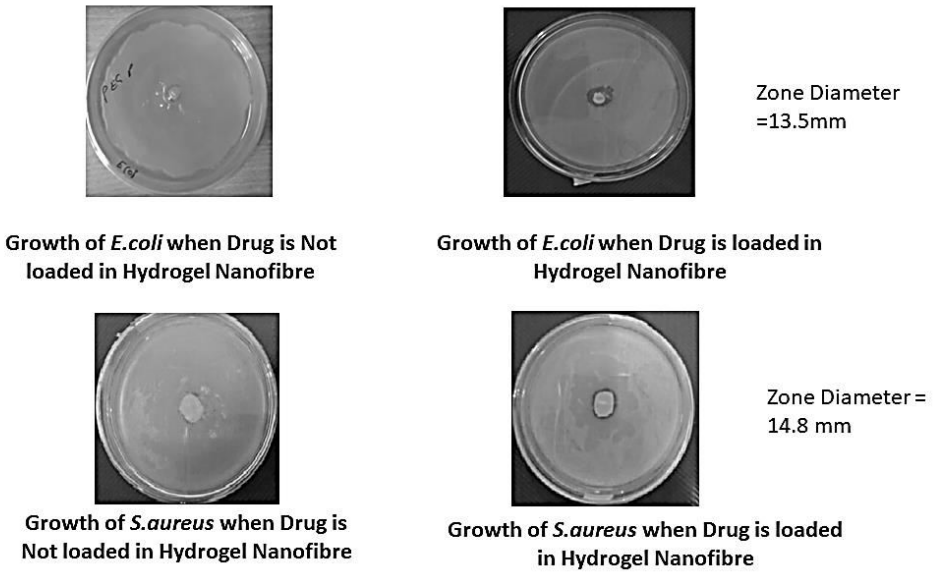

Figure 7.8 Antibacterial Activity of Drug Loaded Hydrogel Nanofibrous Mats

The results showed that amoxicillin drug readily comes out from the nanofibrous mats and show very good zone of inhibition around the samples. The amoxicillin released from the nanofibrous mats ruined the cell walls of both the bacterial strains.

7.7 Drug Release Behaviour

Figure 7.9 shows the amount of drug discharged as a function of time at different pHs.

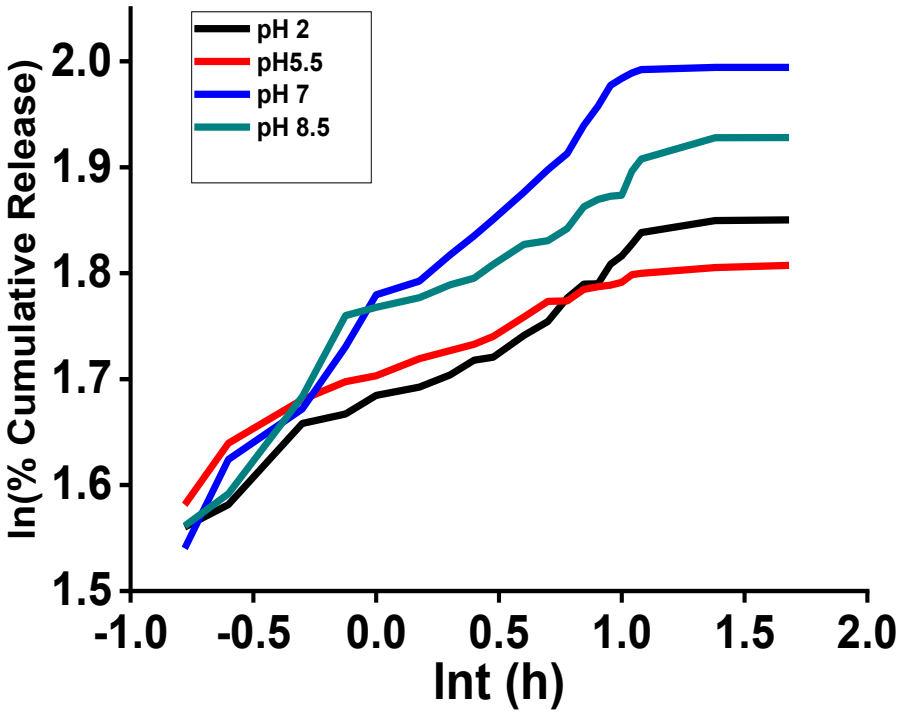

Figure 7.9 Cumulative Drug Release from Hydrogel Nanofibrous Mats

From the Figure it was evident that a considerable amount of drug was discharged at all the pHs and maximum liberation was observed at pH 7.0. Up to 68% of drug came out in first 9 h.

7.7.1 *Drug Release Kinetics*

The drug release data was fitted into various kinetic models like Peppas model, Higuchi model etc. The graphs of Peppas model and Higuchi model are shown in Figure 7.10(a) and (b) respectively.

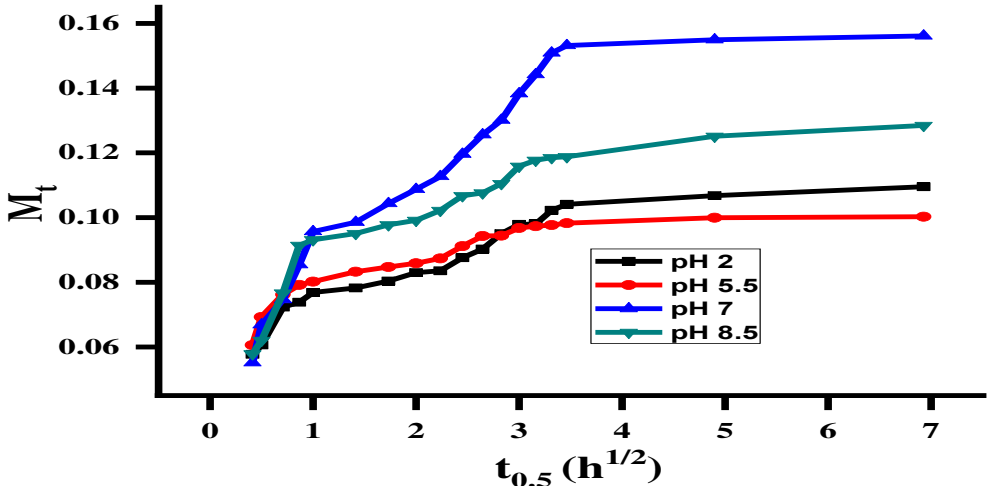

Figure 7.10(a) Plots of Higuchi Model

The graph showing highest linearity was considered as best fit model.

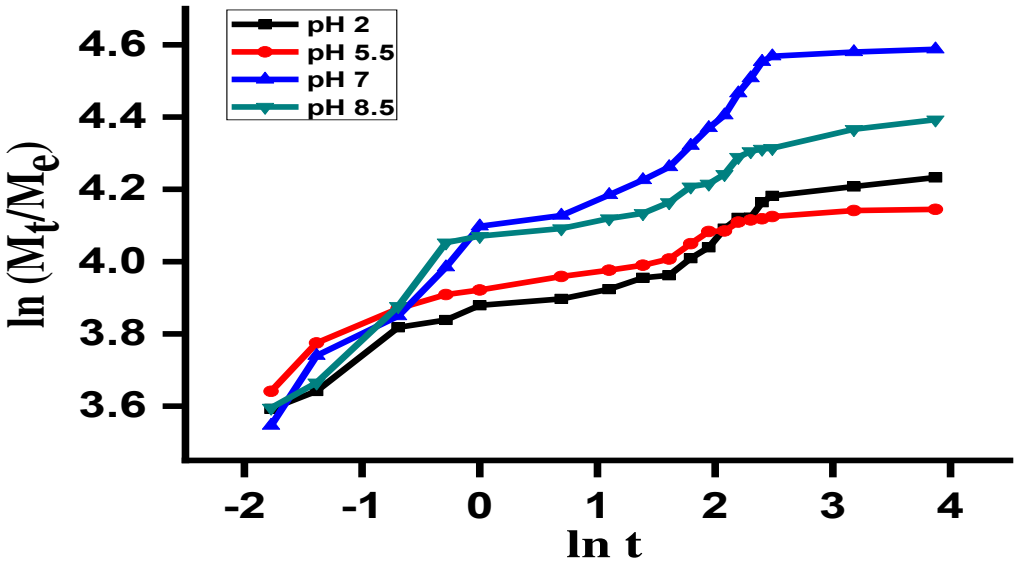

Figure 7.10 (b) Plots of Peppas Model

The kinetic constants for drug release at different pHs for different kinetic models were summarized in Table 7.2.

Table 7.2: Kinetic Constants for Drug Release at Different pH

	Peppas Model			Higuchi Model	
pH	**$(R^2)^a$**	**n^b**	**k^c**	**$(R^2)^a$**	**k^c**
2	0.95	0.12	46.26	0.82	0.008
5.5	0.93	0.21	49.74	0.7	0.006
7	0.95	0.28	54.47	0.78	0.016
8.5	0.91	0.15	52.17	0.74	0.010

[a]Correlation coefficient, [b]Release exponent, [c]Constant of hydrogels

From this table it was clear that drug release kinetics was best described by Peppas-model as the value of correlation coefficient was found to be more than 0.9. Studies suggested that a drug delivery system with slab geometry and values of release exponent (n) < 0.5, 0.5 < n < 1.0 or 1.0 corresponds to Fickian diffusion, anomalous transport and case-II transport (zero order release) respectively. Theophylline release from poly (acrylic acid-co-acrylamide) hydrogels followed an anomalous kinetics[41] while gentamicin sulphate liberation from poly (acrylamide-co-acrylic acid) showed anomalous diffusion at low acrylic acid concentration and Fickian diffusion at high acrylic acid concentration[40].

For hydrogel nanofibrous mat release exponent value was below 0.5 at all the pHs which indicated Fickian diffusion at all the pHs. It means that the drug diffusion rate was less as compared to the relaxation rate of the hydrogel matrix. The table also indicated that value of k raises with increase in pH up to 7.0 and then decreased. Since k is related with the geometry of the hydrogel, so it can be assumed that the pore size in the nanofibers hydrogel was maximum at pH 7.0 because of the repulsion between

the negatively charged carboxylate groups formed due to the ionization of carboxylic acid groups at this pH. However, above this pH, the physical forces working between poly acrylic acid and poly acrylamide diminished and hence pore size reduced resulting in less drug release. A lack towards the study of drug release kinetics from hydrogel nanofibers was appeared in the previous papers. Yuan et al.[52] studied the release of BSA as a model protein from hydrogel nanofibers of CTS-g-PNIPAAm / PEO and reported that BSA release was a diffusion controlled process. Agarwal and Purwar studied the drug release kinetics of hydrogel films of poly (acrylamide-co-acrylic acid) and reported that it fits best in Peppas-model i.e., drug release occur by Fickian diffusion mechanism[139]. This was also in accordance with the results obtained for hydrogel nanofibers.

CHAPTER 8

CONCLUSIONS

Bilayer composites of poly (acrylamide-co-acrylic acid) grafted cotton fabric were prepared using cross-linkers MBAAm and PEG. The optimized conditions for the development of bilayer composites were initiator concentration 5%(w/V), monomer ratio 1:1 (in mol), monomer concentration 15%(w/V), reaction time 55minutes, and reaction temperature 50±5°C. The cross-linker concentration was found to be 0.1% (w/w) in case of composite prepared by using PEG, whereas it was found to be 0.3% (w/w) in the case of the composite prepared using MBAAm as a cross-linker. Sufficiently thick i.e., 0.23±0.05mm thick in case of composite prepared by using PEG and 0.30±0.04mm in case of composite prepared using MBAAm, hydrogel layer were grafted over the cotton fabric. These layers had approximate resemblance with the thickness of the cotton fabric. The grafting yield was 102% and 184% in case of composites prepared by using PEG and MBAAm respectively. These composites were characterised structurally and morphologically using FTIR and SEM techniques. Cross-linking by PEG in the hydrogel was revealed by a characteristic band of C-O-C stretching at 1168cm^{-1} showing the presence of ester linkage in it whereas cross-linking by MBAAm was indicated by a weak band at 2156cm^{-1} showing the presence of C–N bond. SEM micrographs of both the composites revealed formation of a uniform layer of hydrogel over the cotton fabric. Mechanical testing using Universal Testing Machine (Instron-2700) showed a higher tensile strength (6.2 and 4.2MPa respectively for the composite prepared with MBAAm and PEG as cross-linkers) of the composites as compared to the hydrogel film.

Comparison of grafting and swelling ability tests of the grafted composites suggested more grafted and a highly condensed structure in case of composite prepared by using MBAAm but swelling ability of composite prepared by using PEG was just the double in comparison to that prepared with MBAAm at all the pHs studied. However, maximum swelling i.e., 1466% and 720% respectively, for the composites prepared by using PEG and MBAAm was achieved at neutral pH. Swelling of the composite prepared by using PEG followed first-order kinetics at acidic and neutral pH, whereas second-order kinetic model at pH8.5 while that prepared using MBAAm followed second-order kinetic equation at all the pHs studied. The swelling kinetics was also governed by Peppas-model at all pHs. Antimicrobial tests were performed to show the effectiveness of drug loaded within the hydrogel samples. The zone diameter in the discs having *E.coli.* and *S. aureus*. were 17.5mm and 14.0mm in case of composite cell-$(AAm)_n$-$(AAc)_n$-PEG whereas these were found to be 15.0mm and 11.0mm for cell-$(AAm)_n$-$(AAc)_n$-MBAAm. More diameter of zone of inhibition in case of composite cell-$(AAm)_n$-$(AAc)_n$-PEG as compared to the composite cell-$(AAm)_n$-$(AAc)_n$-MBAAm supports the dependency of bactericidal action of composite material upon the amount of drug released, i.e., upon the swelling and drug loading property of the composite. The amount of drug loaded was found to be 76.45% and 55.89% respectively for cell-$(AAm)_n$-$(AAc)_n$-PEG and cell-$(AAm)_n$-$(AAc)_n$-MBAAm. Although a good amount of drug was loaded in both the composites but more drug was loaded in case of cell-$(AAm)_n$-$(AAc)_n$-PEG due to more hydrophilicity and optimum pore size in this case. Release kinetics of gentamicin sulphate from both the composites was studied in phosphate buffer of pH 5.5, 7.0 and 8.5 at 37±0.1°C and observed that it was faster in phosphate buffer of pH 7.0. Up to 68% drug was released in the first 12h in case of cell-$(AAm)_n$-$(AAc)_n$-PEG

while it was only 62% in case of cell-$(AAm)_n$-$(AAc)_n$-MBAAm. On fitting release data in Peppas-model, Higuchi-model, zero-order, first-order and second-order kinetic equations, it was found that drug release was diffusion controlled and followed Fickian diffusion mechanism in case of composite prepared by using PEG as cross-linker whereas it was controlled by diffusion as well as chain relaxation in case of composite prepared by using MBAAm.

Hydrogel nanofibers of copolymer of poly (acrylamide-co-acrylic acid) were also developed using electrospinning machine with a voltage of 23kV, tip to collector distance 15cm and feed rate of 3.5-4$\mu Lmin^{-1}$ followed by cross-linking through heat induced esterification at 145-150°C. The obtained fibers had bead less morphology and average fiber diameter of 275±94.5nm. These mats were highly porous structure with 74% porosity. Swelling of these mats was highest at neutral pH and it followed second-order kinetics at all pHs. Half of the swelling was achieved within a period of two hours. The nanofibrous mats were loaded with amoxicillin drug for antimicrobial activity. Formation of a clear zone of inhibition with both Gram positive and Gram negative bacteria in disc diffusion test confirmed the loading and releasing of the drug from the hydrogel nanofibrous mat. The drug release kinetics followed Fickian diffusion ($n < 0.5$). Initial excessive swelling and a higher initial release rate make the hydrogel nanofibrous mat a potent candidate for making active wound dressings.

FUTURE PROSPECTIVE OF THE RESEARCH

This research work helps in understanding the correlation of drug release with the geometry of the dressing matrix. It opens many new opportunities for the development of several other hydrogel based nanofibers and their use for the release of various nutrients.

This is only an initial step for the development and characterisation of nanofibers of poly (acrylamide-co-acrylic acid). Further study of the rheological properties of hydrogel nanofibers is still unrevealed.

REFERENCES

1. Szycher, M. & Lee, S. J. Modern wound dressings : A systematic approach to wound healing. *J. Biomater. Appl.***7,** 142–213 (1992).

2. Guo, S. & Dipietro, L. A. Factors affecting wound healing. *J. Dent. Res.***89,** 219–229 (2010).

3. Winter GD. A note on wound healing under dressings with special reference to perforated-film dressings. *J. Invest. Dermatol.***45,** 299–303 (1965).

4. Winter, G. D. Formation of the scab and the rate of epithelization of superficial wounds in the skin of the young domestic pig. *Nat. Int. J. Sci.***193,** 293–294 (1962).

5. Ichioka, S., Harii, K., Nakahara, M. & Sato, Y. An experimental comparison of hydrocolloid and alginate dressings, and the effect of calcium ions on the behaviour of alginate gel. *Scand. J. Plast. Reconstr. Surg. Hand Surg.***32,** 311–316 (1998).

6. S. Thomas, Bp. Alginate dressings in surgery and wound management – part 1. *J. Wound Care.***9,** 9–13 (2000).

7. Kuo, C. K. & Ma, P. X. Ionically crosslinked alginate hydrogels as scaffolds for tissue engineering: Part 1. Structure, gelation rate and mechanical properties. *Biomaterials.***22,** 511–521 (2001).

8. M., B. G. Experimental observations on absorbable alginate products in surgery. *J. Surg.***125,** (1946).

9. Dealey, C. Role of hydrocolloids in wound management. *Br. J. Nurs.***2,** 358–365 (1993).

10. Andrew, H. Wound dressings and the drug tariff. *J. Wound Care.***8,** 69–72 (1999).

11. Thomas, S. & Materials, S. A guide to the composition, properties and uses of hydrocolloid dressings and the commercial presentations available. *J. Wound Care.***I,** 127–130 (1992).

12. He, G., Ke, W., Chen, X., Kong, Y., Zheng, H., Yin, Y. & Cai, W. Preparation and properties of quaternary ammonium chitosan-g-poly(acrylic acid-co-acrylamide) superabsorbent hydrogels. *React. Funct. Polym.***111,** 14–21 (2017).

13. Gharekhani, H., Olad, A., Mirmohseni, A. & Bybordi, A. Superabsorbent hydrogel made of NaAlg-g-poly(AA-co-AAm) and rice husk ash: Synthesis, characterization, and swelling kinetic studies. *Carbohydr. Polym.***168,** 1–13 (2017).

14. Zohuriaan-Mehr, M. J., Omidian, H., Doroudiani, S. & Kabiri, K. Advances in non-hygienic applications of superabsorbent hydrogel materials. *J. Mater. Sci.***45,** 5711–5735 (2010).

15. Conaghey, O. M., Corish, J. & Corrigan, O. I. Iontophoretically assisted in vitro membrane transport of nicotine from a hydrogel containing ion exchange resins. *Int. J. Pharm.***170,** 225–237 (1998).

16. Feng, C., Shen, Z., Yang, D., Li, Y., Hu, J., Lu, G. & Huang, X. Synthesis of well-defined amphiphilic graft copolymer bearing poly (2-acryloyloxyethyl ferrocenecarboxylate) side chains via successive SET-LRP and ATRP. *Polymer (Guildf).***47,** 4346–4357 (2009).

17. Mohd Amin, M. C. I., Ahmad, N., Pandey, M. & Jue Xin, C. Stimuli-responsive bacterial cellulose-g-poly(acrylic acid-co-acrylamide) hydrogels for oral controlled release drug delivery. *Drug Dev. Ind. Pharm.***40,** 1340–1349 (2014).

18. Reddy, K. R., Rajgopal, K., Maheswari, C. U. & Lakshmi Kantam, M. Chitosan hydrogel: A green and recyclable biopolymer catalyst for aldol and Knoevenagel reactions. *New J. Chem.***30,** 1549–1552 (2006).

19. Hapiot, F., Menuel, S. & Monflier, E. Thermoresponsive hydrogels in catalysis. *ACS Catal.***3,** 1006–1010 (2013).

20. Tangri, A. Polyacrylamide based hydrogels : Synthesis , characterization and applications. *Int. J. Pharm. Chem. Biol. Sci.***4,** 951–959 (2014).

21. Cheng, W. M., Hu, X. M., Zhao, Y. Y., Wu, M. Y., Hu, Z. X. & Yu, X. T. Preparation and swelling properties of poly(acrylic acid-co-acrylamide) composite hydrogels. *E-Polymers.***17,** 95–106 (2017).

22. Bajpai, S. K. & Dubey, S. Synthesis and swelling kinetics of a pH-sensitive terpolymeric hydrogel system. *Iran. Polym. J. (English Ed.***13,** 189–203 (2004).

23. Dibakar, D., C.K., N. & P.R., C. Super absorbent hydrogels: Interpenetrating networks of poly(acrylamide-co-acrylic acid) and poly (vinyl alcohol): Swelling behavior and structural parameters. *J. Macromol. Sci. Part A Pure Appl. Chem.***A36,** 197–210 (1999).

24. Chavda, H. V. & Patel, C. N. Preparation and characterization of swellable polymer-based superporous hydrogel composite of poly (acrylamide-co-acrylic acid). *Trends Biomater. Artif. Organs.***24,** 83–89 (2010).

25. Jones, A. & Vaughan, D. Hydrogei dressings in the management of a variety of wound types: A review. *J. Orthop. Nurs.***9,** S1–S11 (2005).

26. Purwar, R., Rajput, P. & Srivastava, C. M. Composite wound dressing for drug release. *Fibers Polym.***15,** 1422–1428 (2014).

27. Gupta, P., Bajpai, M. & Bajpai, S. K. Textile technology: Investigation of antibacterial properties of silver nanoparticle-loaded poly (acrylamide-co-itaconic acid)-grafted cotton fabric. *J. Cotton Sci.***12,** 280–286 (2008).

28. Chun, H. J., Cho, S. M., Lee, Y. M., Lee, H. K., Suh, T. S. & Shinn, K. S. Graft copolymerization of mixtures of acrylic acid and acrylamide onto polypropylene film. *J. Appl. Polym. Sci.***72,** 251–256 (1998).

29. Mahdavinia, G. R., Pourjavadi, A., Hosseinzadeh, H. & Zohuriaan, M. J. Modified chitosan 4. Superabsorbent hydrogels from poly(acrylic acid-co-acrylamide) grafted chitosan with salt- and pH-responsiveness properties. *Eur. Polym. J.***40,** 1399–1407 (2004).

30. Li, S., Dong, S., Xu, W., Tu, S., Yan, L., Zhao, C., Ding, J. & Chen, X. Antibacterial Hydrogels. *Adv. Sci.***5,** 1–17 (2018).

31. Sabitha, M. & Rajiv, S. Preparation and characterization of ampicillin-incorporated electrospun polyurethane scaffolds for wound healing and infection control. *Polym. Eng. Sci.***55,** 541–548 (2014).

32. Loh, X. J., Peh, P., Liao, S., Sng, C. & Li, J. Controlled drug release from biodegradable thermoresponsive physical hydrogel nanofibers. *J. Control. Release.***143,** 175–182 (2010).

33. Liu, Z. S. & Rempel, G. L. Preparation of superabsorbent polymers by crosslinking acrylic acid and acrylamide copolymers. *J. Appl. Polym. Sci.***64,** 1345–1353 (1997).

34. Nesrinne, S. & Djamel, A. Synthesis, characterization and rheological behavior of pH sensitive poly(acrylamide-co-acrylic acid) hydrogels. *Arab. J. Chem.***10,** 539–547 (2017).

35. Thakur, A., Wanchoo, R. K. & Singh, P. Structural parameters and swelling behavior of pH sensitive poly (acrylamide- co -acrylic acid) hydrogels. *Chem. Biochem. Eng. Q.***25,** 181–194 (2011).

36. Ueshima, T., Hosoda, Y. & Lieberman, P. E. Process for the production of highly water-absorbing but less water-soluble hydrogels. 1–18 (1982).

37. Parks, L. R. Cross-linked sodium polyacrylate absorbent. *US Pat. Doc.* (1981).

38. Yang, Z., Peng, H., Wang, W. & Liu, T. Crystallization behavior of poly(ε-caprolactone)/layered double hydroxide nanocomposites. *J. Appl. Polym. Sci.***116,** 2658–2667 (2010).

39. Povea, M. B., Monal, W. A., Cauich-Rodríguez, J. V., Pat, A. M., Rivero, N. B., Covas, C. P., Valerio, J., Rodríguez, C., Pat, A. M., Rivero, N. B. & Covas, C. P. Interpenetrated chitosan-poly(acrylic acid-co-acrylamide) hydrogels. Synthesis, characterization and sustained protein release studies. *Mater. Sci. Appl.***2,** 509–520 (2011).

40. Thakur, A., Wanchoo, R. K. & Singh, P. Hydrogels of poly(acrylamide-co-acrylic acid):In-vitro study on release of gentamicin sulfate. *Chem. Biochem. Eng. Q.***25,** 471–482 (2011).

41. Katime, I., Novoa, R.,Apodaca. Dı´az de., Mendizabal, & E., Puig, J., Theophylline release from poly (acrylic acid-co-acrylamide). *Polym. Test.***18,** 559–566 (1999).

42. Martínez-Ruvalcaba, A., Sánchez-Díaz, J. C., Becerra, F., Cruz-Barba, L. E. & González-Álvarez, A. Swelling characterization and drug delivery kinetics of polyacrylamide-co-itaconic acid/chitosan hydrogels. *Express Polym. Lett.***3,** 25–32 (2009).

43. Ray, D., Mohapatra, D. K., Mohapatra, R. K., Mohanta, G. P. & Sahoo, P. K. Synthesis and colon-specific drug delivery of a poly(acrylic acid-co-acrylamide)/MBA nanosized hydrogel. *J. Biomater. Sci. Polym. Ed.***19,** 1487–1502 (2008).

44. Nayak, R. & Padhye, R. Nano fibres by electrospinning, properties and applications. *J. Text. Eng. Fash. Technol.***2,** 486–497 (2017).

45. Chen, H. & Hsieh, Y. Lo. Ultrafine hydrogel fibers with dual temperature- and pH-responsive swelling behaviors. *J. Polym. Sci. Part A Polym. Chem.***42,** 6331–6339 (2004).

46. Zhang, C., Wu, S. & Qin, X. Facile fabrication of novel pH-sensitive poly(aspartic acid) hydrogel by crosslinking nanofibers. *Mater. Lett.***132,** 393–396 (2014).

47. Uppal, R., Ramaswamy, G. N., Arnold, C., Goodband, R. & Wang, Y. Hyaluronic acid nanofiber wound dressing — production , characterization , and in vivo behavior. *J. Biomed. Mater. Biomater.***97B,** 20–29 (2011).

48. Tang, C., Ye, S. & Liu, H. Electrospinning of poly(styrene-co-maleic anhydride) (SMA) and water-swelling behavior of crosslinked/hydrolyzed SMA hydrogel nanofibers. *Polymer (Guildf).***48,** 4482–4491 (2007).

49. Cao, S. & Liu, H. Synthesis of pH-responsive crosslinked poly [styrene- co - (maleic sodium anhydride)] and cellulose composite hydrogel nanofibers by electrospinning. *Polym. Int.***58,** 545–551 (2009).

50. Kim, K., Akada, Y., Kai, W., Kim, B. & Kim, I. Cells attachment property of PVA hydrogel nanofibers incorporating hyaluronic acid for tissue engineering. *J. Biomater. Nanobiotechnol.***2,** 353–360 (2011).

51. Yun, J., Im, J. S., Lee, Y. S. & Kim, H. Il. Electro-responsive transdermal drug

delivery behavior of PVA/PAA/MWCNT nanofibers. *Eur. Polym. J.***47,** 1893–1902 (2011).

52. Yuan, H., Li, B., Liang, K., Lou, X. & Zhang, Y. Regulating drug release from pH- and temperature-responsive electrospun CTS-g-PNIPAAm/poly(ethylene oxide) hydrogel nanofibers. *Biomed. Mater.***9,** 055001 (2014).

53. González, E. & Frey, M. W. Synthesis, characterization and electrospinning of poly(vinyl caprolactam-co-hydroxymethyl acrylamide) to create stimuli-responsive nanofibers. *Polymer (Guildf).***108,** 154–162 (2017).

54. Lubasova, D., Niu, H., Zhao, X. & Lin, T. Hydrogel properties of electrospun polyvinylpyrrolidone and polyvinylpyrrolidone/poly(acrylic acid) blend nanofibers. *RSC Adv.***5,** 54481–54487 (2015).

55. Ding, B., Kim, H. Y., Lee, S. C., Shao, C. L., Lee, D. R., Park, S. J., Kwag, G. B. & Choi, K. J. Preparation and characterization of a nanoscale poly(vinyl alcohol) fiber aggregate produced by an electrospinning method. *J. Polym. Sci. Part B Polym. Phys.***40,** 1261–1268 (2002).

56. S., K. R. & H., E. W. The wound healing process. *Dermatol. Clin.***11,** 629–640 (1993).

57. Kaye, B. B. & Ennis, W. M. Classification of wounds and their treatment. *Am. J. Surg.***59,** 94–98 (1943).

58. Schneider, L. A., Korber, A., Grabbe, S. & Dissemond, J. Influence of pH on wound-healing: A new perspective for wound-therapy? *Arch. Dermatol. Res.***298,** 413–420 (2007).

59. Gethin, G. The significance of surface pH in chronic wounds. *wounds uk.***3,** 52–55 (2007).

60. Moore, O. A., Smith, L. A., Campbell, F., Seers, K., McQuay, H. J. & Moore, R. A. Systematic review of the use of honey as a wound dressing. *BMC Complement. Altern. Med.***1,** (2001).

61. Jones, V. J. The use of gauze: Will it ever change? *Int. Wound J.***3,** 79–88 (2006).

62. Waring, M. J. & Parsons, D. Physico-chemical characterisation of carboxymethylated spun cellulose " bres. *Biomaterials.***22,** 903–912 (2001).

63. Jones, A. M. & San Miguel, L. Are modern wound dressings a clinical and cost-effective alternative to the use of gauze? *J. Wound Care.***15,** 65–69 (2006).

64. Hoekstra, M. J., Hermans, M. H., Richters, C. D. & Dutrieux, R. P. A histological comparison of acute inflammatory responses with a hydrofibre or tulle gauze dressing. *J. Wound Care.***11,** 113–117 (2002).

65. G., O. L. Hanging wet-to-dry dressings out to dry. *Adv. Skin Wound Care* 79–86 (2002).

66. D., H. C. & Howard, M. Effect of air exposure and occlusion on experimental human skin wounds. *Nature.***200,** 378–379 (1963).

67. Compañ, V., Andrio, A., López-Alemany, A., Riande, E. & Refojo, M. F. Oxygen permeability of hydrogel contact lenses with organosilicon moieties. *Biomaterials.***23,** 2767–2772 (2002).

68. Cartmell, J.V., Sturtevant,W. R., & Wolf , M. L., U.S. Patent 5429589A,

Hydrogel gauze wound dressing. (1995).

69. Degreef, H. J. How to heal a wound fast. *Dermatol. Ther.***16,** 365–375 (1998).

70. Liu, X., Liu, J., Lin, S. & Zhao, X. Hydrogel machines. *Mater. Today***xxx,** 14–19 (2020).

71. Caló, E. & Khutoryanskiy, V. V. Biomedical applications of hydrogels: A review of patents and commercial products. *Eur. Polym. J.***65,** 252–267 (2015).

72. Hoffman, A. S. Hydrogels for biomedical applications ☆. *Adv. Drug Deliv. Rev.***64,** 18–23 (2012).

73. van Bemmelen, J. M. The hydrogel and the crystalline hydrate of copper oxide. *J. Inorg. Chem.***5,** 466–483 (1894).

74. Aswathy, S. H., Narendrakumar, U. & Manjubala, I. Commercial hydrogels for biomedical applications. *Heliyon.***6,** e03719 (2020).

75. Wichterle, O. & Lim, D. Process for producing shaped articles from three-dimensional hydrophilic high polymers. 2–5 (1961).

76. Gupta, P., Vermani, K. & Garg, S. Hydrogels: From controlled release to pH-responsive drug delivery. *Drug Discov. Today.***7,** 569–579 (2002).

77. Hoffman, A. S. Environmentally Sensitive Polymers and Hydrogels. *MRS Bull.* 42–46 (1991).

78. Zhang, Y., Wu, F., Li, M. & Wang, E. pH switching on-off semi-IPN hydrogel based on cross-linked poly(acrylamide-co-acrylic acid) and linear polyallyamine. *Polymer (Guildf).***46,** 7695–7700 (2005).

79. Shukla, S. & Bajpai, A. K. Preparation and characterization of highly swelling

smart grafted polymer networks of poly(vinyl alcohol) and poly(acrylic acid-co-acrylamide). *J. Appl. Polym. Sci.***102,** 84–95 (2006).

80. Kabiri, K., Omidian, H., Hashemi, S. A. & Zohuriaan-Mehr, M. J. Synthesis of fast-swelling superabsorbent hydrogels: Effect of crosslinker type and concentration on porosity and absorption rate. *Eur. Polym. J.***39,** 1341–1348 (2003).

81. Ganji, F., Vasheghani-Farahani, S. & Vasheghani-Farahani, E. Theoretical description of hydrogel swelling: A review. *Iran. Polym. J. (English Ed.***19,** 375–398 (2010).

82. Fu, Y. & Kao, W. J. Drug release kinetics and transport mechanisms of non-degradable and degradable polymeric delivery systems. *Expert Opin. Drug Deliv.***7,** 429–444 (2010).

83. Bajpai, A. K., Shukla, S. K., Bhanu, S. & Kankane, S. Responsive polymers in controlled drug delivery. *Prog. Polym. Sci.***33,** 1088–1118 (2008).

84. Sand, A. & Vyas, A. Superabsorbent polymer based on guar gum-graft-acrylamide: synthesis and characterization. *J. Polym. Res.***27,** 43 (2020).

85. Şolpan, D., Duran, S. & Torun, M. Removal of cationic dyes by poly(acrylamide-co-acrylic acid) hydrogels in aqueous solutions. *Radiat. Phys. Chem.***77,** 447–452 (2008).

86. Ritger, P. L. & Peppas, N. A. A simple equation for description of solute release II. Fickian and anomalous release from swellable devices. *J. Control. Release.***5,** 37–42 (1987).

87. Lamprecht, A., Yamamoto, H., Takeuchi, H. & Kawashima, Y. Microsphere design for the colonic delivery of 5-fluorouracil. *J. Control. Release.***90,** 313–322 (2003).

88. Graham, N. B. & McNeill, M. E. Hydrogels for controlled drug delivery. *Biomaterials.***5,** 27–36 (1984).

89. Serra, L., Doménech, J. & Peppas, N. A. Drug transport mechanisms and release kinetics from molecularly designed poly(acrylic acid-g-ethylene glycol) hydrogels. *Biomaterials.***27,** 5440–5451 (2006).

90. Samaha, D., Shehayeb, R. & Kyriacos, S. Modeling and comparison of dissolution profiles of diltiazem modified-release formulations. *Dissolution Technol.***16,** 41–46 (2009).

91. Pourjavadi, A. & Mahdavinia, G. R. Superabsorbency, pH-sensitivity and swelling kinetics of partially hydrolyzed chitosan-g-poly(acrylamide) hydrogels. *Turkish J. Chem.***30,** 595–608 (2006).

92. Peppas, N. A. & Khare, A. R. Preparation, structure and diffusional behavior of hydrogels in controlled release. *Adv. Drug Deliv. Rev.***11,** 1–35 (1993).

93. Sandeep, C., SL, H. & Kanupriya. Hydrogels: A smart drug delivery system. *Int. J. Res. Pharm. Chem.***2,** 603–614 (2012).

94. Xie, Z., Aphale, N. V., Kadapure, T. D., Wadajkar, A. S., Orr, S., Gyawali, D., Qian, G., Nguyen, K. T. & Yang, J. Design of antimicrobial peptides conjugated biodegradable citric acid derived hydrogels for wound healing. *J. Biomed. Mater. Res. - Part A.***103,** 3907–3918 (2015).

95. Lian, Z. & Ye, L. Synthesis and properties of carboxylated poly(vinyl alcohol) hydrogels for wound dressings. *J. Polym. Res.***22,** 1–11 (2015).

96. Li, W., Zhao, H., Teasdale, P. R., John, R. & Zhang, S. Synthesis and characterisation of a polyacrylamide-polyacrylic acid copolymer hydrogel for environmental analysis of Cu and Cd. *React. Funct. Polym.***52,** 31–41 (2002).

97. Turan, E. & Tuncer, C. Swelling and network parameters of pH-sensitive poly (acrylamide- co -acrylic acid) hydrogels. *J. Appl. Polym. Sci.***106,** 2000–2007 (2007).

98. Zhang, Y. Preparation of copolymers of acrylic acid and acrylamide for copper (II) capture from aqueous solutions. *Thesis* (2009).

99. Gupta, B., Agarwal, R. & Alam, M. S. Textile-based smart wound dressings. *Indian J. Fibre Text. Res.***35,** 174–187 (2010).

100. Amit, B., W., R. J. & Paramita, R. *Polymer grafting and cross-linking*. (2009).

101. Borbély, É. & Erdélyi, J. Grafting of Industrial Cellulose Pulp with Vinyl acetate Monomer by Ceric Ion Redox System as Initiator. Acta Polytech. Hungarica 1,86–95(2004).

102. Chen, J. P., Kuo, C. Y. & Lee, W. L. Thermo-responsive wound dressings by grafting chitosan and poly(N-isopropylacrylamide) to plasma-induced graft polymerization modified non-woven fabrics. *Appl. Surf. Sci.***262,** 95–101 (2012).

103. Nazari Pour, S., Ghugare, S. V., Wiens, R., Gough, K. & Liu, S. Controlled in situ formation of polyacrylamide hydrogel on PET surface via SI-ARGET-

ATRP for wound dressings. *Appl. Surf. Sci.***349,** 695–704 (2015).

104. Mostafa, K. M. & . K. M. M. Grafting of Methacrylamide onto Cotton Yarn Part I: Tensile Strength. *J. Appl. Sci.***5,** 341–346 (2005).

105. Khullar, R., Varshney, V. K., Naithani, S. & Soni, P. L. Grafting of acrylonitrile onto cellulosic material derived from bamboo (Dendrocalamus strictus). *Express Polym. Lett.***2,** 12–18 (2008).

106. Jianqin, L., Maolin, Z. & Hongfei, H. Pre-irradiation grafting of temperature sensitive hydrogel on cotton cellulose fabric. *Radiat. Phys. Chem.***55,** 55–59 (1999).

107. Kubota, H. & Shiobara, N. Photografting of N-isopropylacrylamide on cellulose and temperature-responsive character of the resulting grafted celluloses. *React. Funct. Polym.***37,** 219–224 (1998).

108. Tourrette, A., De Geyter, N., Jocic, D., Morent, R., Warmoeskerken, M. M. C. G. & Leys, C. Incorporation of poly(N-isopropylacrylamide)/chitosan microgel onto plasma functionalized cotton fibre surface. *Colloids Surfaces A Physicochem. Eng. Asp.***352,** 126–135 (2009).

109. Ávila, A., Bierbrauer, K., Pucci, G., López-González, M. & Strumia, M. Study of optimization of the synthesis and properties of biocomposite films based on grafted chitosan. *J. Food Eng.***109,** 752–761 (2012).

110. Yang, J. M., Yang, S. J., Lin, H. T., Wu, T. H. & Chen, H. J. Chitosan containing PU/Poly(NIPAAm) thermosensitive membrane for wound dressing. *Mater. Sci. Eng. C.***28,** 150–156 (2008).

111. Ikram, S., Kumari, M. & Gupta, B. Thermosensitive membranes by radiation-induced graft polymerization of N-isopropyl acrylamide/acrylic acid on polypropylene nonwoven fabric. *Radiat. Phys. Chem.***80,** 50–56 (2011).

112. Lopérgolo, L. C., Catalani, L. H., MacHado, L. D. B., Rela, P. R. & Lugão, A. B. Development of reinforced hydrogels - I. Radiation induced graft copolymerization of methylmethacrylate on non-woven polypropylene fabric. *Radiat. Phys. Chem.***57,** 451–454 (2000).

113. Chen, K. S., Tsai, J. C., Chou, C. W., Yang, M. R. & Yang, J. M. Effects of additives on the photo-induced grafting polymerization of N-isopropylacrylamide gel onto PET film and PP nonwoven fabric surface. *Mater. Sci. Eng. C.***20,** 203–208 (2002).

114. Gupta, B., Mishra, S. & Saxena, S. Preparation of thermosensitive membranes by radiation grafting of acrylic acid/N-isopropyl acrylamide binary mixture on PET fabric. *Radiat. Phys. Chem.***77,** 553–560 (2008).

115. Sweeney, I. R., Miraftab, M. & Collyer, G. A critical review of modern and emerging absorbent dressings used to treat exuding wounds. *Int. Wound J.***9,** 601–612 (2012).

116. Dermarite Industries. Hydrogel Dressing | DermaGauze | Sterile Gauze for Assisted Living Facilities. (https://dermarite.com/product/dermagauze/)

117. DermaSyn _ Hydrogel Wound Dressing _ Products for Senior Care Centers. (http://dermarite.com/product/dermasy/) Access date 07/09/2021

118. Neoheal. (http://kikgel.com.pl/en/products/neoheal/) Access date 07/09/2021

119. Geliperm sheet Dressings Datacard.

(http://www.dressings.org/dressings/geliperm.html) Access date 07/09/2021

120. Kai, D., Prabhakaran, M. P., Stahl, B., Eblenkamp, M., Wintermantel, E. & Ramakrishna, S. Mechanical properties and in vitro behavior of nanofiberhydrogel composites for tissue engineering applications. *Nanotechnology.***23,** 1–10 (2012).

121. Visser, J., Melchels, F. P. W., Jeon, J. E., Van Bussel, E. M., Kimpton, L. S., Byrne, H. M., Dhert, W. J. A., Dalton, P. D., Hutmacher, D. W. & Malda, J. Reinforcement of hydrogels using three-dimensionally printed microfibres. *Nat. Commun.***6,** 1–10 (2015).

122. Liu, W., Zhan, J., Su, Y., Wu, T., Ramakrishna, S., Liao, S. & Mo, X. Injectable hydrogel incorporating with nanoyarn for bone regeneration. *J. Biomater. Sci. Polym. Ed.***25,** 168–180 (2014).

123. Sakai, S., Takagi, Y., Yamada, Y., Yamaguchi, T. & Kawakami, K. Reinforcement of porous alginate scaffolds by incorporating electrospun fibres. *Biomed. Mater.***3,** 1–6 (2008).

124. Ekaputra, A. K., Prestwich, G. D., Cool, S. M. & Hutmacher, D. W. Combining electrospun scaffolds with electrosprayed hydrogels leads to three-dimensional cellularization of hybrid constructs. *Biomacromolecules.***9,** 2097–2103 (2008).

125. Anderson, K. D., Lu, D., McConney, M. E., Han, T., Reneker, D. H. & Tsukruk, V. V. Hydrogel microstructures combined with electrospun fibers and

photopatterning for shape and modulus control. *Polymer (Guildf).***49,** 5284–5293 (2008).

126. Mo, X. M., Xu, C. Y., Kotaki, M. & Ramakrishna, S. Electrospun P(LLA-CL) nanofiber: A biomimetic extracellular matrix for smooth muscle cell and endothelial cell proliferation. *Biomaterials.***25,** 1883–1890 (2004).

127. Liu, H., Zhen, M. & Wu, R. Ionic-strength- And pH-responsive poly[acrylamide-co-(maleic acid)] hydrogel nanofibers. *Macromol. Chem. Phys.***208,** 874–880 (2007).

128. Xie, J. & Hsieh, Y. Lo. Ultra-high surface fibrous membranes from electrospinning of natural proteins: Casein and lipase enzyme. in *J. Mater. Sci.***38,** 2125–2133 (2003).

129. Xu, X. lin, Zhou, G. qing, Li, X. jie, Zhuang, X. pin, Wang, W., Cai, Z. jun, Li, M. qin & Li, H. jun. Solution blowing of chitosan/PLA/PEG hydrogel nanofibers for wound dressing. *Fibers Polym.***17,** 205–211 (2016).

130. Kim, S. H., Kim, S. H., Nair, S. & Moore, E. Reactive electrospinning of cross-linked poly(2-hydroxyethyl methacrylate) nanofibers and elastic properties of individual hydrogel nanofibers in aqueous solutions. *Macromolecules.***38,** 3719–3723 (2005).

131. Isik, B. & Kis, M. Preparation and determination of swelling behavior of poly(acrylamide-co-acrylic acid) hydrogels in water. *J. Appl. Polym. Sci.***94,** 1526–1531 (2004).

132. L F, G. & Peppas, N. A. Preparation and Characterization of pH-Sensitive , Interpenetrating Networks of Poly (vinyl alcohol) and Poly (acrylic acid). *J.*

*Appl. Polym. Sci.***55,** 919–928 (1995).

133. Sen, M., Yakar, A. & Güven, O. Determination of average molecular weight between cross-links ($\bar{M}(c)$) from swelling behaviours of diprotic acid-containing hydrogels. *Polymer (Guildf).***40,** 2969–2974 (1999).

134. Singhal, R., Tomar, R. S. & Nagpal, A. K. Effect of cross-linker and initiator concentration on the swelling behaviour and network parameters of superabsorbent hydrogels based on acrylamide and acrylic acid. *Int. J. Plast. Technol.***13,** 22–37 (2009).

135. Tomar, R. S., Gupta, I., Singhal, R. & Nagpal, A. K. Synthesis of poly (acrylamide-co-acrylic acid) based superaborbent hydrogels: Study of network parameters and swelling behaviour. *Polym. - Plast. Technol. Eng.***46,** 481–488 (2007).

136. Majumder, S., Dahiya, U. R., Yadav, S., Sharma, P., Ghosh, D., Rao, G. K., Rawat, V., Kumar, G., Kumar, A. & Srivastava, C. M. Zinc oxide nanoparticles functionalized on hydrogel grafted silk fibroin fabrics as efficient composite dressing. *Biomolecules.***10,** 1–14 (2020).

137. Srivastava, C. M., Purwar, R. & Gupta, A. P. Enhanced potential of biomimetic, silver nanoparticles functionalized Antheraea mylitta (tasar) silk fibroin nanofibrous mats for skin tissue engineering. *Int. J. Biol. Macromol.***130,** 437–453 (2019).

138. Tomar, R. S., Gupta, I., Singhal, R. & Nagpal, A. K. Synthesis of poly(acrylamide-co-acrylic acid)-based super-absorbent hydrogels by gamma radiation: Study of swelling behaviour and network parameters. *Des.*

*Monomers Polym.***10,** 49–66 (2007).

139. Agrawal, A. & Purwar, R. Swelling and drug release kinetics of composite wound dressing. *Indian J. Fibre Text. Res.***43,** 104–111 (2018).

140. Pishbin, F. et al. Electrophoretic deposition of gentamicin-loaded bioactive glass / chitosan composite coatings for orthopaedic implants. *ACS Appl. Mater. Interfaces.***6,** 8796–8806 (2014).

141. Çay, A. & Mohsen Miraftab. Properties of electrospun poly(vinyl alcohol) hydrogel nanofibers crosslinked with 1,2,3,4-butanetetracarboxylic acid. *J. Appl. Polym. Sci.***129,** 3140–3149 (2013).

142. Liu, R., Xu, X., Zhuang, X. & Cheng, B. Solution blowing of chitosan/PVA hydrogel nanofiber mats. *Carbohydr. Polym.***101,** 1116–1121 (2014).

143. Jin, X. & Hsieh, Y. Lo. pH-responsive swelling behavior of poly(vinyl alcohol)/poly(acrylic acid) bi-component fibrous hydrogel membranes. *Polymer (Guildf).***46,** 5149–5160 (2005).

144. Schneider, L. A., Korber, A., Grabbe, S. & Dissemond, J. Influence of pH on wound-healing: A new perspective for wound-therapy? Arch. Dermatol. Res. 298, 413–420 (2007).

145. Wang, H. et al. Synthesis of nanocrystalline cellulose via ammonium persulfate-assisted swelling followed by oxidation and their chiral self-assembly. Cellulose 27, 657–676 (2019).

PUBLICATIONS (FROM THESIS WORK)

Publication in International Journals

1. Preeti Gupta and Roli Purwar, Electrospun pH responsive poly (acrylic acid-co-acrylamide) hydrogel nanofibrous mats for drug delivery, Journal of Polymer Research,27(10):1-10.(Impact Factor: 2.426).

2. Preeti Gupta and Roli Purwar, Influence of Cross-linkers on the properties of Cotton grafted Poly (acrylamide-co-acrylic acid) Hydrogel Composite: Swelling and Drug Release Kinetics, Iranian Polymer journal,30:381-391. (Impact factor:1.89)

3. Preeti Gupta and Roli Purwar, Design and Development of Bilayer Composite using Different Cross-linkers, International Journal of Polymer and Textile Engineering, 7(3):12-17. (Impact factor:0.3)

Conference Publications

1. Preeti Gupta and Roli Purwar, Study of swelling behaviour and drug release kinetics of composite wound dressing material, International Conference on Polymeric Biomaterials, Bioengineering and Biodiagnostics , 27-30 October 2014, Organized by APA and IIT Delhi, New Delhi , India.

2. Preeti Gupta and Roli Purwar, Effect of cross linkers on Drug Delivery from Cotton Grafted hydrogel composite, International Conference on Advances in Polymer Science & Technology, 23-25 November, 2017, Organized by APA and IIT Delhi, New Delhi, India.

3.Preeti Gupta and Roli Purwar, Poly(Acrylamide-co-acrylic acid) Hydrogel Nanofibers: Swelling and Drug Release Behaviour, APA Bioforum International e-Conference on Polymeric Biomaterials &Bioengineering, 27-28 August 2021,Organised by APA Bioforum.

CURRICULUM VITAE

Preeti Gupta

Research Scholar (UGC-JRF)

Fiber Technology Research lab

Department of Applied Chemistry

Delhi Technological University, Delhi-110042

E-mail: preeti.yashvardhan@gmail.com

Area of Research Interest

- Fabrication & Grafting of poly (acrylamide-co-acrylic acid) based hydrogels for wound dressing application, composite dressings, nanofibrous mats, drug delivery kinetics.

Academic Qualification

- Ph.D. (Applied Chemistry) in 2014- present, from Delhi Technological University, Delhi.
- NET-JRF in 2012, from CSIR-UGC.
- M.Sc. (Chemistry) in 2006 from C.C.S University, Meerut (U.P.)
- B.Sc. (Biology) in 2003 from C.C.S University, Meerut (U.P.)
- Intermediate in 1999 from U.P. Board, Allahabad.
- High School in 1997 from U.P. Board, Allahabad.

Teaching Experience

- Working as Chemistry Lecturer from October 2016- till now in L.P.S.S. Inter College, Achalpur, Etah (U.P.)-207123

Other Experience

- Worked as Senior Author from October 2007 to October 2013 in Arihant Publications India Ltd. Meerut, (U.P.)-250103.
- Worked as freelance author for Chitra Publication, Rajeev Publication, SBPD Nageen Publication etc.